



**UNIVERSITY
OF TURKU**

**GALLIUM-68 RADIOLABELING OF
BIOMOLECULES FOR POSITRON
EMISSION TOMOGRAPHY WITH
SPECIAL REFERENCE TO IMAGING
OF INFLAMMATION AND BONE**

Meeri Käkelä



UNIVERSITY
OF TURKU

**GALLIUM-68 RADIOLABELING OF
BIOMOLECULES FOR POSITRON
EMISSION TOMOGRAPHY WITH
SPECIAL REFERENCE TO IMAGING
OF INFLAMMATION AND BONE**

Meeri Käkälä

University of Turku

Faculty of Medicine
Department of Clinical Physiology and Nuclear Medicine
Drug Research Doctoral Programme
Turku PET Centre

Supervised by

Professor Anne Roivainen, PhD
Turku PET Centre and Turku Center for
Disease Modeling
University of Turku, Finland

Adjunct Professor Xiang-Guo Li, PhD
Turku PET Centre
University of Turku, Finland

Reviewed by

Adjunct Professor Kim Bergström, PhD
HUS Medical Imaging Centre, Cyclotron
Unit
University of Helsinki, Finland

Professor Vladimir Tolmachev, DMSc,
MScEng
Department of Immunology, Genetics
and Pathology
Uppsala University, Sweden

Opponent

Assistant and Associate Professor Danielle Vugts, PhD
Department of Radiology
Amsterdam University Medical Center, the Netherlands

The originality of this publication has been checked in accordance with the University of Turku quality assurance system using the Turnitin OriginalityCheck service.

ISBN 978-951-29-7975-2 (PRINT)
ISBN 978-951-29-7976-9 (PDF)
ISSN 0355-9483 (Print)
ISSN 2343-3213 (Online)
Painosalama Oy, Turku, Finland 2020

“...because that challenge is one that we are willing to accept, one we are unwilling to postpone and one we intend to win...”

- John F. Kennedy

UNIVERSITY OF TURKU

Faculty of Medicine

Department of Clinical Physiology and Nuclear Medicine

MEERI KÄKELÄ: Gallium-68 Radiolabeling of Biomolecules for Positron Emission Tomography with Special Reference to Imaging of Inflammation and Bone

Doctoral Dissertation, 106 pp.

Drug Research Doctoral Programme

February 2020

ABSTRACT

Positron emission tomography (PET) radiopharmaceuticals are composed of a positron emitting radionuclide (e.g. gallium-68) and a molecular structure. MicroRNA-21 is a relevant target overexpressed in many diseases, such as osteoporosis and osteosarcoma. Interference of microRNA-21 by anti-microRNA-21 would be a potential medicinal treatment.

3'-NOTA-chelated anti-microRNA-21 was radiolabeled with gallium-68 using the fractionated method and mixed with 5'-alendronate-conjugated microRNA-21. ⁶⁸Ga-labeled double helix was formed rapidly at room temperature. The double helix thus formed was *in vivo* PET imaged to evaluate whether its bone accumulation was increased because of conjugated bis(phosphonate). PET imaging revealed that bis(phosphonate)-conjugated anti-microRNA-21 accumulates in the bone. This observation can be utilized in the future when developing medicinal treatments for diseases involving micro-RNA-21.

Sialic acid-binding immunoglobulin-like lectin-9 (Siglec-9) is a leukocyte ligand of vascular adhesion protein-1 (VAP-1). VAP-1 plays an important role in many inflammatory conditions. Inflammation has a significant part in a number of diseases, such as atherosclerosis and diabetes. PET imaging provides tools for studying the mechanisms related to the process of inflammation and to discover potential targeted therapeutics. [⁶⁸Ga]Ga-DOTA-Siglec-9 can be used as a PET tracer for imaging of inflammation.

The purpose of this thesis was to develop an automated protocol for producing GMP-grade inflammation imaging agent [⁶⁸Ga]Ga-DOTA-Siglec-9 for first-in-human studies. This GMP-grade tracer was produced using a fully automated acetone-based method. It was concluded that this method facilitates efficient production of GMP-grade [⁶⁸Ga]Ga-DOTA-Siglec-9 and the tracer is suitable for human use.

KEYWORDS: ⁶⁸Ga-radiolabeling, acetone-based method, bis(phosphonate)-conjugated anti-microRNA-21, fractionated method, Siglec-9

TURUN YLIOPISTO

Lääketieteellinen tiedekunta

Kliininen fysiologia ja isotooppilääketiede

MEERI KÄKELÄ: Biomolekyylien gallium-68-radioleimaus erityisesti

tulehduksen ja luuston PET-kuvantamiseksi

Väitöskirja, 106 s.

Lääkekehityksen tohtoriohjelma

Helmikuu 2020

TIIVISTELMÄ

Positroniemissiotomografiassa (PET) käytettävät radiolääkkeaineet koostuvat positronisäteilevästä radionuklidista (esim. gallium-68) ja molekyyli-rakenteesta. MikroRNA-21 ylierittyy monissa sairauksissa, kuten osteoporoosissa ja osteosarkoomassa. MikroRNA-21-rakenteen estäminen vastinparilla (anti-mikroRNA-21) on potentiaalinen hoitokeino.

3'-NOTA-kelatoitu anti-mikroRNA-21 radioleimattiin gallium-68:lla käyttämällä fraktiointimenetelmää ja sekoitettiin 5'-alendronaatti-konjugoidun mikroRNA-21:n kanssa. ⁶⁸Ga-radioleimattu kaksoiskierre muodostui nopeasti huoneenlämpötilassa. Rakenne PET-kuvattiin sen arvioimiseksi, lisääkö konjugoiminen bisfosfonaattiin sen luuhakuisuutta. PET-kuvantamisen avulla todettiin, että bisfosfonaatti-konjugoitu anti-mikroRNA-21-rakenne kerääntyy luustoon. Tätä havaintoa voidaan hyödyntää tulevaisuudessa kehitettäessä lääketieteellisiä hoitoja sairauksiin, joihin mikroRNA-21-rakenne liittyy.

Siaalihappoon sitoutuva immunoglobuliinin kaltainen lektiini-9 (Siglec-9) on vaskulaarisen adheesiomolekyylin (VAP-1) ligandi. VAP-1:llä on tärkeä osuus elimistön tulehduksiloissa. Tulehduksella on merkittävä rooli monissa sairauksissa, kuten ateroskleroosissa ja diabeteksessa. PET-kuvantamisen avulla voidaan tutkia tulehdusprosessia ja löytää siihen hoitokeinoja. Radiolääkeainetta [⁶⁸Ga]Ga-DOTA-Siglec-9 voidaan käyttää tulehduksen PET-kuvantamiseen.

Väitöskirjan tarkoituksena oli kehittää automaattinen menetelmä tulehduksen kuvantamiseen käytettävän GMP-laatuisen [⁶⁸Ga]Ga-DOTA-Siglec-9 radiolääkeaineen tuottamiseksi ensimmäisiin kliinisiin tutkimuksiin. Radiolääkeaine valmistettiin käyttämällä automaattista asetonipohjaista menetelmää. Menetelmä mahdollistaa GMP-laatuisen [⁶⁸Ga]Ga-DOTA-Siglec-9 radiolääkeaineen tehokkaan tuotannon. Radiolääkeaine soveltuu kliiniseen käyttöön.

AVAINSANAT: ⁶⁸Ga-radioleimaaminen, asetonipohjainen menetelmä, bisfosfonaatti-konjugoitu anti-mikroRNA-21, fraktiointimenetelmä, Siglec-9

Table of Contents

Abbreviations	9
List of Original Publications	13
1 Introduction	14
2 Review of the Literature	17
2.1 Radiochemistry	17
2.1.1 Radioisotopes of gallium	17
2.1.2 ⁶⁸ Ge/ ⁶⁸ Ga generators and cyclotrons	19
2.2 ⁶⁸ Ga-labeled PET radiopharmaceuticals and their development	22
2.2.1 Bifunctional chelators	23
2.2.1.1 Macrocyclic chelators	24
2.2.1.1.1 Examples of macrocyclic chelators	25
2.2.1.2 Acyclic chelators	27
2.2.1.2.1 Examples of acyclic chelators	29
2.2.1.3 Intermediate between macrocyclic and acyclic chelators	31
2.2.2 Synthesis of ⁶⁸ Ga-labeled PET radiopharmaceuticals	32
2.2.2.1 Elution of the ⁶⁸ Ge/ ⁶⁸ Ga generator and pre- purification of the eluate	33
2.2.2.2 Buffer solutions and purification of ⁶⁸ Ga- labeled peptides	36
2.2.3 Examples of ⁶⁸ Ga-labeled PET radiopharmaceuticals	38
2.2.3.1 ⁶⁸ Ga-somatostatin peptide derivatives	38
2.2.3.2 Prostate-specific membrane antigen	41
2.2.3.3 RGD-based peptides	43
2.2.3.4 Oligonucleotides	44
2.2.3.5 MicroRNA	47
2.2.3.6 Bis(phosphonates)	48
2.2.3.7 Sialic acid-binding immunoglobulin-like lectin 9	50
2.2.4 Quality control of PET radiopharmaceuticals	53
2.2.4.1 Chemical and physical tests	54
2.2.4.2 Biological tests	57

2.2.4.3	Examples of analytical techniques used in quality control of PET radiopharmaceuticals.....	58
2.2.5	Good manufacturing practice.....	61
3	Aims	63
4	Materials and Methods.....	64
4.1	⁶⁸ Ga-labeling and quality control (Subprojects I-III).....	64
4.1.1	Fractionated method for producing nonGMP-grade [⁶⁸ Ga]Ga-DOTA-Siglec-9 and related quality control (Subproject I).....	64
4.1.2	GMP-grade [⁶⁸ Ga]Ga-DOTA-Siglec-9 (Subproject II)...	65
4.1.2.1	Radiosynthesis of GMP-grade [⁶⁸ Ga]Ga-DOTA-Siglec-9 using an acetone-based method and related quality control	65
4.1.2.2	Radiosynthesis on nonGMP-grade 3'-[⁶⁸ Ga]Ga-NOTA-anti-microRNA-21 and related quality control (Subproject III).....	67
4.2	<i>In vitro</i> experiments	68
4.2.1	Plasma protein binding and stability of nonGMP-grade [⁶⁸ Ga]Ga-DOTA-Siglec-9 (Subproject I).....	68
4.2.2	Plasma protein binding and stability of nonGMP-grade ⁶⁸ Ga-labeled oligoribonucleotide (Subproject III).....	69
4.3	<i>In vivo</i> studies	71
4.3.1	<i>In vivo</i> imaging with nonGMP-grade ⁶⁸ Ga-labeled oligoribonucleotide (Subproject III)	71
4.3.2	Blood and urine samples (Subproject III).....	72
4.4	<i>Ex vivo</i> biodistribution experiments (Subproject III)	72
4.5	UV-melting profile analysis of 3'-NOTA-anti-microRNA-21/5'-bis(phosphonate)-microRNA-21 double helix (Subproject III).....	73
4.6	Statistical analyses.....	73
5	Results	74
5.1	Radiosynthesis and quality control (Subprojects I-III)	74
5.1.1	NonGMP-grade [⁶⁸ Ga]Ga-DOTA-Siglec-9 using fractionated method (Subproject I).....	74
5.1.2	GMP-grade [⁶⁸ Ga]Ga-DOTA-Siglec-9 using acetone-based (Subproject II)	74
5.1.2.1	Sticking problem and problem solving.....	78
5.1.3	NonGMP-grade 3'-[⁶⁸ Ga]Ga-NOTA-anti-microRNA-21 using fractionated method (Subproject III)	79
5.2	<i>In vitro</i> experiments	79
5.2.1	Plasma protein binding of nonGMP-grade [⁶⁸ Ga]Ga-DOTA-Siglec-9 (Subproject I).....	79
5.2.2	Stability of nonGMP-grade [⁶⁸ Ga]Ga-DOTA-Siglec-9 (Subproject I).....	80
5.2.3	Plasma protein binding of ⁶⁸ Ga-labeled oligoribonucleotide (Subproject III)	81

5.2.4	Stability of nonGMP-grade ⁶⁸ Ga-labeled oligoribonucleotide (Subproject III)	82
5.3	<i>In vivo</i> studies	84
5.3.1	<i>In vivo</i> imaging with ⁶⁸ Ga-radiolabeled oligoribonucleotide (Subproject III)	84
5.3.2	Blood and urine samples (Subproject III)	85
5.4	<i>Ex vivo</i> biodistribution experiments (Subproject III)	87
5.5	UV melting profile analysis of ⁶⁸ Ga-labeled double helix (Subproject III)	88
6	Discussion	90
6.1	Radiolabeling	90
6.1.1	Fractionated method and ⁶⁸ Ga-radiolabeling	90
6.1.2	Acetone-based method and ⁶⁸ Ga-radiolabeling	93
6.2	<i>In vivo</i> imaging and <i>ex vivo</i> biodistribution experiments	95
6.3	Plasma protein binding and stability <i>in vivo</i> and <i>in vitro</i> experiments	95
6.4	Future considerations	97
7	Conclusions	99
	Acknowledgments	101
	References	104
	Original Publications	113

Abbreviations

ACN	Acetonitrile
Al ₂ O ₃	Aluminium oxide
ASO	Antisense oligonucleotide
BFC	Bifunctional chelator
BPAMD	4-{{[(bis-phosphonomethyl)-carbomoyl]methyl}}-7,10-bis(carboxymethyl)-1,4,7,10-tetraazacyclo-dodec-1-yl-acetic acid
BPAPD	4-{{[(bis-phosphonopropyl)-carbomoyl]methyl}}-7,10-bis-(carboxymethyl)-1,4,7,10-tetraazacyclododec-1-yl-acetic acid
BPPED	Tetraethyl-10-{{[(2,2-bis-phosphonoethyl)hydroxyl-phosphoryl]methyl}}-1,4,7,10-tetraazacyclododecane-1,4,7-triacetic acid
¹¹ C	Carbon-11
CE	Capillary electrophoresis
cGMP	Current Good manufacturing practice
CT	Computed tomography
Cyclen	1,4,7,10-tetraazacyclododecane
DATA	6-amino-1,4-diazepinetriacetic acid
DFO	Deferoxamine
DNA	Deoxyribonucleic acid
DOTA	1,4,7,10-tetraazacyclododecane-1,4,7,10-tetraacetic acid
DOTA-NOC	DOTA-1-NaI ³ -octreotide
DOTA-TATE	DOTA-Tyr ³ -octreotate
DOTA-TOC	DOTA-Tyr ³ -octreotide
EDTA	Ethylenediamine- <i>N,N,N',N'</i> -tetraacetic acid
EOS	End of synthesis
EtOH	Ethanol
¹⁸ F	Fluorine-18
FDA	U.S. Food and Drug Administration
Fe ³⁺	Iron(III)
FID	Flame ionization detector
⁶⁷ Ga	Gallium-67

⁶⁸ Ga	Gallium-68
GaCl ₄	Tetrachlorogallate
GC	Gas chromatography
Ge	Germanium
GMP	Good manufacturing practice
HBED	<i>N,N'</i> -bis(2-hydroxybenzyl)-ethylenediamine- <i>N,N'</i> -diacetic acid
HBED-CC	<i>N,N'</i> -bis[2-hydroxy-5(carboxy-ethyl)benzyl]ethylenediamine- <i>N,N'</i> -diacetic acid
HBr	Hydrogen bromide
HCl	Hydrochloric acid
H ₂ dedpa	6,60-(ethane-1,2 diylbis(azanediy))bis (methylene)dipicolinic acid
HEPES	4-(2-hydroxyethyl)piperazine-1-ethanesulfonic acid
HNO ₃	Nitric acid
H ₃ NOKA	6,6',6''-(1,4,7-triazonane-1,4,7-triyl)tris(methylene)tris(5-hydroxy-2 (hydroxymethyl)-4Hpyran-4-one)
HPLC	High performance liquid chromatography
HPO	3-hydroxy-4-pyridinone
H ₃ PO ₄	Phosphoric acid
iTLC	Instant thin-layer chromatography
i.v.	Intravenously
LAN	Lanreotide
M	Molar
MicroRNA	miRNA
MRI	Magnetic resonance imaging
mRNA	Messenger RNA
¹³ N	Nitrogen-13
N	Normal
Na	Sodium
NaCl	Sodium chloride
NaOAc	Sodium acetate
NET	Neuroendocrine tumor
NH ₄ OAc	Ammoniumacetate
NO ₂ AP	1,4,7-triazacyclononane-1,4-diacetic acid
NOC	[NaI ³]-octreotide
NODAGA	1,4,7-triazacyclononane,1-glutaric acid-4,7-acetic acid
NODAPA-NCS	1,4,7-triazacyclononane-1,4-diacetic acid-7- <i>p</i> -isothiocyanatophenyl-acetic acid
NODAPA-(NCS) ₂	1,4,7-triazacyclononane-1-acetic acid-4,7-di- <i>p</i> -isothiocyanatophenyl-acetic acid

NODAPA-OH	1,4,7-triazacyclononane-1,4-diacetic acid-7- <i>p</i> -hydroxyphenyl-acetic acid
NODASA	1,4,7-triazacyclononane-1-succinic acid-4,7-deacetic acid
NOTA	1,4,7-triazacyclononane-1,4,7-triacetic acid
NOTAM	1,4,7-triazacyclononane-1,4,7-triacetamide
NOTP	1,4,7-triazacyclononane- <i>N,N',N''</i> -tris(methylenephosphonic) acid
NOTPME	1,4,7-triazacyclononane- <i>N,N',N''</i> -tris(methylenephosphonate-monoethylester)
NP-HPLC	Normal-phase chromatography
OSEM3D	Ordered-subsets expectation maximization 3D
PET	Positron emission tomography
Ph. Eur.	European Pharmacopoeia
PP	Pyrophosphate
PSL	Photostimulated luminescence
PSMA	Prostate-specific membrane antigen
QA	Quality assurance
QC	Quality control
RAC	Radioactivity concentration
RCP	Radiochemical purity
RCY	Radiochemical yield
RGD	Arg-Gly-Asp
RNA	Ribonucleic acid
RNAi	RNA interference
ROI	Regions of interest
RP-HPLC	Reversed-phase chromatography
r.t.	Room temperature
SAX	Strong anion-exchange
SCX	Strong cation-exchange
SD	Standard deviation
SG	Silica gel
Siglec	Sialic acid-binding immunoglobulin-like lectin
siRNA	Small interfering ribonucleic acid
SnO ₂	Tin dioxide
SOP	Standard operating procedure
SPE	Solid phase extraction
SPECT	Single photon emission computed tomography
SSTR	Somatostatin receptor
SUV	Standardized uptake value
TAC	Time-radioactivity curve

TACN	1,4,7-triazacyclononane
TACN-TM	1,4,7-tris(2 mercaptoethyl)-1,4,7-triazacyclononane
TATE	[Tyr ³]-octreotate
TFA	Trifluoroacetic acid
THP	Tris(3,4-hydroxypyridinone)
Ti ⁴⁺	Titanium(IV)
TiO ₂	Titanium dioxide
TLC	Thin-layer chromatography
TOC	[Tyr ³]-octreotide
TRAP	Triazacyclononane phosphinic acid
TRAP-H	Triazacyclononane methylphosphinic acid
TRAP-OH	Triazacyclononane methyl- (hydroxymethyl)phosphinic acid
TRAP-Ph	Triazacyclononane methyl(phenyl)phosphinic acid
UPLC	Ultra performance liquid chromatography
UV	Ultraviolet
VAP-1	Vascular adhesion protein-1
⁶⁸ Zn	Zinc-68
⁶⁸ Zn(NO ₃) ₂	Zinc-68 nitrate
ZrO ₂	Zirconium dioxide

List of Original Publications

This dissertation is based on the following original publications, which are referred to in the text by their Roman numerals:

- I Svend B. Jensen, Meeri Käkelä, Lars Jødal, Olli Moisio, Aage K.O. Alstrup, Sirpa Jalkanen, Anne Roivainen. Exploring the radiosynthesis and *in vitro* characteristics of [⁶⁸Ga]Ga-DOTA-Siglec-9. *Journal of Labelled Compounds and Radiopharmaceuticals*, 2017; 60: 439–49.
- II Meeri Käkelä, Pauliina Luoto, Tapio Viljanen, Helena Virtanen, Heidi Liljenbäck, Sirpa Jalkanen, Juhani Knuuti, Anne Roivainen, Xiang-Guo Li. Adventures in radiosynthesis of clinical grade [⁶⁸Ga]Ga-DOTA-Siglec-9. *The Royal Society of Chemistry Advances*, 2018; 8: 8051–6.
- III Satish Jadhav, Meeri Käkelä, Matthieu Bourgery, Kiira Rimpilä, Heidi Liljenbäck, Riikka Siitonen, Jussi Mäkilä, Tiina Laitala-Leinonen, Päivi Poijärvi-Virta, Harri Lönnberg, Anne Roivainen, Pasi Virta. *In vivo* bone-targeting of bis(phosphonate)-conjugated double helical RNA monitored by positron emission tomography. *Molecular Pharmaceutics*, 2016; 13: 2588–95.

The original publications have been reproduced with the permission of the copyright holders.

1 Introduction

Positron emission tomography (PET) provides quantitative images of biological processes *in vivo* at molecular level. It provides clinically important information for tumor diagnosis, cardiovascular diseases, neurological applications (Maisey, 2005) and infection and inflammation (Zhuang and Alavi, 2002). PET radiopharmaceuticals consist of two components: a molecular structure (ligand, vector, vehicle) and a positron emitting radionuclide. In order to make a stable connection between these two parts, a linker may be chemically necessary. The molecular structure defines the biological characteristics. It is responsible for biochemical and chemical interactions within the living organism and it has to provide a high degree of selectivity and specificity towards the target site. These targets can be e.g. antigens or selected receptor systems. The molecular structure either takes part directly in the metabolic processes or interacts with the targets. (Wadsak and Mitterhauser, 2010, Boschi et al., 2013)

The most common radionuclides for PET radiopharmaceuticals include carbon-11 (^{11}C , $t_{1/2} = 20$ minutes), nitrogen-13 (^{13}N , $t_{1/2} = 10$ minutes), oxygen-15 (^{15}O , $t_{1/2} = 123$ seconds), fluorine-18 (^{18}F , $t_{1/2} = 110$ minutes), gallium-68 (^{68}Ga , $t_{1/2} = 68$ minutes) and rubidium-82 (^{82}Rb , $t_{1/2} = 78$ seconds). Radiometals, such as ^{68}Ga , can only be fixed to the molecular structure using a metal-ligand-complex. Radionuclides can be produced using cyclotrons and generators. ^{68}Ga is one of the very early radionuclides applied to PET imaging at a time when not even the wording PET itself was yet established and a long time before the usage of, for example, ^{18}F . (Tsang et al., 1993, Wadsak and Mitterhauser, 2010, Boschi et al., 2013, Rösch, 2013, Huang, 2018)

^{68}Ga -based imaging agents comprising small molecules, large biomolecules and particles have been explored for the imaging and quantitation of various physiological disorders and biological functions. The molecular imaging of oncological diseases has been investigated most extensively for targeting receptors, enzymes and antigens. In addition, visualization of downstream biological processes, such as angiogenesis, apoptosis, hypoxia, glycolysis and proliferation, has also been performed. Probes for non-targeted imaging of pulmonary and

myocardial perfusion and ventilation as well as targeted imaging of inflammation, infection and messenger RNA (mRNA) have also been studied. (Velikyan, 2014)

In general, the production of ^{68}Ga -labeled radiopharmaceuticals involves elution of the generator, pre-purification of the eluate, the heating step, purification of the crude product and formulation of the injection solution. Buffer solutions are used to adjust the optimal reaction mixture pH as necessary for the chelate complexation. Recently, the use of fully automated systems for the production of ^{68}Ga -radiopharmaceuticals has increased. (Boschi et al., 2013)

The purpose of quality control (QC) of PET radiopharmaceuticals is to assure the safety of the product before its release for clinical use. QC involves several specific tests and measurements to ensure product purity, identity, efficacy and biological safety (Ha et al., 2017). Product purity consists of radionuclidic purity and chemical purity. Radionuclidic impurities can impact the quality of PET images. Chemical purity concerns solvents, by-products and other residual components used during the production. All of them can affect radiolabeling negatively. High performance liquid chromatography (HPLC) and thin-layer chromatography (TLC) are commonly used chromatographic methods in the QC of ^{68}Ga -radiopharmaceuticals.

Several peptide analogues of vascular adhesion protein-1 (VAP-1) ligands have been designed for visualization of VAP-1 expressed on endothelial surface in infection and inflammation (Velikyan, 2014). Linear 9-amino acid DOTA-chelated peptide targeting VAP-1 (^{68}Ga]-Ga-DOTAVAP-P1) and its modifications have been introduced and radiolabeled with ^{68}Ga in order to study their stability and potential to function as a PET tracer and to demonstrate specific binding and capability to differentiate between inflammation and infection using animal models (Lankinen et al., 2008, Ujula et al., 2009, Silvola et al., 2010, Aalto et al., 2011, Autio et al., 2011, Ahtinen et al., 2014, Virtanen et al., 2015, Virtanen et al., 2017). One of them is the cyclic peptide CARLSLSWRGLTLCPSK (containing residues 283–297 from sialic acid-binding immunoglobulin-like lectin-9 (Siglec-9)) bearing 1,4,7,10-tetraazacyclo-dodecane-1,4,7,10-tetraacetic acid (DOTA) chelator.

Chemical derivatization of small interfering ribonucleic acid (siRNA) and antisense oligonucleotides (ASO) has continued exhaustively over the past decades (Yamamoto et al., 2011, Winkler, 2013). Different modifications have been prepared and many of them have been evaluated for therapeutic use. There are many challenges related to the therapeutic application of nucleic acid-derived compounds. Delivery to tissues and organs other than the liver has not been achieved in a satisfactory manner yet. For example, it has been observed in some cases that oligonucleotides are rapidly eliminated by renal filtration, thus demanding high doses. (Winkler, 2013)

Good manufacturing practice (GMP) is one aspect of quality assurance for ensuring that medicinal products are consistently produced and controlled according to the relevant quality standards as required by the product specifications. The purpose is to minimize the risks involved in pharmaceutical production that cannot be eliminated through testing the final product. GMP covers all aspects of medicinal production including equipment, starting materials, premises and training of staff. It is highly important to have systems capable of providing documented proof that correct procedures are followed during the manufacturing processes.

The production of PET radiopharmaceuticals must be in compliance with the basic principles of GMP. The fact that PET radiopharmaceuticals are short-lived radiopharmaceuticals brings challenges to QC. The short half-life means that PET radiopharmaceuticals must be released and administered to a patient immediately after their production. The produced batch is authorized for clinical use before completion of all tests and the final release is approved later on (the two-stage release). (World Health Organization, 2003, Poli et al., 2014)

In the research project for this thesis, GMP-grade and nonGMP-grade ^{68}Ga -labeled DOTA-Siglec-9 peptide and nonGMP-grade 3'- ^{68}Ga]Ga-NOTA-anti-microRNA-21 were produced and their QC was carried out using radio-HPLC and/or radio-TLC. *In vitro* stability and plasma protein binding of these potential PET tracers were determined using radio-HPLC. In addition, the *in vivo* stability and bone accumulation of ^{68}Ga -labeled oligoribonucleotide were determined using PET and biodistribution measurements with gamma counter. The research project consists of three subprojects in which radiolabeling protocols for GMP-grade ^{68}Ga]Ga-DOTA-Siglec-9 and nonGMP-grade 3'- ^{68}Ga]Ga-NOTA-anti-microRNA-21 are being developed and the feasibility of these tracers as PET tracers is studied with animal experiments.

2 Review of the Literature

2.1 Radiochemistry

Over one hundred years ago Henri Becquerel discovered the phenomenon of radioactivity (Myasoedov, 2000). The radiotracer technique developed by George (György) de Hevesy in 1924 is the basis of nuclear medicine. The principle of the technique is that changing an atom in a molecule for its radioisotope will not significantly change its biological and chemical behavior, while the distribution, movement and concentration of the molecule and its derivatives can be followed by measuring its radiation. Also, processes in a live animal or human can be studied using external radiation detectors. Modern devices allow for the detection of so small amounts (in terms of molarity) of the tracer that the function of the studied organ is not affected. (Varga, 2012)

Radiochemistry is the science that encompasses the production, separation and purification of radionuclides. In addition, it includes the synthesis of radiolabeled compounds for biological or biochemical research. Radiochemical reactions are performed using very small amounts of the radionuclides. Accordingly, there are practical considerations, such as the risk of having a significant proportion of a radionuclide sample adsorbed onto the reaction glassware. The successful application of radiochemical techniques requires careful attention to all details and plenty of practice. Nowadays, novel applications within medicine and biology for the purposes of diagnostics, study of biomechanical processes, environmental science, and element speciation and migration are being increasingly discovered. (Myasoedov, 2000, Ebenhan et al., 2017)

2.1.1 Radioisotopes of gallium

Gallium (Ga) has two natural stable isotopes, namely ^{69}Ga (60%) and ^{71}Ga (40%). Gamma camera imaging to image lymphoma using the longest-lived radioisotope of Ga, gallium-67 (^{67}Ga , $t_{1/2} = 78$ hours), has been employed regularly in the clinic since the 1980s. Besides of its gamma emissions for single photon emission computed tomography (SPECT) imaging and scintigraphy, ^{67}Ga also emits Auger electrons. Thus, it has potential as a therapeutic radionuclide. Two isotopes,

gallium-66 (^{66}Ga , $t_{1/2} = 9.5$ hours) and ^{68}Ga ($t_{1/2} = 68$ minutes), are suitable for PET imaging. ^{68}Ga ($Q^+ = 2.92$ MeV; $E_{\text{max}} = 1.89$ MeV) decays to 88.91% by positron emission and to 11.09% via electron capture into stable zinc-68 (^{68}Zn). The average positron energy per disintegration is 829.5 keV. (Banerjee and Pomper, 2013, bin Othman et al., 2017, Boschi and Lodi, 2017, Ebenhan et al., 2017, Tsionou et al., 2017)

The physical half-life of ^{68}Ga is compatible with the pharmacokinetics of many PET radiopharmaceuticals of low molecular weight, such as peptides, oligonucleotides, antibody fragments and aptamers (Boschi and Lodi, 2017). ^{68}Ga has demonstrated its feasibility for the radiolabeling of biological macromolecules, small compounds and micro- and nano-particles (Velikyan, 2011). The major application domain is oncology. Potential has been demonstrated for imaging of inflammation and infection as well as lung ventilation, pulmonary perfusion and myocardial perfusion. Imaging of general biologic properties and processes, such as angiogenesis, apoptosis, glycolysis, hypoxia and proliferation, has also been investigated. (Velikyan, 2011, Velikyan, 2014)

Ga can form four-, five- and six-coordinated complexes. Six-coordinated complexes are the most stable with an octahedral coordination sphere. Ga is suitable for complexation with polydentate ligands, both cyclic and open chain structures. The majority of ligands designed for Ga are hexadentate. The Ga^{3+} ion is classified as a hard Lewis acid, forming thermodynamically stable complexes with ligands that are hard Lewis bases containing oxygen, nitrogen and sulfur donor atoms, such as carboxylate, phosphonate, amine and hydroxamate. Softer functional groups, such as phenolate and thiol groups, have also been found to be appropriate. The ligand is called a bifunctional chelator (BFC) if it binds the metal cation and also presents a functionality, often an amino group or a carboxyl group, that allows covalent coupling to a targeting vector. The principal requirements are that ligands should form stable complexes with Ga preferably of octahedral geometry in order to yield stable complexes. (Maecke and André, 2007, Velikyan, 2011, Velikyan, 2014, Boschi and Lodi, 2017)

^{11}C is bound covalently within the vehicle molecule. ^{18}F is also attached covalently to the parent molecule but it has to be added to the original structure.

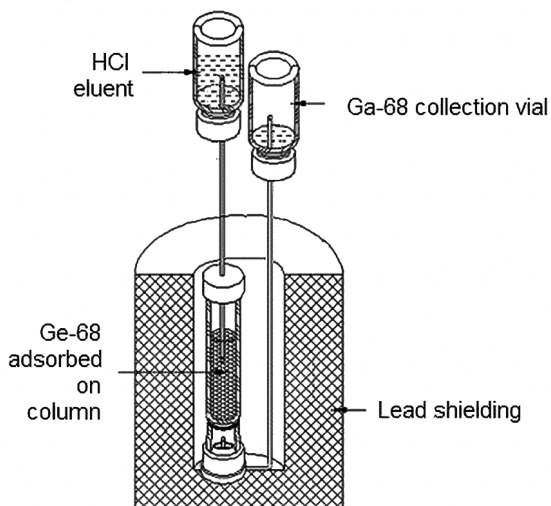


Figure 1. A schematic view of a $^{68}\text{Ge}/^{68}\text{Ga}$ generator. (Costello et al., 2015)

^{68}Ga and other radiometals can only be fixed to the vehicle by using a metal-ligand-complex. Metal-ligand interactions within a complex are usually much weaker than a covalent binding. Metal-ligand-complex leads to significant changes in the electrical and steric configuration. It also changes the pharmacodynamics and pharmacokinetics of the radiopharmaceutical. (Wadsak and Mitterhauser, 2010)

2.1.2 $^{68}\text{Ge}/^{68}\text{Ga}$ generators and cyclotrons

Radionuclide ^{68}Ga can be produced using a cyclotron (Pandey et al., 2014, Alves et al., 2017, Riga et al., 2018) or a cost-effective $^{68}\text{Ge}/^{68}\text{Ga}$ generator, which is simple in use. Pandey and co-workers have developed an automated system for the separation of ^{68}Ga from ^{68}Zn nitrate ($^{68}\text{Zn}(\text{NO}_3)_2$). They performed 30-minutes irradiations with 1.7 molar (M) solutions of $^{68}\text{Zn}(\text{NO}_3)_2$ (99.23% isotopic enrichment) in 0.2 normal (N) nitric acid (HNO_3). They concluded that the enhanced heat transfer allowed irradiation as a closed system. They also pointed out that ^{68}Ga can be produced on a low energy cyclotron in sufficient quantities to provide an alternative to $^{68}\text{Ge}/^{68}\text{Ga}$ generators. Riga and co-workers also showed that $^{68}\text{Zn}(p,n)^{68}\text{Ga}$ nuclear reaction is feasible for the production of ^{68}Ga using medicinal cyclotron. This is an economical alternative to $^{68}\text{Ge}/^{68}\text{Ga}$ generators. It has been proved that the quality of cyclotron-produced ^{68}Ga is equal or even better when compared with the generator-produced ^{68}Ga . (Pandey et al., 2014, Lin et al., 2018, Riga et al., 2018)

Current $^{68}\text{Ge}/^{68}\text{Ga}$ generators can nominally deliver up to 1.85 GBq (50 mCi) of ^{68}Ga per elution. However, ^{68}Ga activity decreases over time due to the decay of the parent nuclide germanium-68 (^{68}Ge). It decays spontaneously with a half-life of 271 days by electron capture. Unfortunately, elution efficiencies around 80% of

present activity are typical. Thus, cyclotrons show potential for large scale production of ^{68}Ga -radiolabeled tracers. (Lin et al., 2018)

Radionuclide generators have the advantage of providing radionuclides on demand. The parent nuclide of ^{68}Ga is ^{68}Ge , which is produced with an accelerator on a gallium oxide target. ^{68}Ge is adsorbed on a stationary material inside the generator (Figure 1.). For GMP use, this enables a shelf-life of the generator of up to a year. Generators provide on-site access to a GMP-grade diagnostic PET radionuclide without the need for cyclotron facilities. (Maecke and André, 2007, Fani et al., 2008, Ebenhan et al., 2017, Tsionou et al., 2017)

From the historical point of view, the availability of ^{68}Ga as a PET radionuclide goes back to the time when ^{18}F -tracers were not yet established. The first $^{68}\text{Ge}/^{68}\text{Ga}$ generator, the so-called positron cow, was developed in 1960. The separation of ^{68}Ge was accomplished by distillation of volatile germanium tetrachloride, the distillate was extracted with carbon tetrachloride and the activity returned to an aqueous phase. Separation of the radionuclides was done utilizing anion-exchange procedures. Acetylacetone was used to extract the carrier-free activity from the acid solution of ^{68}Ge . It was observed that it is possible to return the product to an aqueous phase of 0.1 M hydrochloric acid (HCl). Finally, the injectable preparation was made. (Gleason, 1960, Ebenhan et al., 2017)

An improved generator version was introduced in 1961. It employed an aluminium oxide (Al_2O_3)-based column matrix. ^{68}Ga was eluted with a sodium ethylenediamine-*N,N,N',N'*-tetraacetic acid (Na-EDTA) solution. The next generation of generators was launched in 1974. This made it possible that ^{68}Ga could be eluted directly in an ionic form. The new generator type also set the design of today's commercially available generators. Despite growing clinical use, especially in Europe, the first commercial generator has received marketing authorization as recently as 2014. (Greene and Tucker, 1961, Kopecký and Mudrová, 1974, Blower, 2016, Ebenhan et al., 2017)

Due to the long half-life of ^{68}Ge , a good separation system of mother and daughter nuclides is mandatory to avoid breakthrough (Maecke and André, 2007, Fani et al., 2008). The current generators are modified on metal oxides, such as titanium dioxide (TiO_2), tin dioxide (SnO_2) and Al_2O_3 . In addition, inorganic supports (silica-based) and organic polymer resins are used. Macroporous organic polymer based on *N*-methylglucamine has shown to be suitable as an organic matrix (Nakayama et al., 2002). Pyrogallol-formaldehyde polymer resins allow for the elution of ^{68}Ga as tetrachlorogallate anion ($^{68}\text{GaCl}_4^-$) with 5.5 M HCl followed by purification from low levels breakthrough ^{68}Ge and concentration by adsorption on a small Dowex anion-exchange column as $^{68}\text{GaCl}_4^-$. It is then eluted with water to afford a concentrated solution of $^{68}\text{Ga}^{3+}$ in 0.5 M HCl. This type of a

generator shows a very low breakthrough. (Schuhmacher and Maier-Borst, 1981, Zhernosekov et al., 2007, Ebenhan et al., 2017)

Inorganic matrices were the first to be used for efficient separation. Inorganic ion-exchangers have a high radiolytic stability (Pillay, 1986). Al_2O_3 or zirconium dioxide (ZrO_2) was used and ^{68}Ga was eluted as $[\text{}^{68}\text{Ga}]\text{Ga-EDTA-complex}$, which must be destroyed before the radionuclide can be incorporated into the required PET radiopharmaceutical. This made every synthesis of a radiopharmaceutical tedious and time-consuming. After replacing Al_2O_3 by antimony pentoxide and EDTA by sodium oxalate solution, the elution yield was more stable (Arino et al., 1978). To make the process simpler, attempts were focused on the development of generators that provide $^{68}\text{Ga}^{3+}$ free from any complexing agent. Several systems were proposed, such as Al_2O_3 , ferric hydroxide, HCl, HNO_3 , silicon dioxide and ZrO_2 (Kopecký and Mudrová, 1974, Neirinckx and Davis, 1979). A new type of $^{68}\text{Ge}/^{68}\text{Ga}$ generators based on HCl elution provides ionic $^{68}\text{Ga}^{3+}$ instead of $^{68}\text{Ga-complexes}$. These became commercially available in the early 2000s (Razbash et al., 2005). This development has offered new opportunities for PET radiopharmaceutical chemistry based on trivalent metals. (Greene and Tucker, 1961, Maecke and André, 2007, Fani et al., 2008, Rösch, 2013, Ebenhan et al., 2017)

Nowadays, a commonly used commercially available $^{68}\text{Ge}/^{68}\text{Ga}$ generator is based on a TiO_2 -solid support. ^{68}Ga can be conveniently eluted with up to 10 mL diluted HCl as soluble $^{68}\text{Ga}^{3+}$. SnO_2 is another common column packing material in modern $^{68}\text{Ge}/^{68}\text{Ga}$ generators. ^{68}Ga is eluted as $^{68}\text{Ga}^{3+}$ with HCl while ^{68}Ge , form $^{68}\text{Ge}^{4+}$, remains adsorbed. For fresh generators, ^{68}Ga -eluate yield ranges from 70% to 80%. ^{68}Ge -breakthrough is at levels of about 0.01–0.001%, or even better for fresh generators, increasing over longer periods of generator usage. (Rösch, 2013, Ebenhan et al., 2017)

Nano-zirconia has been studied as a sorbent for the preparation of the $^{68}\text{Ge}/^{68}\text{Ga}$ generator. The results have proved that a major advantage of this kind of a generator is its consistency, which is superior to that of the SnO_2 - and TiO_2 -based $^{68}\text{Ge}/^{68}\text{Ga}$ generators. The major benefits of the nano-zirconia sorbent are proposed to be, for example, its rigidity, which allows the use of high flow rates, and the chemical and radiation stability of the sorbent matrix. The results have also shown that the obtained ^{68}Ga is suitable for preparation of ^{68}Ga -labeled PET radiopharmaceuticals with high labeling yield. These generators are suggested feasible as an option for use in institutions where commercial sources of PET radioisotopes are not readily available. (Chakravarty et al., 2011)

2.2 ^{68}Ga -labeled PET radiopharmaceuticals and their development

The most widely utilized ^{68}Ga -labeled PET radiopharmaceuticals consist of ^{68}Ga coordinated to a chelator that is attached to a peptide, or other molecules, for targeting cell surface receptors of tumors (Tsionou et al., 2017). The kinetic and thermodynamic stability, geometry and lipophilicity of a chelator-metal ion complex are important parameters in the development of radiometal-based PET radiopharmaceuticals. These design principles are valid for the ^{68}Ga -labeling of biological macromolecules, small biologically active organic molecules, and complexes of variable charge, lipophilicity and particles. This means that the chemistry considered in the development of ^{68}Ga -based imaging agents has several cornerstones, including the coordination chemistry and aqueous chemistry of ^{68}Ga , bioconjugate chemistry and design of mono-chelators and BFCs. Nowadays, the biodistribution of ^{68}Ga imaging agents is defined by the vector molecule, and ^{68}Ga may or may not influence biodistribution or affinity to the target. (Velikyan, 2014)

Efficient and quantitative radiolabeling allowing the preparation of PET radiopharmaceuticals without the need of additional purification further simplifies translation of new tracers into clinical practice. Another critical step for clinical translation is the selection of the BFC to adjust the polarity and charge of the overall conjugate as a means to optimize the route of clearance and the pharmacokinetics. For example, the blood clearance of a PET radiopharmaceutical should be sufficiently long to facilitate optimal delivery to the target site but also short enough to avoid unnecessary radiation exposure. For the design of BFCs of high *in vivo* stability, efficient radiolabeling kinetics and favorable pharmacokinetics, a thorough understanding of the coordination chemistry of the radiometal of interest is thus essential. (Bartholomä, 2012)

Great advances in automation technology for ^{68}Ga -radiochemistry and radiopharmacy have been achieved lately. Different automation strategies are now available and they can also be tailored to different needs. Automation technologies have implemented different pre-purification approaches which has led to increased radionuclidic and chemical purity as well as high molar activity of the final preparation. The use of automated systems has many advantages like easier handling, improved reproducibility, higher throughput, improved response to clinical demand, and production in compliance with current Good manufacturing practice (cGMP). (Boschi et al., 2013)

Pre-loaded cassette-based modules, manufactured under cGMP standards, have already represented an improvement in terms of safety and compliance with regulations. In the future, microfluidic approaches could open interesting perspectives. Major concerns include radiolysis due to the high concentration of radionuclide and surface effects. It has been proposed that development of ^{68}Ga -

radiopharmaceuticals as freeze-dried kits may be an alternative to cyclotron-based PET radiopharmaceuticals. (Boschi et al., 2013)

2.2.1 Bifunctional chelators

The biological fate of PET radiopharmaceuticals is determined by the BFC-metal complex, the biological properties of the targeting vector and the tether. The choice of BFC is determined by the nature and oxidation state of the metallic radionuclide. It has been shown that the nature of a BFC-metal complex (lipophilicity, geometry and overall charge) plays a crucial role in determining the biodistribution of targeted PET radiopharmaceuticals. Chelators of high lipophilicity are not very optimal because of their increased uptake in non-target tissues, such as the liver. (Bartholomä, 2012)

The BFC should chelate the radiometal, such as copper, gallium, indium, yttrium or zirconium, rapidly and sufficiently when linked to a macromolecule. The chelator should be kinetically stable to demetallation over a pH range of 4–8 and stable in the presence of other serum cations (calcium ion, magnesium ion, Zn^{2+}). The BFC should be characterized by high radiolabeling efficiency to yield PET radiopharmaceuticals of high molar activity. The receptor population in the diseased organ or tissues is often limited in numbers and low molar activity may result in blockage of the receptor by the unlabeled bioconjugate and impact the efficacy of radiotherapeutics or the image quality. The main objective in the design of metal-based PET radiopharmaceuticals is to select an efficient bifunctional chelating system that forms the radiometal chelator with kinetic inertness and very high thermodynamic stability. This way it is possible to retain the label on the targeting vector and to minimize accumulation of the radiometal in non-target tissues. In addition, it is possible to optimize image contrast and minimize the radiation burden to patients, which is of particular importance for radiotherapeutic applications. (Bartholomä, 2012, Boschi and Lodi, 2017)

The use of radiometals for the labeling of biomolecules generally requires the use of BFCs. The BFC is covalently attached to the targeting biomolecule either directly or through a linker. These chelators bind the metal at one terminus and contain a functional group for the covalent linkage to a targeting vector at the second terminus. In an optimal situation, the BFC is able to form a stable radiometal chelator with high thermodynamic stability and kinetic inertness. The optimal BFC should ideally fulfill several requirements. One requirement is stability, meaning that the BFC should form kinetically inert and thermodynamically stable complexes to prevent hydrolysis or any ligand exchange reactions *in vivo*. A second requirement is rapid complexation kinetics meaning that radiolabeling of the BFC should be efficient and rapid at low temperatures and

low concentration at a pH that is suitable for biological targeting vectors. A third requirement is that the BFC should selectively bind the radiometal of interest because it is important to avoid low molar activity during radiolabeling. Low molar activity might be observed due to the presence of other trace metals (decay products). A fourth requirement is that BFCs should have versatile conjugation chemistry. This means flexibility in the conjugation of the BFC to functional groups of targeting vectors. Flexibility allows optimization of pharmacokinetics by adjusting the polarity of the overall conjugate. A fifth requirement is accessibility, meaning that the preparation of the BFC should be quick, straightforward and cost-effective. The preparation of BFC should be scalable to the preparation of multigram quantities of product with only few reaction steps. (Yang et al., 2008, Bartholomä, 2012)

The two most important parameters of a BFC that influence the *in vivo* properties of PET radiopharmaceuticals are the overall charge and the lipophilicity of the corresponding BFC-metal complex. The success of a BFC is not guaranteed even when all of the abovementioned requirements are completely fulfilled. This is due to the fact that the nature of a BFC can have a profound impact on the pharmacokinetics of a PET radiopharmaceutical such as receptor binding and clearance from non-target tissues. (Bartholomä, 2012)

The main requirement for a ^{68}Ga -BFC is the kinetic inertness towards transferrin (the blood serum protein transporting iron) and higher thermodynamic stability than that of the ^{68}Ga -transferrin complex to avoid any premature ligand exchange *in vivo* during the course of the clinical application. Chelators that quantitatively coordinate ^{68}Ga at room temperature (r.t.), near neutral pH and low concentrations of chelator-bioconjugate will facilitate one-step, kit-based radiolabeling protocols. Such chelators would also be useful for radiolabeling of small proteins. However, they are susceptible to degradation or unfolding at extremes of pH and temperature. BFCs generally fall into one of two broad categories: macrocyclic or acyclic chelators. (Bartholomä, 2012, Charron et al., 2016, Tsionou et al., 2017)

2.2.1.1 Macrocyclic chelators

Macrocyclic chelators are rigid chemical structures designed to ensure that the donor atoms are in the optimal location for metal chelation. Macrocyclic ligands are the most widely used chelator type for ^{68}Ga . This is due to the generally simple synthesis from inexpensive starting materials. In addition, they are also very broadly used for PET metal-ion chelation, as well as components of single SPECT radiopharmaceuticals and magnetic resonance imaging (MRI) contrast agents. (Burke et al., 2014, Charron et al., 2016)

The focus in this area is on the development of novel chelators to overcome the problem related to the high temperature routinely needed for macrocyclic ^{68}Ga -complex formation, which is not suitable for many biomolecules. In recent years, the design of BFCs in general and for ^{68}Ga -chelators, in particular, has mainly focused on ligands based on polyaza-macrocycles, such as 1,4,7,10-tetraazacyclododecane (cyclen) and 1,4,7-triazacyclononane (TACN). This is because of the higher kinetic inertness of macrocycles, as compared with acyclic ligands, due to the macrocyclic effect that minimizes transchelation or loss of metal *in vivo*, which is favorable for PET radiopharmaceutical applications. (Bartholomä, 2012, Burke et al., 2014)

2.2.1.1.1 Examples of macrocyclic chelators

Several multidentate cyclen and TACN derivatives with additional donor groups have been developed to saturate all coordination sites on the six-coordinate Ga^{3+} . The most prominent representative of this category is the aminocarboxylate macrocycle ligand DOTA (Figure 2.). DOTA chelator is the current “gold standard” bifunctional ^{68}Ga -chelator (Berry et al., 2011). The metal center in the ^{68}Ga]Ga-DOTA complex is encapsulated by a N_4O_2 donor set of the cyclen moiety and two carboxylate groups in a *cis*-pseudooctahedral fashion according to the crystal structures of ^{68}Ga]Ga-DOTA and ^{68}Ga]Ga-DOTA-D-PheNH₂ (Heppeler et al., 1999, Viola et al., 2006). The third carboxylic acid group is deprotonated and does not coordinate to the metal. The fourth carboxylic acid function is either conjugated to the amino acid via the amide in ^{68}Ga]Ga-DOTA-D-PheNH₂ or is not involved in metal coordination in ^{68}Ga]Ga-DOTA. (Heppeler et al., 1999, Viola et al., 2006, Bartholomä, 2012)

DOTA has proven to be a very suitable chelator for a number of trivalent metal cations. It can be attached to various somatostatin analogues, such as [Tyr³]-octreotide (TOC), [Tyr³]-octreotate (TATE), [NaI³]-octreotide (NOC), lanreotide (LAN) and other peptides, without loss of receptor specificity or binding affinity. However, DOTA has several drawbacks as a ^{68}Ga chelator (Berry et al., 2011). Due to the kinetic inertness of the macrocycle, the kinetics of complex formation of DOTA is slow (Bartholomä, 2012). Several chelators have been evaluated and developed for ^{68}Ga -labeling of biomolecules to avoid the limitations of DOTA. (Meyer et al., 2004, Petrik et al., 2011, Tsionou et al., 2017)

TACN-based chelators, such as 1,4,7-triazacyclononane-1,4,7-triacetic acid (NOTA), (Figure 2.) show favorable characteristics for ^{68}Ga -radiolabeling. NOTA has proven interesting because of its fast and high *in vivo* stability and reaction kinetics, efficient radiolabeling at r.t. and high selectivity towards ^{68}Ga due to cavity size. Ga^{3+} forms thermodynamically less stable complexes with DOTA-like

than with NOTA-like chelators (Clarke and Martell, 1991, Kubíček et al., 2010). This is a consequence of the excellent fit of the small Ga^{3+} into the cavity of the nine-membered triazamacrocycle of NOTA. Among the macrocyclic chelators, the triazacyclononanes display high conformational and size selectivity towards ^{68}Ga due to the smaller dimensions of the corresponding cavity in comparison with DOTA. (Velikyán et al., 2008, Bartholomä, 2012, Burke et al., 2014)

A macrocyclic chelator, 6,6',6''-(1,4,7-triazonane-1,4,7-triyl)tris(methylene)tris(5-hydroxy-2 (hydroxymethyl)-4Hpyran-4-one) (H_3NOKA) (Figure 2.) with pendant 3-hydroxy-4-pyrone arms, is also based on TACN. Solution and solid state analyses have revealed that this chelator acts as a hexadentate ligand with all six donors (three amine-N atoms and three enolate-O atoms) bonding to the metal center. It has been suggested that NOKA-derivatives might be useful as bifunctional chelators for ^{68}Ga -labeling of small biomolecules. (Yang et al., 2008)

Three triazacyclononane phosphinic acid (TRAP) (Figure 2.) ligands bearing methylphosphinic (TRAP-H), methyl(phenyl)phosphinic (TRAP-Ph) or methyl-(hydroxymethyl)phosphinic acid (TRAP-OH) pendant arms have been investigated as members of a new family of efficient ^{68}Ga -chelators. All of them are TACN-derivatives. The results have proved that all these are suitable alternatives for the development of ^{68}Ga -radiopharmaceuticals. As compared with common DOTA-derivatives, they show fast complexation of $^{68}\text{Ga}^{3+}$ over a broad pH range. All these complexes are kinetically inert in both acidic and alkaline solutions. Complex formation studies in acidic solutions indicate that ^{68}Ga -complexes of the phosphinate ligands are formed quantitatively and quickly, in minutes, even at pH below 2. (Šimeček et al., 2012, Notni et al., 2014)

Several derivatives of NOTA (Figure 2.) have been developed and investigated. Among these are examples of hexadentate ligands 1,4,7-triazacyclononane-1-succinic acid-4,7-deacetic acid (NODASA) (Andre et al., 1998), 1,4,7-triazacyclononane- N,N,N' -tris(methylenephosphonic) acid (NOTP), which is a phosphonate analog of NOTA (Prata et al., 2000, Fellner et al., 2011), 1,4,7-triazacyclononane- N,N,N' -tris(methylenephosphonate-monoethylester) (NOTPME) (Prata et al., 1999) and 1,4,7-tris(2 mercaptoethyl)-1,4,7-triazacyclononane (TACN-TM) (Ma et al., 1995). All these have demonstrated octahedral coordination geometry, high thermodynamic stability and identical plasma and *in vivo* stability. (Velikyán et al., 2008)

One example of the bifunctional modifications of NOTA is a macrocyclic chelator 1,4,7-triazacyclononane,1-glutaric acid-4,7-acetic acid (NODAGA) (Figure 2.). NODAGA has three carboxyl groups for coordination with ^{68}Ga after conjugation with peptide. It is known to form highly stable complexes with ^{68}Ga . Higher target to background ratios have been reported with NODAGA-derivatized

peptides in direct comparison with their DOTA counterparts, which is related to lower plasma protein binding of the ^{68}Ga -labeled peptide. (Fani et al., 2008, Decristoforo et al., 2012, Satpati et al., 2018)

Other bifunctional NOTA-derivatives include 1,4,7-triazacyclononane-1,4-diacetic acid-7-*p*-hydroxyphenyl-acetic acid (NODAPA-OH), 1,4,7-triazacyclononane-1,4-diacetic acid-7-*p*-isothio-cyanatophenyl-acetic acid (NODAPA-NCS) (Figure 2.) and 1,4,7-triazacyclononane-1-acetic acid-4,7-di-*p*-isothiocyanatophenyl-acetic acid (NODAPA-(NCS)₂) (Riss et al., 2008). All these derivatives show comparable radiolabeling efficiency comparable to that of NOTA. It has been reported that, at pH 2.8, up to 85% of these derivatives are radiolabeled within three minutes, at 45°C for NODAPA-OH and at 75°C for NODAPA-(NCS)_n (n = 1–2). The stability of the corresponding ^{68}Ga -complexes is in a similar range as that of the congener NOTA. (Bartholomä, 2012)

2.2.1.2 Acyclic chelators

The macrocyclic effect generally results in kinetically more inert and thermodynamically more stable metal complexes of macrocyclic chelators in comparison with the acyclic ones. Thus, BFCs based on macrocycles are more attractive for radiopharmaceutical applications. However, a number of acyclic chelators have been described that perform quite successfully *in vivo*. A significant advantage of acyclic chelators, especially in the case of shorter-lived radiometals such as ^{68}Ga , is the faster metal binding kinetics as compared with macrocyclic complexes of corresponding stability, thus resulting in faster radiolabeling. (Bartholomä, 2012, Charron et al., 2016)

Acyclic chelators undergo a conformational change to effectively place the donor atoms in the ideal geometry for chelation. Acyclic chelators for ^{68}Ga offer great potential due to the fast kinetics involved in the complex formation. Recent work in the area has focused on the design of novel chelators, which retain the kinetic advantages whilst addressing the issue of low *in vivo* stability. (Burke et al., 2014, Charron et al., 2016)

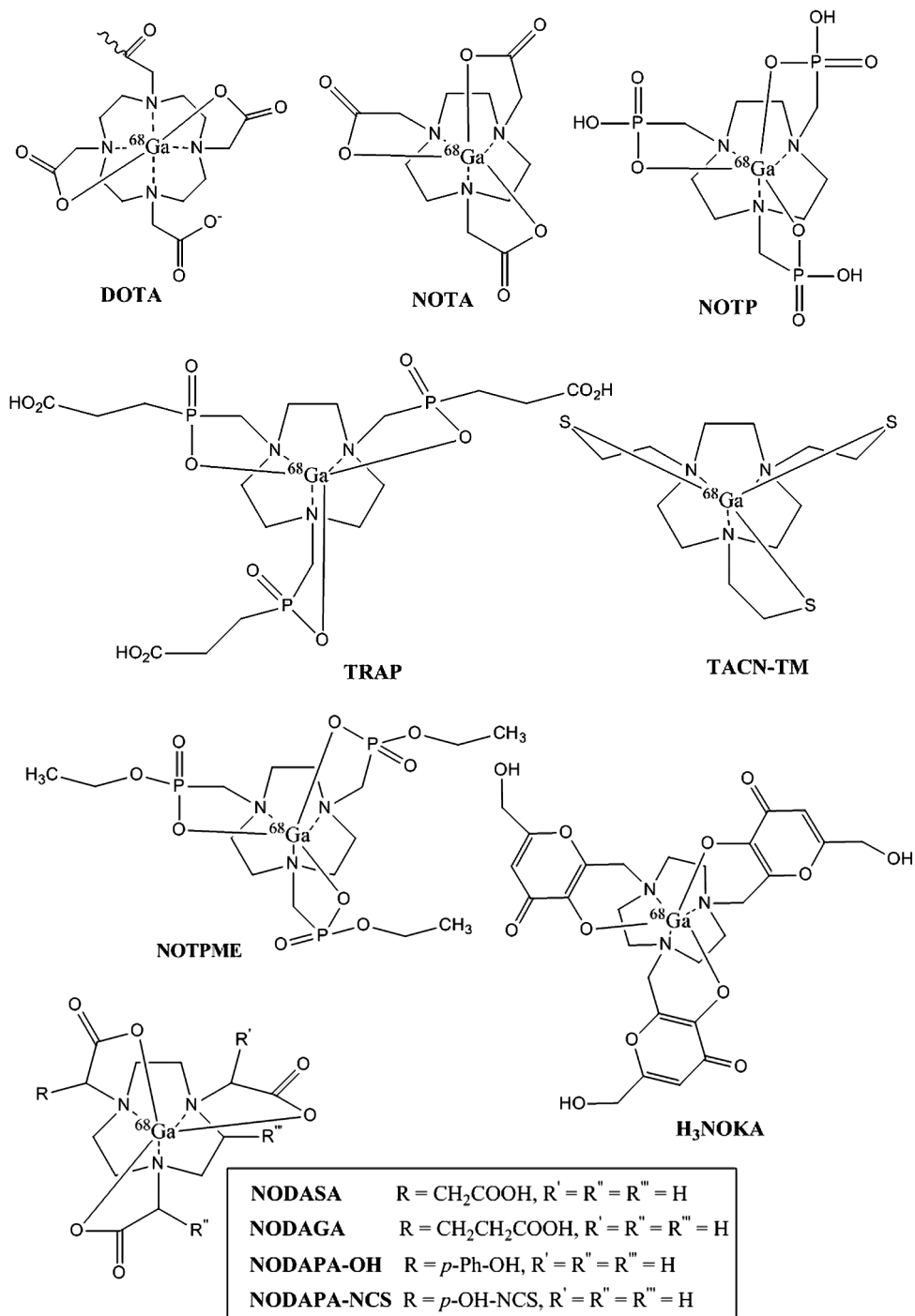


Figure 2. Examples of ^{68}Ga -chelated macrocyclic chelators.

2.2.1.2.1 Examples of acyclic chelators

The acyclic ligand *N,N'*-bis(2-hydroxybenzyl)ethylenediamine-*N,N'*-diacetic acid (HBED) (Figure 3.) is based on an EDTA-type framework with two pendant phenol arms. It has received attention for the design of BFCs for PET radiopharmaceutical applications. The acyclic bifunctional ligand *N,N'*-bis[2-hydroxy-5(carboxyethyl)benzyl]ethylenediamine-*N,N'*-diacetic acid (HBED-CC) (Figure 3.) is characterized by efficient and rapid radiolabeling at r.t. and high *in vivo* stability. It has been employed for ^{68}Ga -labeling of thermo-sensitive biomolecules (Eder *et al.* 2008).

Deferoxamine (DFO) (Figure 3.) forms ^{68}Ga -complexes of high thermodynamic stability. Its usefulness as a BFC for ^{68}Ga -radioisotopes has been proved in combination with peptides and small molecules. It has been observed that the labeling of DFO with $^{68}\text{Ga}^{3+}$ is pH dependent. [^{68}Ga]Ga-DFO-folate has been prepared with high radiochemical purity (RCP) (Mathias *et al.* 2003). DFO-octreotide has also been ^{68}Ga -labeled successfully. However, [^{68}Ga]Ga-DFO-octreotide suffers considerable radiation damage when left in the labeling buffer for prolonged periods of time (Smith-Jones *et al.* 1994, Bartholomä 2012).

Hexadentate tris(3,4-hydroxypyridinone) (THP) (Figure 3.) chelators have high affinity for oxophilic trivalent metal ions. This has led to their development for new applications as BFCs for ^{68}Ga . It has been proved that the THP-peptide bioconjugates complex ^{68}Ga quantitatively and rapidly at ambient temperature, neutral pH and micromolar concentrations of ligand. ^{68}Ga -labeled THP-peptides accumulate at target tissue *in vivo* and are excreted largely via a renal pathway providing thus high quality PET-images. It has been concluded that THP-chelators can be used for simple, efficient labeling of ^{68}Ga -biomolecules under mild conditions suitable for peptides and proteins (Ma *et al.* 2016, Cusnir *et al.* 2017).

The acyclic hexadentate chelator 6,60-(ethane-1,2 diylbis(azanediy)) bis(methylene)dipicolinic acid (H_2dedpa) (Figure 3.) and its bifunctional derivatives are one example of acyclic chelators. Several H_2dedpa derivatives, such as H_2dedpa -propyl_{pyr}-FITC, H_2dedpa -propyl_{pyr}-FITC-(*N,N'*-propyl-2-NI) and H_2dedpa -propyl_{pyr}-NH₂, have been prepared. All of these ligands possess strong ^{68}Ga coordinating atoms contained within dedpa^{2-} that are ideal for radiolabeling with $^{68}\text{Ga}^{3+}$ (Boros *et al.* 2010, Ramogida *et al.* 2016).

In the series of 3-hydroxy-4-pyridinone (HPO)-based ligands, a hexadentate HPO chelator, CP256 and its bifunctional version YM103 (Figure 4.), have shown remarkable labeling efficiency at r.t. Radiochemical yield (RCY) of 98–100% after a 5-minute reaction time has been achieved. ^{68}Ga -labeling succeeds also at low concentrations. The results indicate that the [^{68}Ga]Ga-CP256 complex is highly stable for an acyclic chelator (Berry *et al.* 2011, Bartholomä 2012, Burke *et al.* 2014).

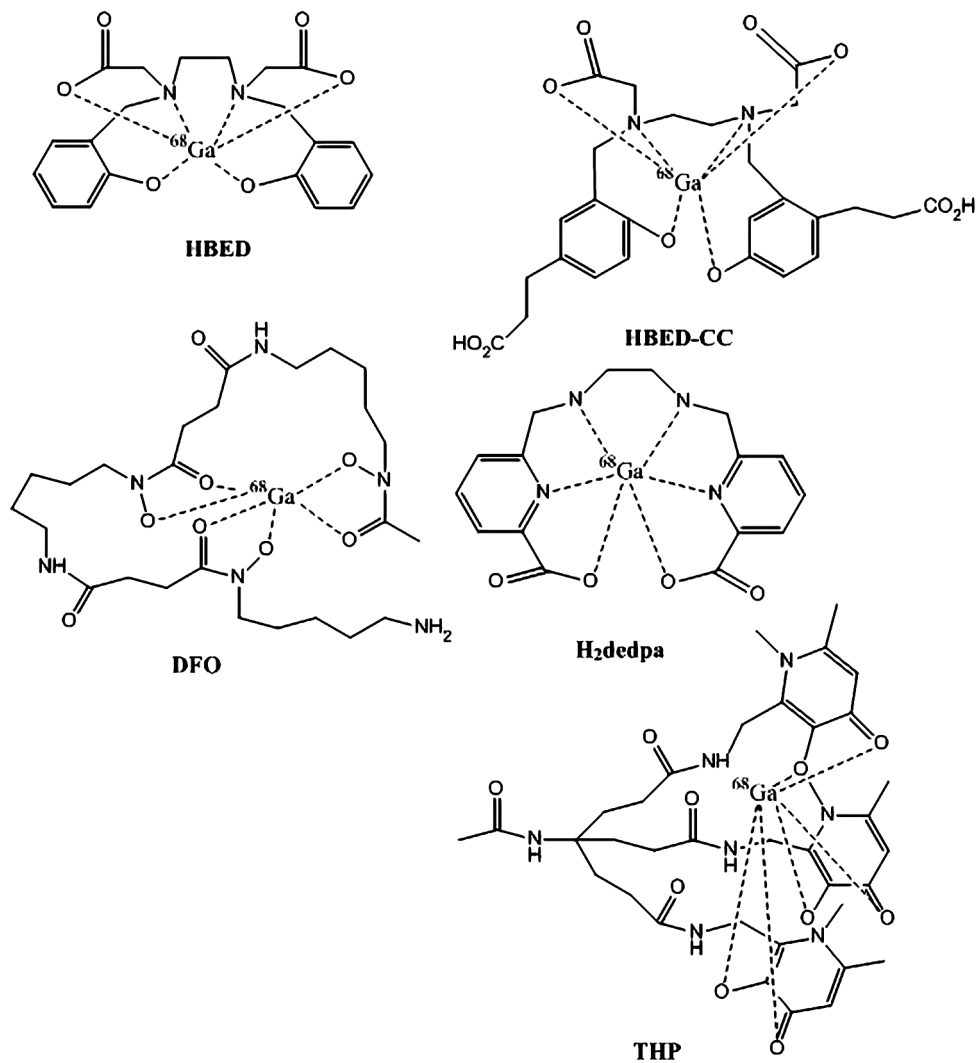


Figure 3. Examples of ^{68}Ga -chelated acyclic chelators.

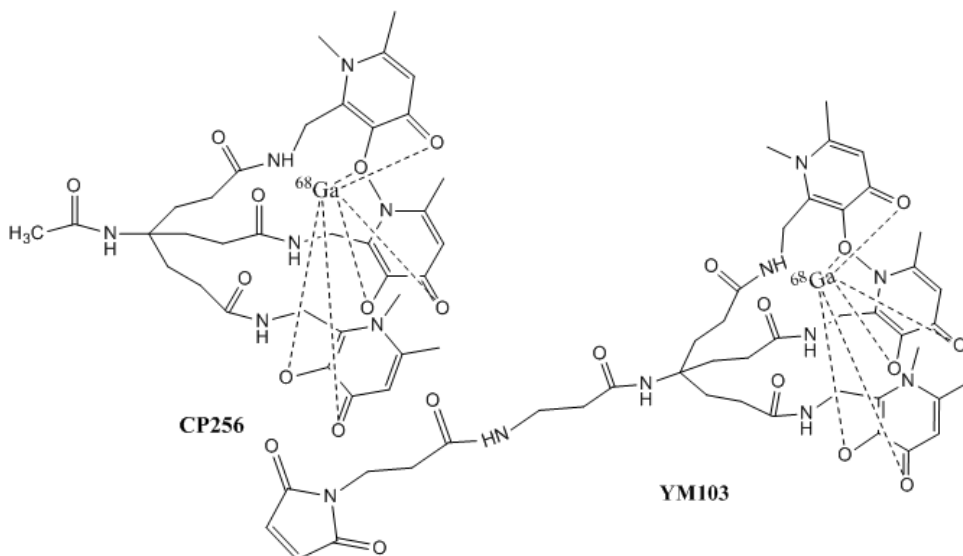


Figure 4. HPO-based ^{68}Ga -chelated ligands CP256 and YM103.

2.2.1.3 Intermediate between macrocyclic and acyclic chelators

6-Amino-1,4-diazepinetriacetic acid (DATA) chelators (Figure 5.) are a class of tri-anionic ligands. DATA chelators are intermediates between macrocyclic and acyclic chelators. They undergo quantitative radiolabeling more rapidly and under milder conditions as compared with macrocyclic chelators based on the cyclen scaffold like DOTA. Several DATA chelators (DATA^m , DATA^p , DATA^{Ph} and DATA^{PPh}) have been labeled with ^{68}Ga . Research has shown the extraordinary potential of this class of chelators for application in molecular imaging using ^{68}Ga -PET. It has been reported that the hexadentate DATA^m ligand and its bifunctional analogue DATA^{5m} rapidly form complexes with ^{68}Ga in high RCY. At pH 7.4 and at 25°C , the half-lives of the dissociation of $[\text{}^{68}\text{Ga}]\text{Ga-DATA}^m$ and $[\text{}^{68}\text{Ga}]\text{Ga-DATA}^{5m}$ are 11 hours and 44 hours, respectively. Based on equilibrium and kinetic data, it has been suggested that the $[\text{}^{68}\text{Ga}]\text{Ga-DATA}^{5m}$ complex is a good candidate as a ^{68}Ga -based radiodiagnostic agent. (Seemann et al., 2015, Farkas et al., 2017, Nock et al., 2017)

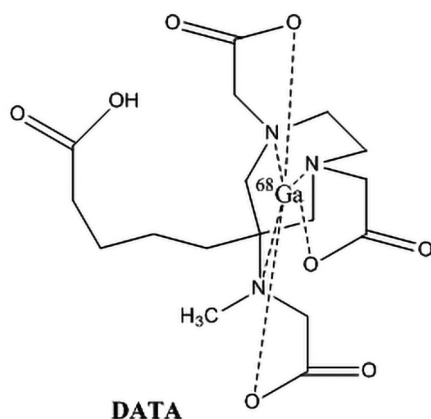


Figure 5. [^{68}Ga]Ga-DATA chelator.

2.2.2 Synthesis of ^{68}Ga -labeled PET radiopharmaceuticals

The RCY of a ^{68}Ga -radiolabeling reaction is influenced by several different parameters, such as radiolysis, concentration, temperature, reaction time, pH value, stoichiometry, metal contamination of the precursor and the targeting agent itself. Typical radiolabeling conditions entail heating. The high temperature and low pH are unsuitable for many proteins of interest for molecular imaging. The long radiolabeling time allows extensive decay during labeling. In addition, the presence of metal ion impurities can affect the labeling efficiency. The labeling procedure has to be optimized for each targeting agent. Optimization is also needed to meet the requirements of radiolabeled products, which are high RCP and radiochemical stability. (Meyer et al., 2004, Petrik et al., 2011, Chakravarty et al., 2013, Seemann et al., 2015, Gijs et al., 2016, Tsionou et al., 2017)

High molar activity of the final radiolabeled product is desired because high molar activity allows the administration of a minimal amount of unlabeled compounds. This might improve the signal-to-background ratios. Correspondingly, when administering lower doses of a PET radiopharmaceutical, simpler toxicology protocols and regulations can be applied. High molar activity can be obtained when the ^{68}Ga -eluate from $^{68}\text{Ge}/^{68}\text{Ga}$ generator is highly concentrated and free of metal contaminants, when radiolabeling yields are quantitative and when the final product needs no further post-labeling purification. (Gijs et al., 2016)

2.2.2.1 Elution of the $^{68}\text{Ge}/^{68}\text{Ga}$ generator and pre-purification of the eluate

The major limitations for the direct use of ^{68}Ga in the radiolabeling of peptides for clinical PET applications are ^{68}Ge breakthrough, potential metallic impurities, such as Zn^{2+} generated from the decay of ^{68}Ga , titanium(IV) (Ti^{4+}) or other potential impurities from the column material, as well as iron(III) (Fe^{3+}), large volumes of generator eluate and high proton concentration (Zhernosekov et al., 2007, Ocak et al., 2010). The relatively high concentration of HCl may protonate functional groups of ligands and bifunctional ligands needed for the labeling of ^{68}Ga . In principle, the long physical half-life of the parent ^{68}Ge should allow the use of a generator for, at least, one year. (Rösch, 2013)

Pre-purification of the eluate has several advantages especially for the radiolabeling of peptides. Pre-purification leads to the concentration of the eluate, which allows the use of all available activity for radiolabeling. It also ensures that accidental breakthrough of ^{68}Ge is eliminated before radiolabeling and facilitates the removal of potential metallic impurities competing with the radiolabeling procedure. Metallic impurities may be present in the eluate, which may adversely affect the ^{68}Ga yield as well as the molar activity of the labeled product. Several methods to purify the eluate from impurities have been developed. (Zhernosekov et al., 2007, Ocak et al., 2010, Boschi et al., 2013)

One option is to use strong anion-exchange (SAX) resins (Hofmann et al., 2001, Meyer et al., 2004, Velikyan et al., 2004) (Figure 6.). ^{68}Ga is adsorbed on the micro-column, and the column is washed with 5.5 M HCl and flushed with a stream of nitrogen. The purpose of nitrogen is to blow off most of the strong HCl. ^{68}Ga is eluted from the micro-column by using pure water. This leads to the decomposition of the tetrachloro-complex and release of ^{68}Ga as aqueous $^{68}\text{Ga}^{3+}$. In order to concentrate ^{68}Ga from generators eluted with 0.1 M HCl, the eluate is adjusted to a concentration of 5.5 M HCl by the addition of the required volume of 30% HCl. As a result, $^{68}\text{GaCl}_4^-$ is formed, and treated as described above. Both the pyrogallol/formaldehyde type and titanium dioxide-based generators have been tested successfully. It has been found that the concentration process will clean ^{68}Ga from any potential ^{68}Ge breakthrough. It does not provide sufficient purification of Ga^{3+} from, for example, Zn^{2+} and Fe^{3+} . These could interfere with the ^{68}Ga -labeling if present. (Meyer et al., 2004)

It has been found that the best agent for eluting ^{68}Ga from the small anionic cartridges is deionized water. Using the sodium acetate (NaOAc) solution directly as the eluting agent is not recommended because the recovery yield of ^{68}Ga is very poor. This is most likely due to the anionic Ga-acetate complex adsorbing to the resin. 50% Ethanol (EtOH) has been proposed as an alternative eluting agent. It has shown nearly the same recovery properties as pure water alone. The parent nuclide

^{68}Ge is not retained on the anion resin. This means that the concentration step can also be seen as a purification of ^{68}Ga from ^{68}Ge breakthrough. In the same way, the original generator eluate has been purified from Ti by 90%. With respect to the eluted ^{68}Ga activity, the ^{68}Ge breakthrough is 0.001–0.007%. (Velikyan et al., 2004)

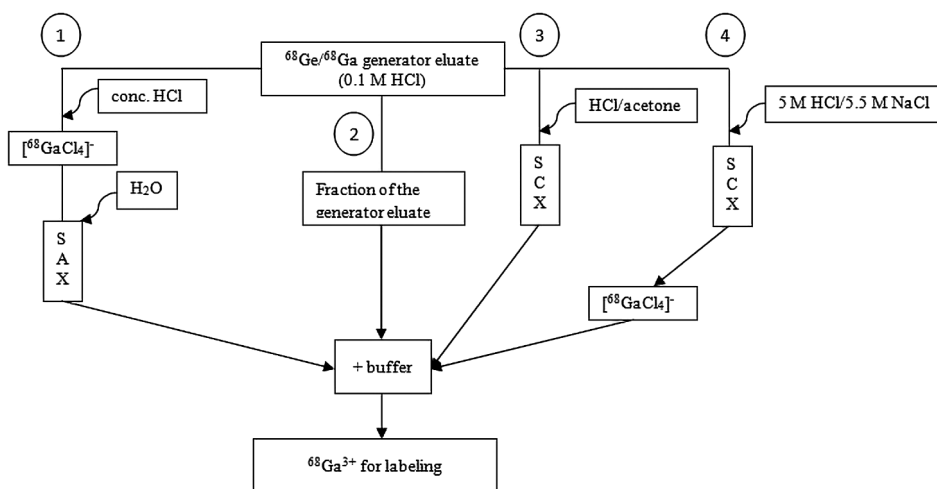


Figure 6. Schematic diagram of the $^{68}\text{Ge}/^{68}\text{Ga}$ generator eluate pre-purification methods. The $^{68}\text{Ge}/^{68}\text{Ga}$ generator is eluted using 0.1 M HCl. The eluate can be purified using (1) strong anion-exchange (SAX) resin, (2) fractionation, (3) strong cation-exchange (SCX) resin with 97.6% acetone/0.05 M HCl, or (4) SCX resin with NaCl/HCl. (Modified from Mueller et al., 2012)

Fractionation (Figure 6.) is one approach to overcome problems, such as content of ^{68}Ge and chemical impurities, acidic pH and eluate volume. The fractionated generator eluate has been used directly without any further purification step to achieve high molar activity of the radiolabeled peptide. Fractionation is based on the fact that about two-thirds of the total ^{68}Ga activity elute within an activity peak of $\sim 1\text{--}2$ mL. Because of the low eluate volume used, the contents of ^{68}Ge and metallic impurities are lower. However, they are not chemically removed before the ^{68}Ga -labeling steps. This approach only decreases the metallic impurities but does not eliminate them. (Breeman et al., 2005, Zhernosekov et al., 2007, Asti et al., 2008, Boschi et al., 2013)

An efficient and simplified method for the preparation of ^{68}Ga -labeled PET radiopharmaceuticals using a microchromatography column containing cation-exchange resins has also been reported (Figure 6.). Using this method, the eluted ^{68}Ga is purified from ^{68}Ge , Zn^{2+} , Ti^{4+} and even Fe^{3+} . It has been proved that the significant removal of almost the entire ^{68}Ge breakthrough on the SCX using the

97.6% acetone/0.05 M HCl systems fulfill the basic requirements relevant to the medical use of the radionuclide generator. The SCX resin represents a guarantee for avoiding the transfer of ^{68}Ge breakthrough to the labeling system or to the patient. In addition, this method extends the useful life of the $^{68}\text{Ge}/^{68}\text{Ga}$ generator systems. It has been proposed that the initial ^{68}Ge breakthrough of a newly installed generator may be acceptable but the breakthrough might increase as a consequence of frequent elutions. This limits the long-term or high-volume application of a generator. (Zhernosekov et al., 2007)

It has been demonstrated that the amount of $^{68}\text{Ge}^{4+}$ remaining in the free volume of the SCX column is further reduced by washing with the 80% acetone/HCl solutions. The final ^{68}Ga -fraction contains <0.01% of ^{68}Ge relative to the initial eluate. Zn^{2+} is quantitatively adsorbed (>99%) from the 0.1 M HCl eluate along with Ga^{3+} . It has been found that Zn^{2+} is desorbed by the 80% acetone/HCl purification step, whereas Ga^{3+} remains on the resin. Ti^{4+} is almost completely adsorbed on the SCX resin directly from the 0.1 M HCl solution. The remaining Ti^{4+} is eluted from the SCX resin almost completely in 4 M HCl. This allows the column to be cleaned. For Fe^{3+} , the best separation factors are provided at an HCl concentration of 0.1 M, but a large volume of the eluent has to be applied. An 80% acetone/0.15 M HCl solution provides the best ratio of eluted amounts of Fe relative to the loss of ^{68}Ga . (Zhernosekov et al., 2007)

A sodium chloride (NaCl)-based, highly efficient ^{68}Ga -eluate concentration and labeling procedure for DOTA-conjugated peptides has been introduced. The method has been proposed to be well-suited for routine production and clinical use, and it has the potential to be expanded to other ligands as well. The procedure is based on the assumption that ^{68}Ga adsorbed onto an SCX cartridge is elutable with a concentrated NaCl solution by conversion of adsorbed $^{68}\text{Ga}^{3+}$ to $^{68}\text{GaCl}_4^-$ anion in the presence of a high concentration of chloride anions (Figure 6.). The $^{68}\text{Ge}/^{68}\text{Ga}$ generator is eluted with 0.1 M HCl and generator eluate is collected and adsorbed onto the SCX cartridge and eluted using a mixture of 5 M NaCl/5.5 M HCl. It has been found that the ^{68}Ga activity is almost quantitatively elutable directly from the SCX cartridge by addition of a minimal amount of HCl to the 5 M NaCl solution. It has been proved that also this eluate could be used directly for ^{68}Ga -labeling of DOTA-conjugated peptides in buffered reaction mixtures. (Mueller et al., 2012)

Pandey and co-workers used a cyclotron for producing ^{68}Ga . After irradiation, the target dump was received in a collection vial along with a 1.6 mL water rinse of the target. The dump and rinse solutions were mixed and passed through a cation-exchange column. The column was preconditioned by washing with 15 mL of water followed by air. Both ^{68}Zn and ^{68}Ga were effectively trapped on the cation-exchange column. The column was washed with water after trapping to remove short-lived ^{11}C and ^{13}N isotopes. ^{68}Zn was eluted from the column using 0.5 N

hydrogen bromide (HBr) in 80% acetone solution and collected in a separate vial, followed by a water rinse to remove any remaining HBr-acetone. ^{68}Ga was finally eluted with 3 N HCl into a product vial. (Pandey et al., 2014)

2.2.2.2 Buffer solutions and purification of ^{68}Ga -labeled peptides

Both pre-concentration methods and eluate fractionation use HCl in the eluent and thus require buffers for the correct pH adjustment necessary for the ^{68}Ga complexation. Weak complexation capacity of the buffer is essential in order to prevent $^{68}\text{Ga}^{3+}$ precipitation and colloid formation and thus act as a stabilizing agent. A number of buffering systems have been evaluated. (Ebenhan et al., 2017)

As already mentioned, Ga^{3+} can form four-, five- and six-coordinated complexes. The coordination reaction of Ga^{3+} requires buffering. DOTA- and NOTA-derivatives can easily be labeled with ^{68}Ga in a reproducible manner and with high yield in a buffer like acetate or 4-(2-hydroxyethyl) piperazine-1-ethanesulfonic acid (HEPES) or in water. Buffers with weak complexing strength are used in labeling synthesis to keep ^{68}Ga in solution, prevent precipitation and colloid formation and provide pH required for formation of the desired complex. Various buffers, such as NaOAc, HEPES, formate, glutamate, lactate, oxalate, succinate, tartrate and tris, have been investigated. Among these, NaOAc, HEPES and succinate have proven to be the most promising for labeling purposes. The use of HEPES buffer has resulted in preparation of tracers with higher molar activity as compared with NaOAc. Other buffers mentioned above have led to poor RCYs. (Velikyan et al., 2004, Bauwens et al., 2010, Velikyan, 2011, Boschi et al., 2013, Velikyan, 2013)

HEPES is a biologically compatible buffer and provides high molar activity and high radioactivity incorporation (>95%) (Velikyan et al., 2004, Velikyan et al., 2008, Bauwens et al., 2010, Velikyan et al., 2010). The drawback of using HEPES is that the European Pharmacopoeia (Ph. Eur.) defines this buffer as an impurity and sets it a specified limit (Ph. Eur., 2013, Pfaff et al., 2018). This means that, prior to clinical use, the PET radiopharmaceutical should be purified from HEPES and additional QC must be performed to ensure that the buffer does not exceed the limit. The use of NaOAc has the advantage of being approved for human use. (Bauwens et al., 2010, Velikyan, 2014, Gijssels et al., 2016)

Syntheses of [^{68}Ga]Ga-DOTA peptides have originally been performed manually or by means of a semi-automated system (Figure 7.). In these procedures, open standard reagent vials containing peptide and pure preheated water are used. Buffers like NaOAc and HEPES buffer solution are applied (Velikyan et al., 2004). The pre-concentrated and purified ^{68}Ga is added and the reaction mixture is heated.

Different options, such as heating in an oil bath (Meyer et al., 2004) or using microwave heating (Velikyan et al., 2004), are available (Boschi et al., 2013).

Methods for the radiolabeling of peptides with ^{68}Ga for clinical applications are required to provide PET radiopharmaceuticals within a short time period in high yields and with high molar activity and pharmaceutical quality. The possibility of quantitative incorporation of ^{68}Ga into microgram amounts of DOTA-derivatized peptides is a major advantage of ^{68}Ga over ^{18}F . In general, DOTA-derivatives require a high temperature (80–100°C) for labeling with ^{68}Ga . NOTA, and particularly conjugates of some of its bi-functional derivatives, mainly NODAGA, can be labeled at r.t. Under acidic conditions, the radiolabeling yield is >95% within 10 minutes. (Meyer et al., 2004, Velikyan et al., 2004, Zhernosekov et al., 2007, Decristoforo et al., 2012, Boschi et al., 2013)

After the heating step, the solution is transferred to a pre-conditioned C18 reversed phase cartridge for purification by a solid phase extraction (SPE) (Figure 7.). ^{68}Ga -labeled peptides are retained on this type of column, while colloids, non-incorporated $^{68}\text{Ga}^{3+}$ and $^{68}\text{Ge}^{4+}$ are not retained (de Blois et al., 2011). The cartridge is washed with water or NaCl and the ^{68}Ga -labeled peptide is recovered from the cartridge with a very small volume of EtOH directly into the final product vial. The EtOH-eluate containing pure ^{68}Ga -labeled peptide is dissolved in an appropriate volume of sterile NaCl or corresponding and sterilized by filtration through a membrane filter. A final EtOH-content even <5% is yielded. The manual and semi-automated procedures facilitate the preparation of injectable ^{68}Ga -labeled DOTA-peptides within 20–30 minutes. (Meyer et al., 2004, Decristoforo et al., 2007, Gabriel et al., 2007, Zhernosekov et al., 2007)

The influence of SPE on different parameters has been studied for labeling DOTA-TOC with ^{68}Ga . It has been observed that, before and after SPE purification, RCP values increased, mainly due to the removal of colloidal ^{68}Ga as determined by TLC. In addition, the content of ^{68}Ge reduced by a factor of >100 and pH values increased from 3.7 to 5.8. The fixation of the radiolabeled peptide on the SPE cartridge allows the removal of all other components used in the synthesis. It also allows washing with sterile NaCl or corresponding for injection after synthesis. It is suggested that SPE purification should be included even when pre-absorption of the eluate on an ion-exchange column is used as a part of the synthesis protocol. (Decristoforo et al., 2007)

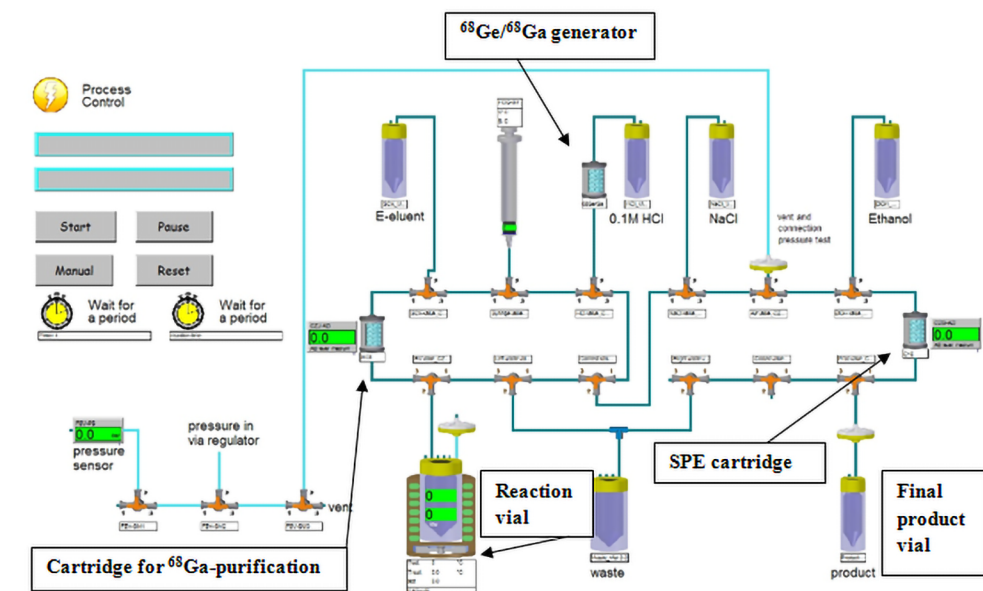


Figure 7. Schematic diagram of an automated system for ^{68}Ga -labeling of peptides including generator elution. As an example, for the labeling of DOTA-conjugated peptides using the NaCl-based method, the $^{68}\text{Ge}/^{68}\text{Ga}$ generator is eluted with a total of 10 mL of 0.1 M HCl. ^{68}Ga of the generator eluate is collected on a SCX cartridge and eluted with minimal loss (1–2%) using a mixture of 5 M NaCl/5.5 M HCl. The eluate is slowly added to a reaction vial in a heating block containing buffer (1 M, 200–400 μL) and the DOTA-conjugated peptide (DOTA-Tyr³-octreotide (DOTA-TOC) or DOTA-Tyr³-octreotate (DOTA-TATE), 40 μg) in 3 mL of water. The pH of the buffer solution is adjusted with glacial acetic acid to 4.5 beforehand. After mixing, the final pH of the radiolabeling reaction mixture is approximately 3.6. The reaction mixture is heated at 90°C for 7 minutes and then neutralized with, for example, sterile saline or sodium phosphate buffer. ^{68}Ga -labeled peptide is transferred to a solid phase extraction (SPE) cartridge for purification. The ^{68}Ga -labeled peptide is eluted from the cartridge using EtOH, through a sterile filter into the final product vial and formulated using sterile NaCl. DOTA-TOC is radiolabeled using an automated synthesis module and the total duration of the synthesis is 14 minutes. (Mueller et al., 2012) (Modified from the Modular-Lab PharmTracer® schematic by Eckert & Ziegler Eurotope)

2.2.3 Examples of ^{68}Ga -labeled PET radiopharmaceuticals

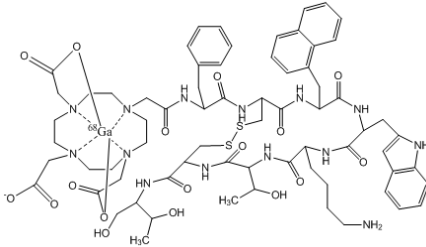
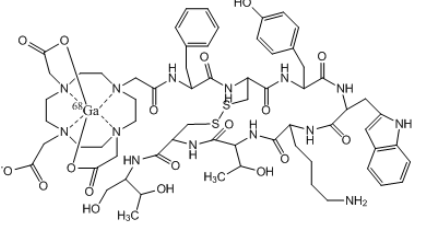
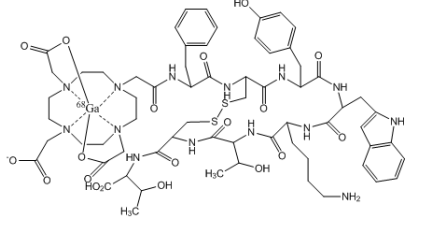
2.2.3.1 ^{68}Ga -somatostatin peptide derivatives

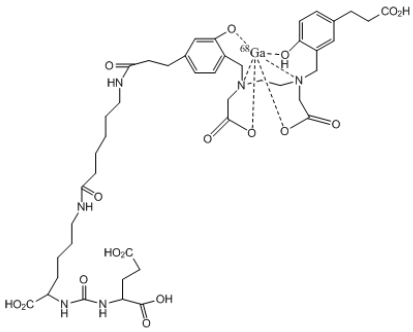
Somatostatin is a cyclic peptide hormone that exerts different biological effects in various parts of the body, such as the gut, the pancreas, the brain, the pituitary and some components of the immune system. The effects include cell proliferation, inhibition of hormone secretion and modulation of neurotransmission. Five different somatostatin receptor subtypes (SSTR 1–5) have been cloned and characterized. They are responsible for different biological responses. Some of

these receptors are overexpressed in several human tumors, especially neuroendocrine tumors (NETs) and their metastases. SSTR 2 is the most representative subtype in NETs, SSTR 3 and SSTR 5 are also represented on NET cell surface. SSTRs have been found to be overexpressed also in breast cancer, prostate cancer, renal cell carcinoma, small cell lung cancer and malignant lymphoma. ^{68}Ga -labeled DOTA-conjugated somatostatin derivatives for the diagnosis of NETs have been well established. Three derivatives are in use: DOTA-1-Nal³-octreotide (DOTA-NOC), DOTA-TOC and DOTA-TATE (Table 1.). In terms of radiolabeling, e.g. yields and molar activity, there is no relevant difference between these somatostatin analogues. (Wild et al., 2003, Antunes et al., 2007, Ambrosini et al., 2008, Decristoforo et al., 2012, Jalilian, 2016)

It has been proved that [^{68}Ga]Ga-DOTA-NOC detects significantly more lesions than the SSTR 2-specific radiotracer [^{68}Ga]Ga-DOTA-TATE in patients with NETs (Jalilian, 2016). SSTR-PET with [^{68}Ga]Ga-DOTA-TOC is superior for the detection of NETs as compared with diagnostic computed tomography (CT) and SPECT in various clinical situations like initial diagnosis, staging and follow-up (Gabriel et al., 2007). Carcinoid tumors, which are rich in SSTR, show typically high-level uptake of [^{68}Ga]Ga-DOTA-TOC (Jindal et al., 2010). The U.S. Food and Drug Administration (FDA) has approved [^{68}Ga]Ga-DOTA-TATE as an imaging agent for the detection of NETs. (Hofmann et al., 2001, Jindal et al., 2010, Hofman et al., 2012, Ocak et al., 2013, Yang et al., 2014, Deppen et al., 2016, Barrio et al., 2017, Mahajan and Cook, 2017)

Table 1. Examples of ^{68}Ga -labeled PET radiopharmaceuticals.

^{68}Ga -labeled PET radiopharmaceutical	Mechanism	Intended use	References
<p>^{68}Ga]Ga-DOTA-NOC</p> 	Binds to SSTR 2, SSTR 3 and SSTR 5.	Identification of tumor site and selection of patients as candidates for radioimmunotherapy.	Ambrosini et al., 2009
<p>^{68}Ga]Ga-DOTA-TOC</p> 	Binds to SSTR 2 and SSTR 3, lower affinity for SSTR 5.	PET/CT imaging in the diagnosis of prostatic cancers, NETs, thyroid malignancies and meningiomas. Evaluation of primary lung cancers, particularly the small-cell form.	Hofmann et al., 2001, Jindal et al., 2010
<p>^{68}Ga]Ga-DOTA-TATE</p> 	SSTR 2 specific.	Detection of NETs (high specificity and sensitivity), a major role in clinical practice of neuroendocrine and other somatostatin-avid malignancies.	Hofman et al., 2012, Barrio et al., 2017

^{68}Ga-labeled PET radiopharmaceutical	Mechanism	Intended use	References
<p data-bbox="189 236 384 262">^{68}Ga]Ga-PSMA-11</p> 	<p data-bbox="678 236 826 338">PSMA is expressed in prostate cancer.</p>	<p data-bbox="853 236 1001 319">PET imaging of prostate carcinomas.</p>	<p data-bbox="1024 236 1166 346">Silver et al., 1997, Charron et al., 2016</p>

2.2.3.2 Prostate-specific membrane antigen

Prostate-specific membrane antigen (PSMA), also called glutamate carboxypeptidase II, is a membrane-type zinc protease. PSMA appears to be highly expressed in normal prostate tissue as well as in primary and nodally metastatic prostate cancer. It has been shown that carcinomas arising in the kidney, colon and bladder do not appear to express PSMA. (Silver et al., 1997, Eder et al., 2014, Pfob et al., 2016)

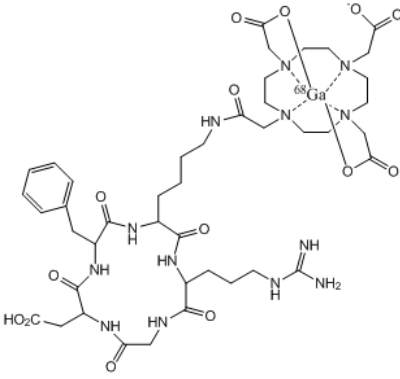
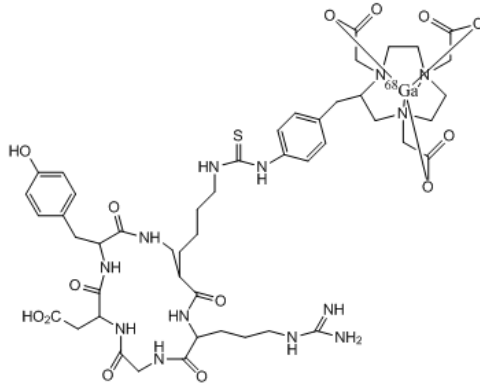
^{68}Ga]Ga-PSMA-HBED-CC, also known as ^{68}Ga]Ga-PSMA-11 ((Glu-NH-CO-NH-Lys-(Ahx)-[^{68}Ga]Ga-HBED-CC)) (Table 1.), is an extracellular PSMA-ligand for PET imaging that has gained significant attention during the past years. Similarly ^{18}F -labeled PSMA, such as ^{18}F -PSMA-1007, have received increasing interest recently (Giesel et al., 2016, Cardinale et al., 2017, Giesel et al., 2017). The acyclic chelator HBED-CC linked to the PSMA ligand can selectively target the hydrophobic pocket of PSMA in prostate carcinomas. (Eder et al., 2014, Charron et al., 2016, Pfob et al., 2016, Baranski et al., 2018)

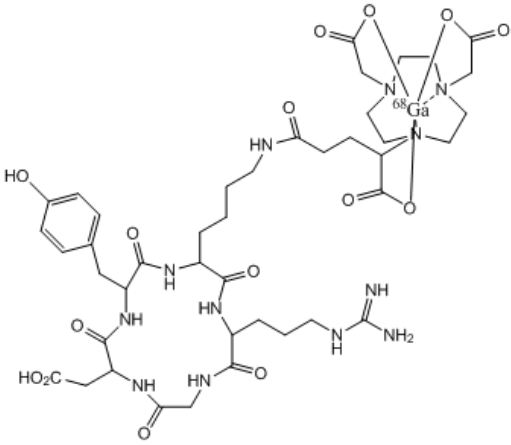
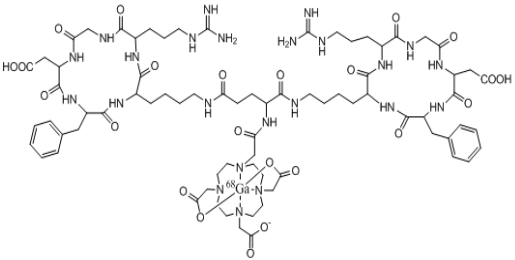
It has been reported that HBED-CC forms three diastereomers during ^{68}Ga -complexation (Schuhmacher et al., 1992). In a standard labeling protocol, ^{68}Ga]Ga-PSMA-HBED-CC is incubated at pH of ~ 4 and heated at 95°C . The thermodynamically favored diastereomer is formed. However, a small fraction of one of the other two formed diastereomers is still present in the reaction mixture and would be part of the final formulation prepared for patients. It is important to assess the biological activity of the two major diastereomers according to their biological activity in cell-based assays. (Eder et al., 2014)

Other PSMA inhibitors that can be used as theranostic agents have been described as well. In comparison with PSMA-HBED-CC, DOTA-conjugated

PSMA inhibitor PSMA-617 seems to be more attractive for endoradiotherapy because of its lower spleen accumulation, higher tumor uptake at later time points, and the highly efficient clearance from the kidneys. It has been observed that [^{68}Ga]Ga-PSMA-617 shows lesions of prostate cancer with high contrast, especially in late images. Maximal contrast of tumor lesions is usually seen between three and four hours after injection. (Afshar-Oromieh et al., 2015, Benešová et al., 2015)

Table 2. Examples of RGD-based ^{68}Ga -labeled PET radiopharmaceuticals.

^{68}Ga -labeled PET radiopharmaceutical	Mechanism	Intended use	References
<p>[^{68}Ga]Ga-DOTA-RGD</p> 	<p>Binds to integrins $\alpha_v\beta_3$, $\alpha_v\beta_5$.</p>	<p>Cancer theranostic, cardiovascular diseases.</p>	<p>Chen et al., 2016, Gnesin et al., 2017</p>
<p>[^{68}Ga]Ga-NOTA-RGD</p> 			

^{68}Ga-labeled PET radiopharmaceutical	Mechanism	Intended use	References
<p data-bbox="181 268 438 297">^{68}Ga]Ga-NODAGA-RGD</p> 			
<p data-bbox="181 773 495 801">^{68}Ga]Ga-DOTA-E-[c(RGDfK)]₂</p> 	Binds to integrin $\alpha_v\beta_3$.	Integrin affinity and tumor uptake.	Dijkgraaf et al., 2011

2.2.3.3 RGD-based peptides

Integrins play a very important role in tumor angiogenesis and metastasis (Chen, 2011). Most of the integrin-targeting imaging tracers are based on the tripeptide Arg-Gly-Asp (RGD) acid sequence because of its high affinity and specificity for integrin $\alpha_v\beta_3$ (Chen et al., 2016). Several proteins of the extracellular matrix like fibrinogen, fibronectin and vitronectin interact with integrin $\alpha_v\beta_3$ via the RGD sequence. Molecular imaging of $\alpha_v\beta_3$ integrin expression with PET is a promising technique that allows for visualization of tumor angiogenesis. (Ruoslahti, 1996, Gilad et al., 2016, Lobeek et al., 2018)

The feasibility of ^{68}Ga]Ga-DOTA-RGD (Table 2.) binding to the $\alpha_v\beta_3/\alpha_v\beta_5$ integrin in the assessment of the degree of inflammation and the vulnerability of atherosclerotic plaques has been studied (Haukkala et al., 2009). In addition to the monomeric DOTA-RGD peptide, a dimeric RGD-peptide (^{68}Ga]Ga-DOTA-E-[c(RGDfK)]₂ (Table 2.) (Dijkgraaf et al., 2011, Kiugel et al., 2014) and a tetrameric

RGD-peptide ($[^{68}\text{Ga}]\text{Ga-DOTA-E}\{\text{E}[\text{c}(\text{RGDfK})]_2\}_2$) (Dijkgraaf et al., 2011) have been evaluated for PET imaging in animal studies. (Haukkala et al., 2009, Dijkgraaf et al., 2011, Kiugel et al., 2014)

Radiolabeling of NOTA-RGD (Table 2.) with ^{68}Ga has been found to be straightforward and stable. $[^{68}\text{Ga}]\text{Ga-NOTA-RGD}$ was synthesized in high yield and found to be a promising radioligand for the imaging of angiogenesis with high affinity, high stability, high specificity and excellent pharmacokinetic properties. (Jeong et al., 2008)

According to the results obtained, $[^{68}\text{Ga}]\text{Ga-NODAGA-RGD}$ (Table 2.) shows high affinity for integrin $\alpha_v\beta_3$, high metabolic stability, receptor-selective tumor uptake, good tumor to background ratios, low protein-bound activity and rapid, predominantly renal elimination. $[^{68}\text{Ga}]\text{Ga-NODAGA-RGD}$ can be produced straightforward with high RCP and high yield, thus making it suitable for synthesis in an automated system. NODAGA-RGD has been labeled with ^{68}Ga in a fully automated, cGMP compliant process (Pohle et al., 2012). It has been demonstrated that $[^{68}\text{Ga}]\text{Ga-NODAGA-RGD}$ is well tolerated and metabolically stable in humans. (Haubner et al., 2016)

2.2.3.4 Oligonucleotides

Oligonucleotides are short, single- or double-stranded deoxyribonucleic acid (DNA) or ribonucleic acid (RNA) molecules (Figure 8.). They include ASO, RNA interference (RNAi) and aptamer RNAs. Both ASO- and RNAi-oligonucleotides are mainly intended for modulating gene and protein expression. Aptamers are single-stranded DNA or RNA sequences that can bind to proteins with high affinity. Aptamers have features that make them ideal candidates for use in therapeutics, diagnostics and other applications. (Syed and Pervaiz, 2010, Kerlin and Li, 2013, Gijs et al., 2016)

Oligonucleotides are soluble in water. They are particularly chemically stable molecules. This is because of the robustness of their phosphodiester backbone. Oligonucleotides can be advantageous in comparison with proteins and antibodies because of their low toxicity, immunogenicity and smaller size. Oligonucleotides are chemically synthesized with high batch fidelity. In addition, they can be easily chemically modified to enhance their bioavailability, pharmacokinetics and stability. However, any modifications of oligonucleotides must be made without compromising their specificity or hybridization properties. Oligonucleotides are

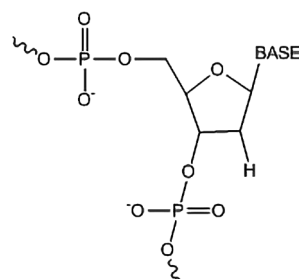


Figure 8. Schematic illustration of an oligonucleotide.

quite unreactive molecules and radiolabeling usually requires functionalization of oligonucleotides with a reactive group. This reactive group can be introduced during chemical synthesis without difficulty by the use of functionalized nucleotides. Nucleotides are easily functionalized with reactive groups, such as an alkyne, alkyl amino group, disulfide group or other, which can be introduced at the 5'- or 3'-end or internally. (Roivainen et al., 2004, Winkler, 2013, Gijs et al., 2016)

Turning oligonucleotides into PET radiopharmaceuticals is not straightforward and there are several challenges. Harsh chemical conditions can affect the stability of oligonucleotides. Oligonucleotides are sensitive to slow acid-catalyzed depurination. They can be hydrolyzed completely at high temperatures and very low pH. Oligonucleotides precipitate in most organic solvents. At least part of these properties are attributed to oligonucleotides' hydrophilicity, ready interaction with degrading enzymes and multiple anionic charges. (Winkler, 2013, Gijs et al., 2016)

Various radiolabeling conditions like temperature, buffer system, incubation time and oligonucleotide concentration have been optimized in order to obtain ^{68}Ga -labeled oligonucleotides with high stability and high labeling efficiency. It has been suggested that radiolabeling of oligonucleotides should occur in pH conditions close to neutral to avoid hydrolysis or acid-catalyzed depurination during the labeling process. (Gijs et al., 2016)

Esterified precursors of DOTA and NOTA ligands bearing a dimethoxytritylated hydroxyl side arm have been prepared and immobilized via an ester linkage to long chain alkylamine derivatized controlled pore glass. After that, oligonucleotide chains are assembled on the hydroxyl function, and the conjugates are released and deprotected. The 3'-DOTA- and 3'-NOTA-conjugated oligonucleotides thus prepared are converted to ^{68}Ga -chelators (Figure 9.) Labeling of the conjugates has proven to be straightforward. According to the results obtained by *in vivo* imaging with PET, differences in biodistribution were mainly caused by oligonucleotide length and/or sequence, and marginally by the chelators. (Kiviniemi et al., 2012)

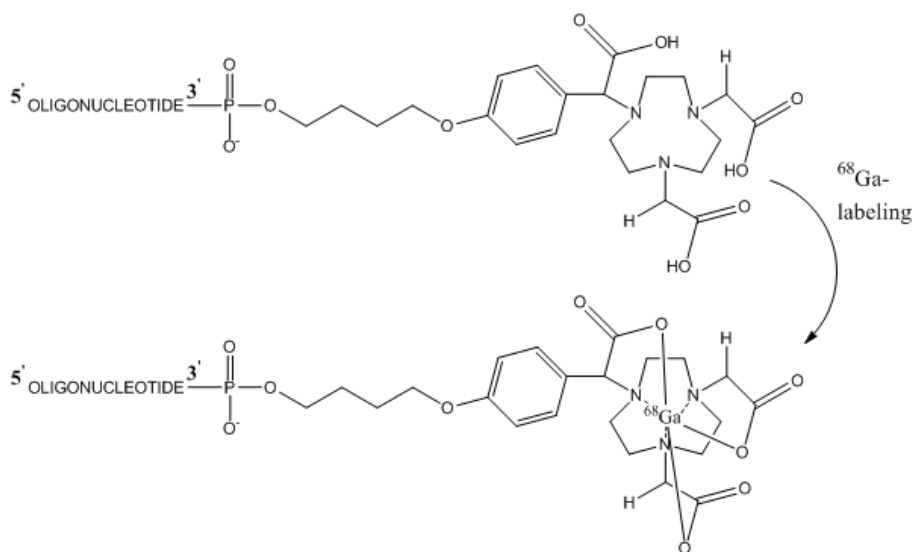


Figure 9. ^{68}Ga -labeling of 3'-NOTA-conjugated oligonucleotide. ^{68}Ga is obtained from a $^{68}\text{Ge}/^{68}\text{Ga}$ generator by elution with HCl. NaOAc is added and the pH is adjusted to 3.5 with HCl. NOTA-conjugate is added and the reaction mixture is incubated at 95°C for 10–15 minutes. (Modified from Kiviniemi et al., 2012)

Three different forms of oligonucleotides, namely 2'-deoxyphosphodiester, 2'-deoxyphosphorothioate and 2'-*O*-methyl phosphodiester, have been researched. These oligonucleotides are conjugated to the DOTA-chelator before radiolabeling with ^{68}Ga . NaOAc buffer is added to the eluate obtained from the $^{68}\text{Ge}/^{68}\text{Ga}$ generator to give pH 5.5. DOTA-oligonucleotide is added and the mixture is incubated at 100°C for 10 minutes. The [^{68}Ga]Ga-DOTA-oligonucleotide remains stable in water at r.t. for up to four hours. According to researchers' experience, the method is easily transferable between laboratories and requires only minor investments. (Roivainen et al., 2004)

^{68}Ga -labeling of DOTA-oligonucleotides using microwave activation has also been described. Microwave activation is used to speed up the complexation of ^{68}Ga with the DOTA chelator. Four modified and functionalized 17-mer oligonucleotides with a hexylamine group in the 3'- or 5'-position have been researched. These oligonucleotides are conjugated to the DOTA chelator and radiolabeled with ^{68}Ga successfully. The same reaction mixture as described above is vortexed and microwave activation is applied for one minute. It has been found that the modifications of the oligonucleotides, such as the substitution of non-bridging oxygens by sulfur, introduction of hexylaminolinker either at the 3'- or 5'-end or introduction of *O*-methyl group at sugar 2'-position, do not influence the

radiolabeling and conjugation result or the hybridization ability of the oligonucleotides. Radiolabeled products are stable in water and EtOH over four hours. (Velikyán et al., 2004)

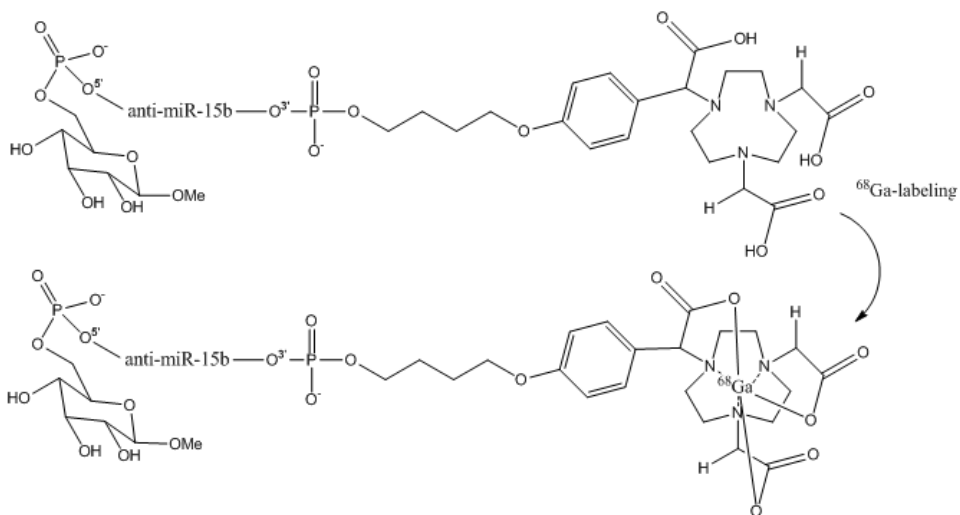


Figure 10. ^{68}Ga -labeling of 2'-O-methyl oligoribonucleotide bearing one *D*-galactopyranoside residue. ^{68}Ga is obtained from a $^{68}\text{Ge}/^{68}\text{Ga}$ generator by elution with HCl. NaOAc buffer is added and the pH is adjusted to 3.5 with HCl. An oligonucleotide conjugate is added and the reaction mixture is incubated at 95°C for 10–15 minutes. (Modified from Mäkilä et al., 2014)

Biokinetics of ^{68}Ga -labeled oligonucleotides in rats has been examined. Intravenously (i.v.) injected ^{68}Ga -oligonucleotides of 17-mer length have resulted in high-quality PET images and thus allowed for quantification of the biokinetics in tumors and major organs. The results show that the simple and rapid ^{68}Ga -labeling of oligonucleotides is a convenient approach for *in vivo* PET imaging of the biodistribution and quantification of oligonucleotide biokinetics in living animals. (Roivainen et al., 2004)

2.2.3.5 MicroRNA

MicroRNAs (miRNAs) are a class of short non-coding RNAs that have been demonstrated to regulate the expression of genes governing tumorigenic processes by targeting mRNAs for translational inhibition or degradation (Xia et al., 2017). Changes in miRNA expression profile are correlated with cancer progression, tumor pathogenesis and drug resistance (Calin and Croce, 2006). For example, it

has been shown that microRNA-21 (miR-21) is overexpressed in all kinds of tumors. miR-21 has been demonstrated to play an important role in the radioresistance of cancers, including breast cancer, glioblastoma and rectal cancer (Xia et al., 2017). It has been demonstrated that miR-21 is significantly overexpressed in osteosarcoma tissues. The results suggest that miR-21 expression plays a key role in regulating cellular processes in osteosarcoma, and it may serve as a therapeutic target. (Ziyan et al., 2011)

⁶⁸Ga-radiolabeled 2'-*O*-methyl oligoribonucleotides (anti-miR-15b) bearing one (Figure 10.), three or seven *D*-galactopyranoside residues have been prepared. *In vivo* imaging with PET in rats has shown remarkable galactose-dependent liver targeting for the conjugates. (Mäkälä et al., 2014)

2.2.3.6 Bis(phosphonates)

Bis(phosphonates), which are pyrophosphate (PP) analogs, are the most widely utilized bone-binding ligands. This is due to the fact that the molecular structure of bis(phosphonates) greatly affects the binding affinity to hydroxyapatite mineral. This binding affinity has led to the widespread use of bis(phosphonates) as drugs to treat metabolic bone disorders. Bis(phosphonates) have been synthesized as a more chemically stable analog of PP. The oxygen molecule bound to the two phosphonate molecules in pyrophosphate (P-O-P) is replaced by a carbon (P-C-P). This elemental substitution results in bonds that are resistant to degradation. Substitution also creates biologically active molecules that are similar in structure to PP and capable of being delivered to bone *in vivo* without degradation by hydrolysis. The first synthesized and studied bis(phosphonates) have shown to significantly impair *in vivo* bone resorption in rats. This has increased interest in exploring bis(phosphonate) compounds as therapeutic agents for bone diseases. (Francis et al., 1969, Cole et al., 2016)

The idea of conjugating bis(phosphonates) to proteins that promote bone formation and healing was introduced almost twenty years ago. A bis(phosphonate), 1-amino-1,1-diphosphonate methane, was conjugated to a protein, albumin. According to the results, the conjugated albumin exhibited a high affinity to hydroxyapatite, which was proportional to the extent of conjugation. It was concluded that conjugation of bis(phosphonates) to albumin imparted a high bone affinity to the protein. These conjugates can be potentially targeted to bone. However, it has been shown that most proteins do not exhibit specific binding to hydroxyapatite but have ubiquitous targets throughout the body. This means that bis(phosphonate) molecules could be conjugated to proteins to reduce the required dose, improve bone-targeting and reduce extraosseous accumulation of the proteins. Studies where bis(phosphonates) have been conjugated to many model

proteins, such as bovine serum albumin, IgG and lysozyme, have been performed. These studies suggest that bis(phosphonates) can be used as a targeting ligand to deliver proteins to bone tissue. (Uludag et al., 2000, Cole et al., 2016)

A promising DOTA-conjugated bis(phosphonate), 4-[[bis-phosphonomethyl]-carbamoyl]methyl}-7,10-bis(carboxymethyl)-1,4,7,10-tetraazacyclododec-1-yl-acetic acid (BPAMD, also called DOTAM^{BP}) (Figure 11.), has been radiolabeled with ⁶⁸Ga. Optimum reaction parameters for the ⁶⁸Ga-complex formation were identified through variation of reaction pH (pH = 1–5), reaction time (1–10 minutes), temperature (60°C to 100°C) and different amounts of the complex ligands. The results of radiolabeling kinetics showed best efficiency at pH = 3–5 and at 100°C for 10 minutes. Complex formation of [⁶⁸Ga]Ga-BPAMD is reported to be fast and resulting in high yields. (Fellner et al., 2012, Meckel et al., 2013)

In addition, two DOTA-based bis(phosphonates), 4-[[bis-phosphonopropyl]-carbamoyl]methyl}-7,10-bis-(carboxymethyl)-1,4,7,10-tetraazacyclododec-1-yl-acetic acid (BPAPD, also called DOTAP^{BP}) and tetraethyl-10-[[2,2-bis-phosphonoethyl]hydroxyl-phosphoryl]methyl}-1,4,7,10-tetraazacyclododecane-1,4,7-triacetic acid (BPPED, also called DO3AP^{BP}), have been radiolabeled with ⁶⁸Ga (Figure 11.). According to the results high bone uptake values were observed for all these three ⁶⁸Ga-labeled bis(phosphonates) at 60 minutes post injection. The results obtained suggest that these ligands could be useful in ⁶⁸Ga imaging of bone metastases. (Meckel et al., 2013)

⁶⁸Ga-radiolabeling of NOTA-like ligands with a bis(phosphonate)-containing side arm connected to a metal-binding cage through acetamide (1,4,7-triazacyclononane-1,4,7-triacetamide, NOTAM^{BP}) or methylphosphinate (1,4,7-triazacyclononane-1,4-diacetic acid, NO2AP^{BP}) pendant arms has also been described. According to the results, they showed efficient complexation of ⁶⁸Ga. It was reported that the phosphinate derivative was shown to bind metal ion better than the acetamide derivative under any used conditions. Radiolabeling with ⁶⁸Ga was rapid at temperatures above 60°C for the phosphinate and at 90°C for the acetamide ligand. (Holub et al., 2015)

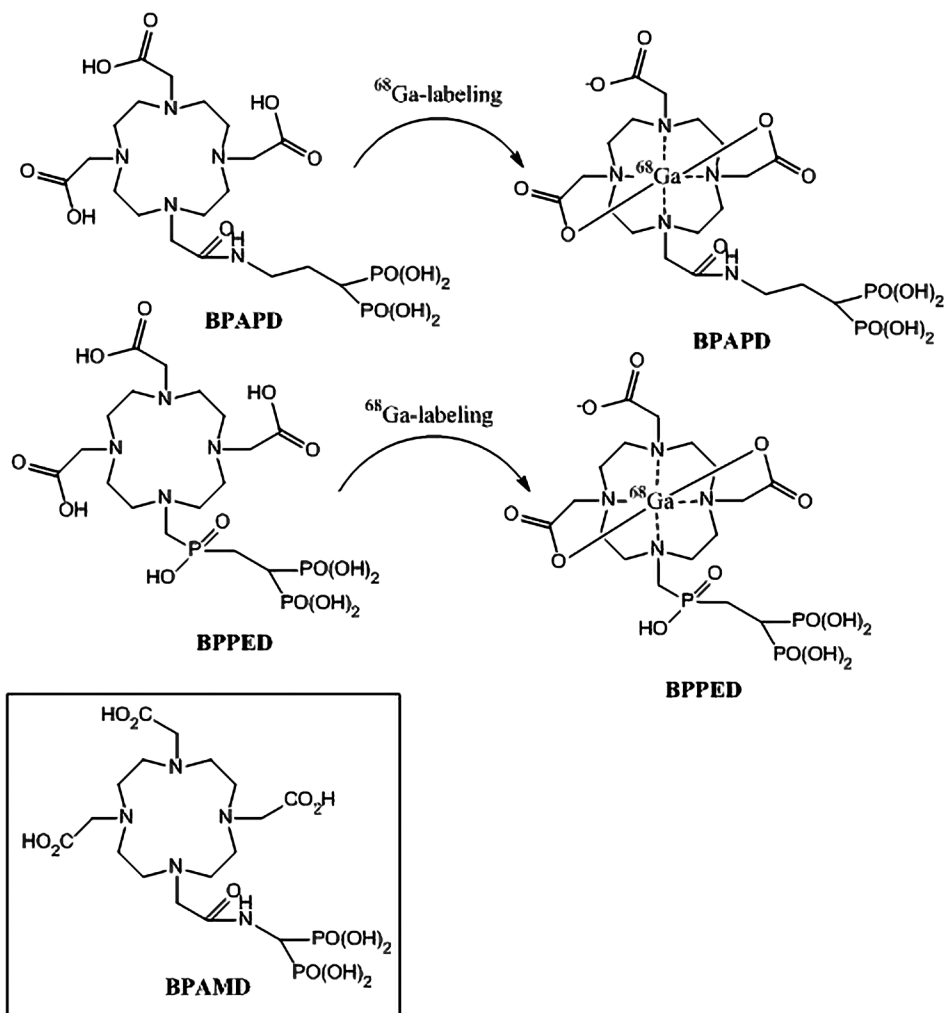


Figure 11. ^{68}Ga -labeling of BPAPD and BPPED. Radiolabeling is performed in ammonium acetate buffer by adding the processed ^{68}Ga -eluate, thus giving a labeling pH of 3.75. The ligand is added and the solution is shaken in a heating block for 10 minutes at 100°C . (Modified from Meckel et al., 2013)

2.2.3.7 Sialic acid-binding immunoglobulin-like lectin 9

Sialic acids are α -keto acids and they consist of a 9-carbon backbone. Sialic acids are located at the distal part of the non-reducing end of glycan and thus they play a special role in physiological processes. Siglecs are single-pass transmembrane cell-surface proteins found predominantly on leukocytes. Siglecs are characterized by their ability to bind specific sialic acid structures. The Siglec family is divided into

two subsets, a rapidly evolving CD33-related subset and a highly conserved subset. Both groups include both activating and inhibitory receptors. Siglecs are mostly located on the cell surface of hematopoietic cells (Varki and Angata, 2006), but cells outside the immune system can also express Siglecs. (Bornhöfft et al., 2018, Carroll et al., 2018)

Human primary amine oxidase, also known as VAP-1, is an endothelial cell molecule involved in leukocyte trafficking from blood into the tissues during inflammatory responses. VAP-1 is stored in vesicles in the endothelial cells and, upon inflammatory stimuli, it is expressed on the endothelial cell surface and prevails there during inflammation (Salmi and Jalkanen, 2014). This makes VAP-1 a good target for visualizing inflammation. Siglec-9 peptides targeted to VAP-1 have been used for PET imaging of inflammation and cancer using different animal models. (Li et al., 2013, Virtanen et al., 2015, Retamal et al., 2016, de Carvalho *et al.*, 2018)

The cyclic peptide CARLSLSWRGLTLCPSK, containing residues 283–297 from Siglec-9 and with cysteines forming a disulfide bridge, has been identified as a VAP-1 ligand (Aalto et al., 2011). The ^{68}Ga -labeled tracer [^{68}Ga]Ga-DOTA-Siglec-9 contains an 8-amino-3,6-dioxaoctanoyl linker, which is a polyethylene glycol derivative, between the peptide and DOTA chelator. Radiolabeling of DOTA-Siglec-9 and another VAP-1-selective peptide named DOTAVAP-P1 has been described (Figure 12.). (Ujula et al., 2009, Aalto et al., 2011, Virtanen et al., 2015)

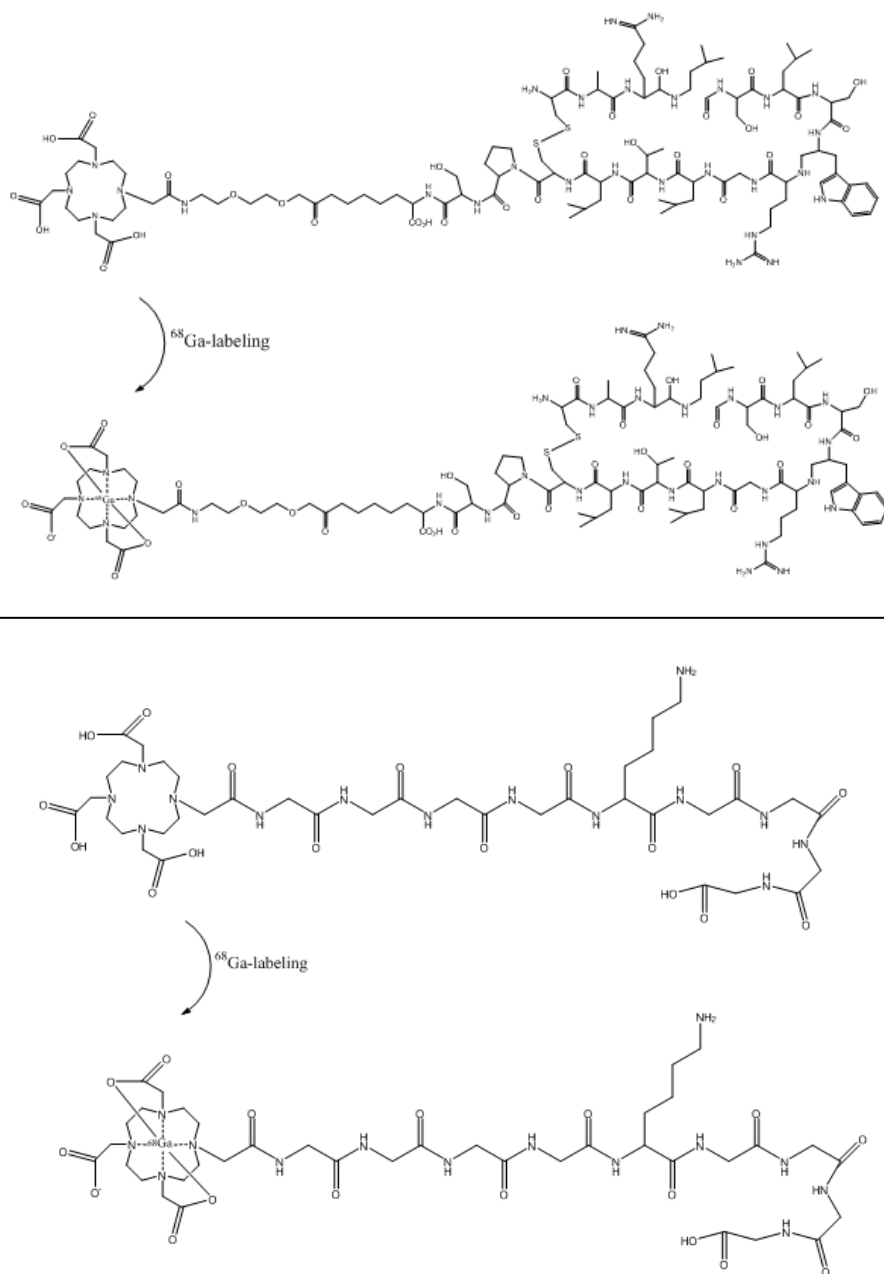


Figure 12. ^{68}Ga -labeling of DOTA-Siglec-9 (top) and DOTAVAP-P1 (bottom). ^{68}Ga is obtained from a $^{68}\text{Ge}/^{68}\text{Ga}$ generator by elution with 0.1 M HCl. ^{68}Ga -eluate is mixed with HEPES to give a pH of approximately 4.1 (DOTA-Siglec-9) or with NaOAc to give a pH of approximately 5.5 (DOTAVAP-P1). Peptide is added and the reaction mixture is heated at 100°C for 15 minutes (DOTA-Siglec-9) or at 100°C for 20 minutes (DOTAVAP-P1). No further purification is performed. (Modified from Ujula et al., 2009, Virtanen et al., 2015)

2.2.4 Quality control of PET radiopharmaceuticals

PET radiopharmaceuticals are treated as drugs. It is required that the effect, i.e. the PET image quality, is guaranteed throughout the PET radiopharmaceutical's shelf life. QC of PET radiopharmaceuticals is important to ensure the safety of the product before its release for clinical use. Because these compounds are injected into humans, there are strict regulatory requirements for performing QC testing of the purified, formulated product of each produced batch to ensure their safety (Fermi, 2009). PET radiopharmaceuticals have to be manufactured, QC tested and administered to patients within a short period of time due to the short half-life of the radionuclides. Because the half-life ranges from minutes to hours, there is no time for all quality parameters to be assessed before releasing the PET radiopharmaceutical for clinical use. In compliance with the risk assessment, it must be specified which parameters can be determined retrospectively. Such parameters include the determination of levels of residual solvents and sterility testing. Sterility testing is performed post release. As a surrogate of sterility testing, endotoxin testing should be performed before release, if possible. (Ballinger and Koziorowski, 2017, Ha et al., 2017, Lodi and Boschi, 2017, Schmidt et al., 2017)

Several quick and efficient tests have been adopted to check the quality of PET radiopharmaceutical preparations before they are released for clinical use in nuclear medicine. Specific procedures for QC of PET radiopharmaceuticals have been published in each country or region (Ph. Eur., United States Pharmacopeia and British Pharmacopoeia). QC of PET radiopharmaceuticals involves several specific tests and measurements to ensure product purity, identity, efficacy and biological safety. The QC tests can be divided into chemical tests, physical tests and biological tests. The chemical and physical tests include, among other things, the visual inspection, the control of pH, and the chemical purity, RCP and radionuclidic purity determination. Biological tests establish sterility and bacterial endotoxins contents. Performing and documenting these required QC tests is time-consuming and cumbersome. It requires, at least, an array of expensive analytical chemistry equipment and significant dedicated laboratory space. For most tests, visual assessment and manual handling and loading of samples leads to significant radiation exposure to personnel. (Ha et al., 2017, Lodi and Boschi, 2017)

Another way to categorize tests is to divide them into radioactive tests and pharmaceutical tests. Radioactive test, such as RCP, radiochemical identity, radioactivity concentration (RAC), radioisotope identity and radioisotope purity, are required to ensure that there are no radionuclidic or radioactive impurities that could interfere with the biodistribution or imaging protocol. Pharmaceutical tests involving, for example, color and clarity, pH, chemical purity, residual solvents, pyrogenicity and sterility, are required to ensure the physiological compatibility of the final preparation and the absence of microbiological, pyrogenic, chemical or

particulate contamination. The goal is to ensure the proper patient dose. (Ha et al., 2017, Lodi and Boschi, 2017)

2.2.4.1 Chemical and physical tests

Visual inspection of the PET radiopharmaceutical solution should be performed before clinical use to ensure that the injectable solution is free from particle contaminations. The purpose is to confirm the color, turbidity or absence of visible particles. The color and clarity of each PET radiopharmaceutical preparation should be checked and the appearance characteristics are reported in the monograph on the radiopharmaceutical. In general, only a clear and colorless, particle-free solution should be used for injection. Generally, the test is performed manually via a qualitative visual inspection. This results in variability in the readout. Formulated PET tracers are generally colorless due to the lack of appreciable absorbance by the tiny amounts of tracer used. Any coloration would indicate a significant quantity of an impurity. (Ha et al., 2017, Lodi and Boschi, 2017, Schmidt et al., 2017)

pH must be controlled to ensure the stability of the formulated PET radiopharmaceutical and to establish that no degradation has occurred between manufacturing and injection. In addition, the physiological compatibility of the formulated PET radiopharmaceutical with the patient should be controlled. The pH of a preparation can be checked using a pH paper indicator strip or a calibrated pH meter. PET radiopharmaceuticals must be formulated at appropriate pH. Due to the relatively small injection volume, typically 1–10 mL, and the high buffer capacity of the blood, a relatively wide pH range, typically 4.5–8.5, is considered to be acceptable from a physiological point of view. (Ha et al., 2017, Lodi and Boschi, 2017, Schmidt et al., 2017)

The radionuclidic identity of PET radionuclides is generally identified by half-life or by gamma-ray spectrometry or by both. The half-life is determined within a suitable period of time, for example 15 minutes, by taking a minimum of three radioactivity measurements of a sample. All these measurements have the same geometry. The half-life is measured with a suitable detection apparatus, such as a Geiger-Müller counter, a scintillation counter or an ionization chamber. (Ph. Eur., 2013, Lodi and Boschi, 2017)

RAC has to be measured in every batch of the final drug preparation at the end of synthesis (EOS) (Fermi, 2009). The total amount of radioactivity in the vial containing the final drug preparation is usually measured using a calibrated dose calibrator. RAC is needed to determine how much volume to dispense for each individual patient dose, meaning decay-corrected to the expected time of injection. (Ha et al., 2017, Schmidt et al., 2017)

Enantiomeric purity has to be verified where appropriate. In the clinical use of chiral PET radiopharmaceuticals, high enantiomeric purity is important. The limit for each enantiomeric impurity is reported in the pharmacopoeia monograph of the radiopharmaceutical, if it has such. (Lodi and Boschi, 2017)

Radiochemical identity can be defined as the molecular structure of the compound that contains the positron-emitting radionuclide. The radiochemical identity of a PET radiopharmaceutical is determined by using a non-radioactive reference standard. Both the standard and the PET radiopharmaceutical are analysed chromatographically. An identical response for the two compounds in terms of retention time when using HPLC with a radiation detector (radio-HPLC), retardation factor when using radio TLC scanner (radio-TLC) or migration time when using capillary electrophoresis (CE) with a radiation detector (radio-CE), demonstrates the structural identity of the PET radiopharmaceutical. (Ha et al., 2017, Lodi and Boschi, 2017)

In addition to confirming the identity of the product, it is also necessary to ensure the absence of radioactive impurities. RCP is defined as the ratio of the activity of the radionuclide concerned which is present in the PET radiopharmaceutical preparation in stated chemical form, to the total radioactivity of that radionuclide present in the PET radiopharmaceutical preparation. RCP is expressed as a percentage. The nature of contaminants will depend on the radionuclide production, on the production process of the PET radiopharmaceutical and the impurity profile of the used starting material. (Ha et al., 2017, Lodi and Boschi, 2017)

The control of radiochemical impurities is essential because any radiochemical impurity can potentially affect the biodistribution of the PET radiopharmaceutical, thus giving a misleading imaging result. It is also important to avoid the patient being subjected to unnecessary radiation exposure. Measurement of RCP requires the use of a method to separate the different labeled chemical species which may be present in the PET radiopharmaceutical preparation. (Ha et al., 2017, Lodi and Boschi, 2017)

Chromatographic methods are commonly used in radiochemical determination because they can effectively separate and quantify the radioactive species in the sample. RCP is typically determined via radio-HPLC. In addition, for accurate determination of RCP, an analysis by radio-TLC may also be necessary. This is because of the fact that certain radioactive species can be under-represented in HPLC. For ^{68}Ga -labeled radiopharmaceuticals, RCP by HPLC is the main test that must be performed before medical use to determine the percentage of free ^{68}Ga . The presence of ^{68}Ga in colloidal form is possible to check, for example, by TLC. In general, the RCP should be >95%. (Lamesa et al., 2015, Ha et al., 2017, Lodi and Boschi, 2017, Schmidt et al., 2017)

Radionuclidic purity is the ratio of the desired radionuclide activity to the total activity. Radionuclidic purity is expressed as a percentage. The purpose of testing radionuclidic purity is to ensure that the PET radiopharmaceutical is not contaminated with other radionuclides. While using $^{68}\text{Ge}/^{68}\text{Ga}$ generators, the potential breakthrough of ^{68}Ge with eluted ^{68}Ga must be taken into account. Cyclotron production of ^{68}Ga eliminates the possibility of ^{68}Ge breakthrough. Radionuclidic impurities can impact the image quality and contribute significantly to the patient's overall radiation dose. The pharmacopoeia monographs prescribe the required radionuclidic purity and may set limits for specific radionuclidic impurities. (Ha et al., 2017, Lodi and Boschi, 2017, Schmidt et al., 2017, Lin et al., 2018)

Chemical purity concerns non-radioactive materials in PET radiopharmaceuticals. It involves by-products, solvents and other residual components used in the production process as well as non-radioactive materials like additives and stabilizers that are intentionally added to the PET radiopharmaceuticals. All non-radioactive substances that can either affect radiolabeling or directly produce adverse biological effects in patients are considered chemical impurities. (Ha et al., 2017, Lodi and Boschi, 2017)

In pharmacopoeia monographs chemical purity is controlled by setting specific limits on chemical impurities. Impurities are typically determined by chromatographic techniques. For example, HPLC or TLC can be used to characterize and determine the quantity of potential chemical contaminants in the final product. The purpose of testing is to ensure that the purification process has reduced residual amounts of impurities to below allowed limits. Impurities are typically quantified using HPLC combined with ultraviolet (UV) absorbance detection (HPLC/UV). Ultra performance liquid chromatography (UPLC) is also used for analysing PET radiopharmaceuticals (Franck et al., 2009, Kryza and Janier, 2013). This technique offers the advantages of faster separation times and more compact separation columns. For those PET radiopharmaceuticals that are labeled by a chelation reaction, the most significant impurity is unlabeled radioisotope, which can be detected via radio-TLC. (Ha et al., 2017, Lodi and Boschi, 2017)

The identity of each peak in the detected chromatogram is determined by comparison of retention time with reference standards. The quantity is generally determined from the peak area. In the case of known impurities, the amount present in the sample is compared with allowed regulatory limits. Regarding unknown impurities, as long as these impurities are below the limit of observed adverse effects in preclinical toxicology studies, they may be safe for injection. (Ha et al., 2017)

Residual solvents are defined as organic volatile chemicals that are used or produced in the manufacture of drug substances or excipients, or in the preparation of drug products. Residual solvents may be the result of the PET radiopharmaceutical synthesis or originate from packaging and storage. Residual solvents in the final formulation may exhibit a variety of toxic effects. The remaining amounts of all solvents used during the synthesis and purification process must be monitored to ensure residual amounts are below safe limits. For example, Ph. Eur. sets a specified limit for EtOH content (Ph. Eur., 2013). Residual solvents are usually determined by chromatographic techniques such as gas chromatography (GC) in conjunction with a flame ionization detector (FID). (Ha et al., 2017, Lodi and Boschi, 2017)

2.2.4.2 Biological tests

One example of a QC criterion specific to short-lived PET radiopharmaceuticals is the permission to release them before completion of all tests. PET radiopharmaceutical preparations must be manufactured using precautions designed to exclude microbial contamination and to ensure sterility. However, sterility tests, for example, are not compatible with the short half-life. Thus, sterilization of the final product or final sterile filtration (0.22 μm filter) and performance of a filter integrity test, bubble point test, is required prior to the release. (Ha et al., 2017, Lodi and Boschi, 2017, Schmidt et al., 2017)

The test for sterility is carried out under aseptic conditions by inoculating the sample in two culture media, and by incubating for not less than 14 days. Because the timeframe is much longer than the half-life of PET radioisotopes, a quick, short-term test is allowed to be used to facilitate early release of the PET radiopharmaceutical. In the short-term test, the integrity of the filter membrane is assessed, typically via a bubble point test, after completing sterile filtration. Compressed gas is applied to the inlet of the wetted filter and pressure is increased until bubbling appears at the outlet, the bubble point. If the bubble point exceeds a threshold pressure, it can be assured that the membrane is intact and pores do not exceed the specified size. A drawback of this test is that the operator has to manually handle the active filter membrane. (Ha et al., 2017, Lodi and Boschi, 2017)

Bacterial endotoxins (pyrogens) are polysaccharides from bacterial gram-negative membranes which are heat stable, water-soluble and filterable. Their presence in a PET radiopharmaceutical preparation can cause fever and also leucopenia in immunosuppressed patients. To minimize the presence of pyrogens, it is important that preparations are manufactured and dispensed under aseptic conditions. Endotoxins can contaminate a solution even if the bacteria have been

thoroughly removed via sterile filtration. Therefore, it is necessary to test PET radiopharmaceutical formulations for the presence of endotoxins. Modern automated endotoxin testers are able to provide valid results within a few minutes. Bioburden analysis can be achieved by running synthetic steps without radioactivity. The effluent is collected at intermediate steps and at the endpoint of the synthetic process without filter sterilization and subsequent sterility testing. (Elsinga et al., 2010, Ha et al., 2017, Lodi and Boschi, 2017, Schmidt et al., 2017)

2.2.4.3 Examples of analytical techniques used in quality control of PET radiopharmaceuticals

Chromatographic separation methods are commonly employed in the QC of PET radiopharmaceuticals. Chromatography is an analytical technique based on the separation of two or more compounds by the distribution between two phases, a stationary phase and a mobile phase. The two phases can be solid-liquid, liquid-liquid or gas-liquid. Chromatographic separation methods are commonly employed in radiochemical, chemical and enantiomeric purity determinations. HPLC, TLC and GC are commonly used chromatographic methods. (Lodi and Boschi, 2017)

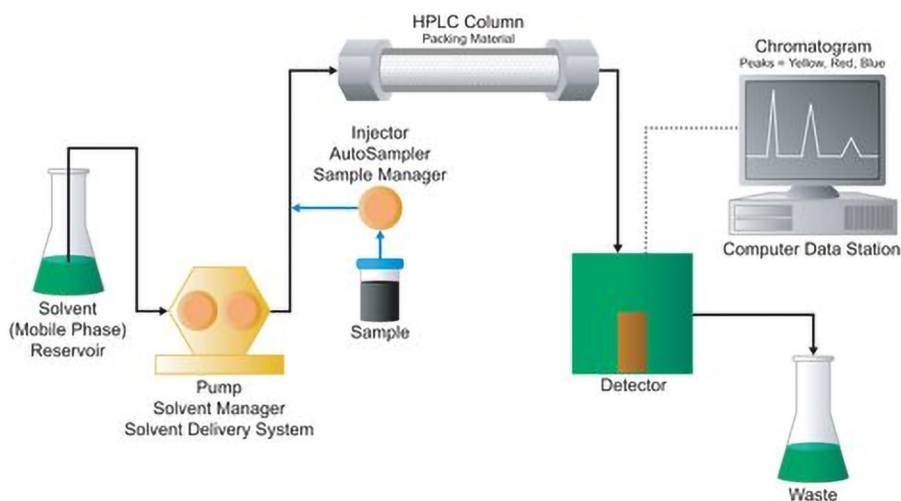


Figure 13. HPLC system. (Waters Corporation, 2014)

HPLC is a type of liquid chromatography used to separate and quantify compounds that have been dissolved in a solution. HPLC consists of a number of components, including reusable columns that hold packing material, stationary phase, and high

pressure pumps that move the mobile phase through the columns (Figure 13.). Column packings consist of small particles designed to provide high separation efficiencies. Other components are an injector to introduce the sample in a small volume and a detector that shows the retention time of the molecules for identification and quantitation. Retention time varies depending on the specific chemical or physical interactions between the stationary phase, the solvent used as a mobile phase and the molecules being analysed. The coupling of radioactivity detectors to the system makes it possible to apply HPLC to PET radiopharmaceuticals. Radioactivity detectors are used to determine the RCP. The ratios of the areas under the peaks give the ratios or percentage of the RAC of the compounds. In addition, the retention time of each compound allows for radiochemical identification. This is performed by comparing the solutions of the same non-radioactive chemical substances, referred to as “cold standard”, using a suitable detection method. (Nunn and Fritzberg, 1986, Lodi and Boschi, 2017)

Types of HPLC generally depend on the phase system used in the process. Normal-phase chromatography (NP-HPLC), reversed-phase chromatography (RP-HPLC) and ion-exchange chromatography are the commonly used types of HPLC in the QC of PET radiopharmaceuticals. NP-HPLC separates analytes based on polarity. RP-HPLC has a non-polar stationary phase and an aqueous, moderately polar mobile phase. RP-HPLC operates on the principle of hydrophobic interactions. They result from repulsive forces between non-polar stationary phase, the relatively non-polar analyte and a polar eluent. Polar compounds are weakly retained and are rapidly eluted by largely aqueous solvent systems. Non-polar compounds are more strongly retained and require increased proportions of organic solvent for elution. The most common type of packing for RP-HPLC is silica gel to which non-polar or alkyl groups are

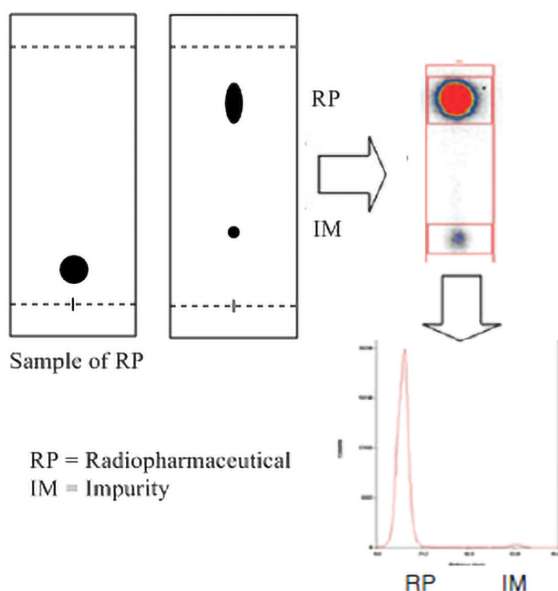


Figure 14. Principle of TLC and development of the plate. (Modified from Lodi and Boschi, 2017)

covalently attached. (Nunn and Fritzberg, 1986, Lodi and Boschi, 2017)

TLC is based on distribution of analyte between a thin layer of sorbent on a solid support and liquid phase moving along the sorbent by capillary force. TLC technique can be used to verify RCP. A small sample of the PET radiopharmaceutical is applied on the marked origin spot on the TLC plate (Figure 14.) and the TLC plate is placed in the development chamber filled with a small amount of mobile phase. The solvent travels from the bottom of the chamber up to the layer of adsorbent by capillary action, passes over the spot and moves the compounds in the mixture up the plate at different rates. The result is the separation of the compounds due to the differences in their affinity to the stationary phase and because of differences in solubility in the solvent. The position of radioactive spots is detected by autoradiography or by measurement of radioactivity over the length of the chromatogram using suitable collimated counters (Figure 14.). TLC can also provide a chromatographic measurement known as retardation factor. (Lodi and Boschi, 2017)

GC is a gas-liquid chromatography which involves a sample being vaporized and injected onto the head of the chromatographic column (Figure 15.). GC is a technique for the separation of components of mixtures. GC consists of the capillary, i.e. the open-tubular column, liquid and solid stationary phases, carrier gas as the mobile phase, the key mechanisms of the interaction of the solutes migrating through a column with the stationary phase, as well as temperature and pressure programming. The sample is transported through the column by the flow of inert, gaseous mobile phase. Commonly used mobile phases are nitrogen, helium and argon. The most commonly used detector type is the FID. Due to the volatility of organic solvents, GC is commonly used to identify and quantify the presence of residual solvents, such as acetone and EtOH, in PET radiopharmaceutical preparations. (Blumberg, 2012, Ph. Eur., 2013, Lodi and Boschi, 2017)

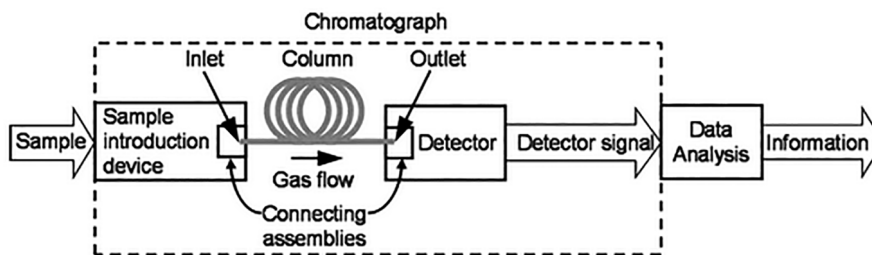


Figure 15. GC system. (Blumberg, 2012)

2.2.5 Good manufacturing practice

A comprehensively designed and correctly implemented quality assurance (QA) system is of utmost importance in order to achieve the quality objectives. QA system is necessary to ensure that the safety and quality of ^{68}Ga -labeled PET radiopharmaceuticals are adequate for the intended use. All instruments, equipment and technologies that may affect the quality of the product should undergo proper qualification protocols. Written and approved protocols specifying the acceptance criteria, critical steps and qualification procedure should be established. (Boschi et al., 2013)

The aim of pharmaceutical GMP is to ensure the delivery of a consistently high-quality product that is appropriate for its intended use. The product also has to meet the specifications of its marketing authorization. FDA has released the cGMP requirements and guidance documents for PET drug products in 2005. The cGMP regulations are the minimum set of requirements for a facility to develop agents for commercial use. (Chi et al., 2014, Ballinger and Kozirowski, 2017)

The main components of GMP are personnel, procedures and documentation, as well as facilities and equipment. All these are governed by a quality management system. Personnel must be adequately trained in any procedures they carry out. The training record must indicate that the member of staff has read the Standard operating procedure (SOP) and has demonstrated competence with evidence of a certain number of monitored activities. Persons who perform aseptic procedures must undergo periodic revalidation of their competence. The authorities and responsibilities at each level of staff must be specified. (Ballinger and Kozirowski, 2017)

There has to be a person designated as production manager, or sometimes called responsible person. This person is responsible for the routine operation of the facility. Production manager ensures that the PET radiopharmaceuticals are produced according to the GMP standard (Ballinger and Kozirowski, 2017)

All SOPs must be written down, approved and reviewed at regular intervals. QA results must include evidence that the analytical equipment has been properly calibrated. The quality of starting materials is one of the underpinning features of GMP. Precursors must be obtained from approved vendors. There must be a process for inspecting or auditing vendors. All chemicals that remain in the final formulation of the PET radiopharmaceutical must be obtained from certified pharmaceutical suppliers, and active pharmaceutical ingredients must be obtained from a certified GMP source. Peptides derivatized with a suitable chelator for ^{68}Ga must be certified to meet the requirements described in the relevant pharmacopoeial monograph, or in the absence of such a monograph, a monograph of the manufacturer approved by pharmaceutical authorities. Several commonly used peptides are commercially available in GMP quality with a certificate of

analysis. However, their cost is relatively high and they are not readily available in all countries. In the future, an increasing number of peptides with potential as precursors for ^{68}Ga -labeled PET radiopharmaceuticals will come commercially available with a GMP certificate but some time may still be required. (Decristoforo et al., 2012, Ballinger and Kozirowski, 2017)

The design and construction of facilities must afford a clean environment. Surfaces must be impervious and able to withstand regular cleaning. Proper operation of the facility must be documented by routine environmental and microbiological monitoring. Generally, radiosynthesis can be carried out in a Grade C environment. However, sterile filtration and dispensing must be carried out in a Grade A environment. These are generally achieved with a hot cell, laminar airflow cabinet or pharmaceutical isolator. All equipment must be kept in good working order with regular checks of performance and records of maintenance undertaken. (Ballinger and Kozirowski, 2017)

The application of GMP to the production of PET radiopharmaceuticals has two separate challenges. The first challenge is related to the short half-lives of most radionuclides used in PET and, thus, the QC of these PET radiopharmaceuticals. The second challenge is related to the small-scale production. There should be clear segregation of responsibilities for production and QC. In addition, there should be independent release. Small-scale production of a range of products is carried out with a small number of automated synthesis units. In the past, this often involved reusable apparatus. Accordingly, there had to be a validated cleaning procedure between operations and a strict regime of segregation. Nowadays, sterile single-use cassettes are available for many products, which will make the production less risky and more reliable. Before a new product is introduced, there must be a number of validation runs with full analysis to establish the reproducibility and the quality of the product. (Ballinger and Kozirowski, 2017)

3 Aims

The purpose of this study was to prepare GMP-grade ^{68}Ga -labeled DOTA-Siglec-9 available for clinical studies so that its suitability for PET imaging of inflammation in humans can be evaluated in the future. *In vitro* plasma protein binding studies were also performed to determine how [^{68}Ga]Ga-DOTA-Siglec-9 translates between different species.

In addition, the purpose of this study was to examine bis(phosphonate)-induced bone accumulation of ^{68}Ga -labeled NOTA-chelated bis(phosphonate)-conjugated oligoribonucleotide. Biodistribution analysis of ^{68}Ga -labeled oligoribonucleotide was performed using PET imaging.

More specifically, the aims of the study were:

1. To develop a fully automated protocol for producing GMP-grade [^{68}Ga]Ga-DOTA-Siglec-9 for clinical studies.
2. To study the stability and plasma protein binding of [^{68}Ga]Ga-DOTA-Siglec-9 in blood *in vitro* in five different species, including human.
3. To prepare ^{68}Ga -labeled NOTA-chelated bis(phosphonate)-conjugated anti-microRNA-21/microRNA-21 double helix.
4. To study the bone accumulation, whole-body biodistribution and *in vivo* stability of ^{68}Ga -labeled NOTA-chelated bis(phosphonate)-conjugated anti-microRNA-21/microRNA-21 double helix in healthy rats.

4 Materials and Methods

All radiation work complied with the regulations of the Radiation and Nuclear Safety Authority of Finland. All animal experiments were approved by the National Animal Experiment Board in Finland and the Regional State Administrative Agency for Southern Finland. All animal experiments were conducted in accordance with the EU Directive on the protection of animals used for scientific purposes.

4.1 ^{68}Ga -labeling and quality control (Subprojects I-III)

4.1.1 Fractionated method for producing nonGMP-grade [^{68}Ga]Ga-DOTA-Siglec-9 and related quality control (Subproject I)

The synthesis was performed manually using the fractionated method. ^{68}Ga was eluted with 0.1 M HCl (6 mL) from a $^{68}\text{Ge}/^{68}\text{Ga}$ generator (IGG100, 50 mCi (1850 MBq); Eckert & Ziegler AG). Activity in MBq means the activity of parent isotope ^{68}Ge adsorbed on the column at the assay date of the generator. A fraction (0.7–1.0 mL) with the highest RAC (280–360 MBq) was collected for subsequent use. The ^{68}Ga -eluate (0.5 mL) was mixed with HEPES (120 mg) to give a pH of approximately 4.1. The pH was measured using pH paper (Macherey Nagel). DOTA-Siglec-9 peptide (Peptide Specialty Laboratories GmbH, nonGMP-grade) was stored in freezer as a 1 mM solution dissolved in deionized water and was let to melt before use. DOTA-Siglec-9 peptide (3–35 nmol, 7.3–85 μg) was added and the reaction mixture was heated at 100 °C for 15 minutes. The pH was adjusted between 6–8 by adding 1 M NaOH (85 μL), if needed for injection. No further purification was performed. Total synthesis time was approximately 20 minutes, starting from the $^{68}\text{Ge}/^{68}\text{Ga}$ generator elution.

RCP of nonGMP-grade [^{68}Ga]Ga-DOTA-Siglec-9 was determined using radio-HPLC. The radio-HPLC system consisted of LaChrom Instruments (Hitachi, Merck) and a Radiomatic 150TR radioisotope detector (Packard). C18 column

(Phenomenex Jupiter, 4.6 × 150 mm, 300Å, 5 µm) with the following HPLC conditions was used (Table 3.). Solvent A was water containing 0.1% trifluoroacetic acid (TFA) and solvent B was acetonitrile (ACN) containing 0.1% TFA. Flow rate was 1 mL/min and $\lambda = 215$ nm.

Table 3. Gradient for [⁶⁸Ga]Ga-DOTA-Siglec-9.

t/min	0.1 % TFA/H ₂ O (%)	0.1 % TFA/ACN (%)
0.0	82	18
2.0	82	18
11.0	40	60
15.0	82	18
20.0	82	18

4.1.2 GMP-grade [⁶⁸Ga]Ga-DOTA-Siglec-9 (Subproject II)

4.1.2.1 Radiosynthesis of GMP-grade [⁶⁸Ga]Ga-DOTA-Siglec-9 using an acetone-based method and related quality control

For the synthesis, the Modular-Lab PharmTracer radiosynthesis device and C4-GA68-PP cassettes (Eckert & Ziegler AG) were used. In this acetone-based method, ⁶⁸Ga was eluted from a ⁶⁸Ge/⁶⁸Ga generator (IGG100, 50 mCi (1850 MBq); Eckert & Ziegler AG) using 0.1 M HCl (6 mL) and loaded onto a Strata-XC cation exchange cartridge. [⁶⁸Ga]GaCl₃ was passed through the Strata-XC cation exchange cartridge and acidified acetone (0.8 mL, containing 0.02 M HCl and 3.25% water) was used to elute the radionuclide ⁶⁸Ga from the Strata-XC into the reaction vial. The reaction vial contained GMP-grade DOTA-Siglec-9 precursor (80 µL, 40 µg, 16.5 nmol; ABX Advanced Biomedical Compounds GmbH), 0.2 M NaOAc buffer (2 mL, pH 4.0) and absolute EtOH (0.2 mL). The reaction mixture was kept at 65°C for 6 minutes (Figure 16.). Acetone was gradually evaporated into the waste vial via vent tubing during the reaction time.

Reaction mixture was diluted using 4 mL physiological saline (0.9 mg/mL) and passed through a tC18 cartridge, which was washed twice with physiological saline (8 mL). Purified [⁶⁸Ga]Ga-DOTA-Siglec-9 was eluted from the tC18 cartridge into an end product vial with 70% EtOH (1.3 mL) via a filter (0.22 µm) and formulated into physiological saline (8.7 mL). Total synthesis time was 25 minutes, starting from the ⁶⁸Ge/⁶⁸Ga generator elution until the final product is ready for administration to human use.

The QC analysis of the GMP-grade [^{68}Ga]Ga-DOTA-Siglec-9 consisted of chemical, physical and biological tests. Appearance of the final product was assessed by visual inspection, pH was measured using pH indicator strips (Macherey Nagel), radionuclidic identity was determined by measuring half-life using a dose calibrator, and radionuclidic purity was measured using a gamma counter. RCP, chemical purity and identity were analyzed using HPLC. RCP was also analyzed using TLC. Integrity of the sterile filter (0.22 μm) was controlled immediately after the radiosynthesis as a short-time test by a bubble-point test. Residual solvents (EtOH and acetone content) were measured post-release by GC-FID using the standard protocols of Turku PET Centre GMP production unit. Also, radionuclidic purity was measured post-release after complete decay of ^{68}Ga ($t \geq 48$ hours). Tests for sterility and bacterial endotoxins were carried out post-release.

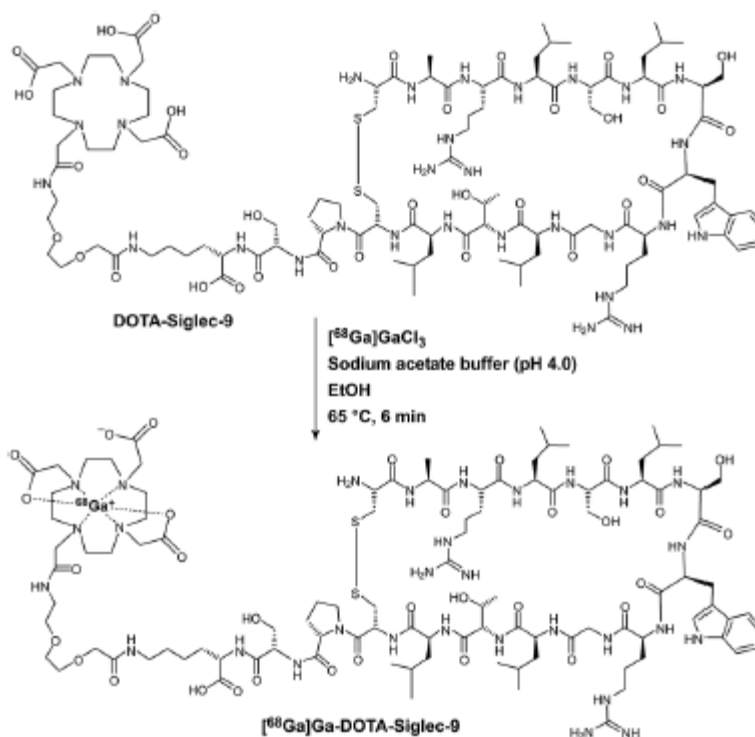


Figure 16. Radiosynthesis of GMP-grade [^{68}Ga]Ga-DOTA-Siglec-9.

The HPLC system (Shimadzu Prominence) was equipped with a radiodetector (Ortec, Model 266). C18 column (Phenomenex Kinetex, 4.6 \times 75 mm, 100 \AA , 2.6 μm) with the following HPLC conditions was used. Solvent A was water containing 0.16% TFA and solvent B was ACN containing 0.16% TFA. Linear

gradient from 18% B to 50% B over 12 minutes was in use. Flow rate was 1 mL/min and $\lambda = 220$ nm.

The eluent used for the instant thin-layer chromatography (iTLC) analyses was 50% methanol in 1 M ammonium acetate buffer (pH 3.5) and iTLC silica gel (SG) paper (Varian Inc.) was used. A very small amount (0.5 μ L) of the sample was applied to the iTLC-SG paper and the sample was developed (development path length 5–7 cm). The iTLC-SG paper was exposed against the imaging plate for a suitable time depending on the activity of the sample. The imaging plate was scanned with Fuji FLA-5100 Imager Reader (FUJIFILM Life Science) and Aida Image Analysis software (Elysia Raytest) was used.

4.1.2.2 Radiosynthesis on nonGMP-grade 3'-[⁶⁸Ga]Ga-NOTA-anti-microRNA-21 and related quality control (Subproject III)

The synthesis was performed manually using the fractionated method. ⁶⁸Ga was eluted with 0.1 M HCl (6 mL) from a ⁶⁸Ge/⁶⁸Ga generator (IGG100, 50 mCi (1850 MBq); Eckert & Ziegler AG). The radioactive elution peak was collected for the ⁶⁸Ga-labeling of nonGMP-grade 3'-NOTA-anti-microRNA-21. The ⁶⁸Ga-eluate (0.5 mL) was mixed with NaOAc (18 mg) to give a 0.2 M solution with regard to NaOAc. The pH was adjusted to approximately 3.5 by adding 2 M HCl (47 μ L). The pH was measured using pH paper (Macherey Nagel). 3'-NOTA-anti-microRNA-21 was stored in freezer as a 0.7 mM solution dissolved in deionized water and was let to melt before use. 3'-NOTA-anti-microRNA-21 (20 nmol) was added and the reaction mixture was heated at 95°C for 10 minutes. No further purification was performed. Total synthesis time was approximately 20 minutes, starting from the ⁶⁸Ge/⁶⁸Ga generator elution. After ⁶⁸Ga-labeling, 5'-alendronate-conjugated microRNA-21 (none, 1, 2 or 4 equivalents) was added to the reaction mixture and the mixture was kept at r.t. for approximately 10 minutes to form the double helix (Figure 17.).

RCP of both nonGMP-grade 3'-[⁶⁸Ga]Ga-NOTA-anti-microRNA-21 and the ⁶⁸Ga-labeled double helix structure was determined using a radio-HPLC. The radio-HPLC system consisted of LaChrom Instruments (Hitachi, Merck) and a Radiomatic 150TR radioisotope detector (Packard). C18 column (Waters μ Bondapak, 3.9 \times 150 mm, 125Å, 10 μ m) with the following HPLC conditions was used. Solvent A was ACN, solvent B was 50 mM ammonium acetate (NH₄OAc) and solvent C was 50 mM phosphoric acid (H₃PO₄). Gradient elution from 0% to 50 % ACN in 50 mM NH₄OAc over 17 minutes, followed by washing with aqueous 50 mM H₃PO₄ was used. Flow rate was 1 mL/min and $\lambda = 220$ nm.

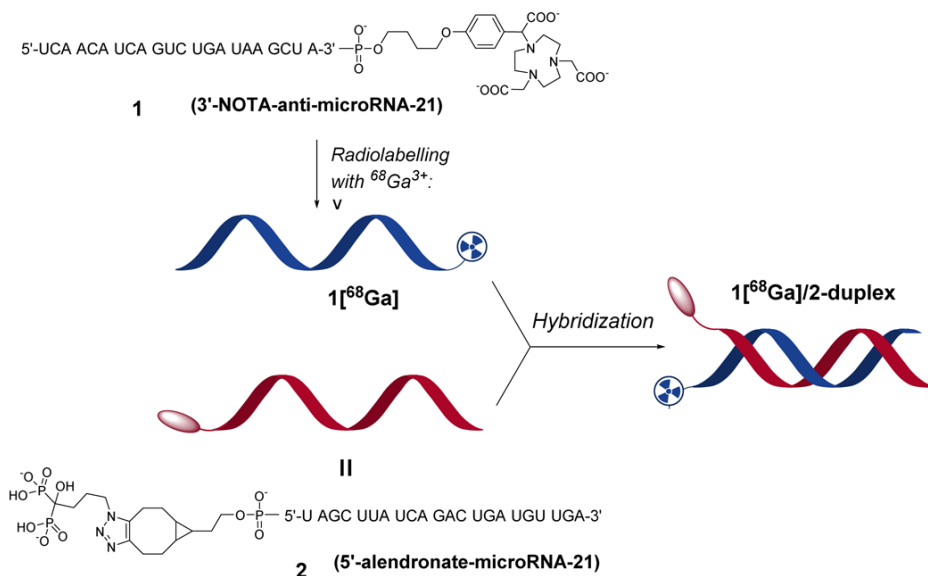


Figure 17. Radiosynthesis of nonGMP-grade 3'-[^{68}Ga]Ga-NOTA-anti-microRNA-21 and hybridization with 5'-alendronate-conjugated microRNA-21 to form the double helix.

4.2 *In vitro* experiments

4.2.1 Plasma protein binding and stability of nonGMP-grade [^{68}Ga]Ga-DOTA-Siglec-9 (Subproject I)

Venous blood samples from five different species were collected in heparinized tubes. These species were male Sprague-Dawley rats ($n = 3$), healthy male C57BL/6N mice ($n = 3$), male New Zealand White rabbits ($n = 3$), female human subjects ($n = 3$) and a male Finnish landrace pig ($n = 1$). Plasma was separated from whole blood by centrifugation. Approximately 1 mL of plasma was transferred to an Eppendorf tube and approximately 0.8 MBq of nonGMP-grade [^{68}Ga]Ga-DOTA-Siglec-9 was added and mixed. The tube was incubated at $+37^\circ\text{C}$ and three parallel sample series (80–100 μL) at 3, 30, 90, 145, 210 and 250 minutes time points were taken. ACN (1:1, v/v) was added to precipitate the plasma proteins. In addition, 10% sulfosalicylic acid (1:1, v/v) was used to precipitate the plasma proteins in order to compare the results (at 90 minutes time point, unpublished material). The mixtures were vortexed and centrifuged (4 minutes, 14,500 rpm). To measure the plasma protein binding, the tubes were counted in a gamma counter (1480 Wizard 3" gamma counter; PerkinElmer/Wallac). After that, the supernatant and precipitate were separated and counted in the gamma counter.

An aliquot of the supernatant was analyzed for tracer stability. The time points for the analyses were 3, 30, 90, 145, 210 and 250 minutes. The aliquot was diluted with 0.1% TFA/H₂O and analyzed by radio-HPLC. The radio-HPLC system consisted of LaChrom Instruments (Hitachi, Merck) and a Radiomatic 150TR radioisotope detector (Packard). C18 column (Phenomenex Jupiter, 10 × 250 mm, 300Å, 5 μm) with the following HPLC conditions was used (Table 4.). Solvent A was 0.1% TFA/H₂O and solvent B was 0.1% TFA/ACN. Flow rate was 5 mL/min and λ = 215 nm.

Table 4. Gradient used for analyzing the stability of [⁶⁸Ga]Ga-DOTA-Siglec-9 (unpublished material).

t/min	0.1 % TFA/H ₂ O (%)	0.1 % TFA/ACN (%)
0.0	82	18
2.0	82	18
11.0	40	60
14.0	40	60
15.0	82	18
20.0	82	18

4.2.2 Plasma protein binding and stability of nonGMP-grade ⁶⁸Ga-labeled oligoribonucleotide (Subproject III)

Approximately 0.5 MBq of nonGMP-grade 3'-[⁶⁸Ga]Ga-NOTA-anti-microRNA-21 or 3'-[⁶⁸Ga]Ga-NOTA-anti-microRNA-21 + 1, 2 or 4 equivalents of 5'-alendronate-conjugated microRNA-21 was added to an Eppendorf tube containing rat's plasma (approximately 1 mL) and mixed. The tube was incubated at +37°C and three parallel sample series (100 μL) at 10, 30 and 60 minutes time points were taken. ACN (1:1, v/v) was added to precipitate the plasma proteins. The mixtures were vortexed and centrifuged (4 minutes, 14,500 rpm). The tubes were counted in a gamma counter (1480 Wizard 3" gamma counter; PerkinElmer/Wallac), and the supernatant and precipitate were separated and counted in the gamma counter to measure plasma protein binding (unpublished material).

An aliquot of the supernatant was analyzed for stability (unpublished material). The aliquot was diluted using 50 mM NH₄OAc and analyzed by radio-HPLC. C18 column (Waters μBondapak, 7.8 × 300 mm, 125Å, 10 μm) with the following HPLC conditions was used. Flow rate was 5 mL/min and λ = 260 nm. Solvent A was 50 mM NH₄OAc, solvent B was ACN and solvent C was 50 mM H₃PO₄. Two slightly different gradients were used (Table 5. and Table 6.).

Table 5. Gradient 1 used for analyzing the stability of 3'-[⁶⁸Ga]Ga-NOTA-anti-microRNA-21 (unpublished material).

t/min	50 mM NH ₄ OAc (%)	ACN (%)	50 mM H ₃ PO ₄ (%)
0.0	100	0	0
17.0	50	50	0
18.0	0	0	100
25.0	0	0	100
27.0	100	0	0
30.0	100	0	0

Table 6. Gradient 2 used for analyzing stability of 3'-[⁶⁸Ga]Ga-NOTA-anti-microRNA-21 + 1, 2 or 4 equivalents of 5'-alendronate-conjugated microRNA-21.

t/min	50 mM NH ₄ OAc (%)	ACN (%)	50 mM H ₃ PO ₄ (%)
0.0	100	0	0
11.0	50	50	0
12.0	0	0	100
16.0	0	0	100
18.0	100	0	0
20.0	100	0	0

Stability of the nonGMP-grade ⁶⁸Ga-labeled oligoribonucleotide at r.t. was also studied (unpublished material). NonGMP-grade 3'-[⁶⁸Ga]Ga-NOTA-anti-microRNA-21 or 3'-[⁶⁸Ga]Ga-NOTA-anti-microRNA-21 + 1, 2 or 4 equivalents of 5'-alendronate-conjugated microRNA-21 was kept at r.t. Aliquots (1 μL) were taken and analyzed at 0, 60, 120 and 180 minutes time points. C18 C18 column (Waters μBondapak, 7.8 × 300 mm, 125Å, 10 μm) with the following HPLC conditions was used. Solvent A was 50 mM NH₄OAc, solvent B was ACN and solvent C was 50 mM H₃PO₄. Flow rate was 5 mL/min and λ = 260 nm. Three slightly different gradients were used (Table 5., Table 6. and Table 7.).

Table 7. Gradient 3 used for analyzing the stability of 3'-[⁶⁸Ga]Ga-NOTA-anti-microRNA-21 + 1 equivalent of 5'-alendronate-conjugated microRNA-21.

t/min	50 mM NH ₄ OAc (%)	ACN (%)	50 mM H ₃ PO ₄ (%)
0.0	100	0	0
25.0	50	50	0
26.0	0	0	100
32.0	0	0	100
33.5	100	0	0
35.0	100	0	0

4.3 *In vivo* studies

4.3.1 *In vivo* imaging with nonGMP-grade ⁶⁸Ga-labeled oligoribonucleotide (Subproject III)

Mature and healthy male Sprague-Dawley rats (weight 441 ± 41 g, $n = 4$ per experiment) were anesthetized with isoflurane. 3'-[⁶⁸Ga]Ga-NOTA-anti-microRNA-21 or 3'-[⁶⁸Ga]Ga-NOTA-anti-microRNA-21 + 1, 2 or 4 equivalents of 5'-alendronate-conjugated microRNA-21 were i.v. injected via tail vein (25 ± 1.5 MBq (6.4 ± 0.47 nmol)). The concentration of oligoribonucleotide in blood circulation immediately after the injection was 0.23 ± 0.037 μ M based on the estimated total volume of blood.

In vivo imaging and the whole-body distribution kinetics of i.v. administered radioactivity were evaluated using a high-resolution research tomograph PET camera (Siemens Medical Solutions). Two rats were imaged at the same time. Rats were kept on a warm pallet during the imaging procedure. Data acquired for 60 minutes in a list mode, starting at the same as the injection, were iteratively reconstructed with the ordered-subsets expectation maximization 3D (OSEM3D) algorithm. Quantitative analysis was performed by defining regions of interest (ROI) in several organs (heart, kidney cortex, kidney medulla, knees, liver and urinary bladder) with Carimas software version 2.9 (Turku PET Centre). The average RAC in the ROI (kBq/mL) was used for further analyses. The uptake was reported as standardized uptake value (SUV) and time-radioactivity curves (TACs). SUV was calculated as the RAC of the ROI divided by the relative injected radioactivity expressed per animal bodyweight. Also the radioactivity remaining in the injection site (tail) was compensated.

In addition, the bone uptake of ⁶⁸Ga-labeled oligoribonucleotide was studied in more detail using PET/CT camera. Four male, small Sprague-Dawley rats were

PET/CT imaged with a dedicated small animal scanner (Inveon Multimodality, Siemens Medical Solutions). Prior to PET, CT was performed for attenuation correction and anatomical reference. After that, rats (weight 85 ± 12 g) were i.v. injected with nonGMP-grade ^{68}Ga -labeled oligoribonucleotide (22 ± 0.4 MBq, $n = 1$ per compound). The PET data acquired for 60 minutes was reconstructed with OSEM3D. PET/CT images were visually observed with Inveon Research Workplace 4.1 software (Siemens Medical Solutions).

4.3.2 Blood and urine samples (Subproject III)

Rats were i.v. injected with nonGMP-grade $3'-[^{68}\text{Ga}]\text{Ga-NOTA-anti-microRNA-21}$ or $3'-[^{68}\text{Ga}]\text{Ga-NOTA-anti-microRNA-21} + 1, 2$ or 4 equivalents of $5'$ -alendronate-conjugated microRNA-21. Blood and urine samples were obtained after 60 minutes PET imaging. ACN (1:1, v/v) was added to precipitate the plasma proteins. The mixtures were vortexed and centrifuged (4 minutes, 14,500 rpm). The supernatant and precipitate were separated and an aliquot of the supernatant was analyzed for the stability. The aliquot was diluted using 50 mM NH_4OAc and analyzed by radio-HPLC. C18 column (Waters $\mu\text{Bondapak}$, 7.8×300 mm, 125\AA , $10\ \mu\text{m}$) was used, flow rate was 5 mL/min and $\lambda = 260$ nm. Solvent A was 50 mM NH_4OAc , solvent B was ACN and solvent C was 50 mM H_3PO_4 . Two slightly different gradients were used (Table 5. and Table 6.).

Urine samples were diluted using 50 mM NH_4OAc and analyzed by radio-HPLC. C18 column (Waters $\mu\text{Bondapak}$, 7.8×300 mm, 125\AA , $10\ \mu\text{m}$) was used, flow rate was 5 mL/min and $\lambda = 260$ nm. Solvent A was 50 mM NH_4OAc , solvent B was ACN and solvent C was 50 mM H_3PO_4 . Two slightly different gradients were used (Table 5. and Table 6.).

4.4 *Ex vivo* biodistribution experiments (Subproject III)

Ex vivo biodistribution was determined after the PET imaging. Rats were euthanized after PET imaging and the RAC in excised organs and tissues was measured with a gamma counter (1480 Wizard 3" gamma counter; PerkinElmer/Wallac). Measured radioactivity was corrected for decay, weight of the organs, and animal and background radioactivity. Measured radioactivity was expressed as SUV. Examined organs and tissues were bone, bone marrow, heart, kidneys, liver, lungs, pancreas, plasma, salivary glands, skin, spleen and urine.

4.5 UV-melting profile analysis of 3'-NOTA-anti-microRNA-21/5'-bis(phosphonate)-microRNA-21 double helix (Subproject III)

UV-melting profile analysis of 3'-NOTA-anti-microRNA-21/5'-bis(phosphonate)-microRNA-21 double helix was performed. Melting curves were measured at 260 nm on a UV-VIS light spectrometer equipped with a multiple cell holder and a Peltier temperature controller. The temperature was changed at a rate of 0.5 °C/min. The measurements were performed in aqueous solutions of 2 µM of 3'-NOTA-anti-microRNA-21 and 5'-alendronate-conjugated microRNA-21, with 10 mM sodium cacodylate and 0.1 M NaCl (pH 7.0) and of 1 µM of 3'-[^{69/71}Ga]^{69/71}Ga-NOTA-anti-microRNA-21 and 5'-alendronate-conjugated microRNA-21, with 0.2 M NaOAc and 0.05 M NaCl (pH 9.0) (⁶⁸Ga-labeling conditions mimicked).

4.6 Statistical analyses

All data are expressed as the mean ± standard deviation (SD) with two significant figures. Different tissues from the same subject were compared using Student's t-test for paired data and unpaired Student's t-test for comparison between two study groups. P-values less than 0.05 were considered statistically significant.

5 Results

5.1 Radiosynthesis and quality control (Subprojects I-III)

5.1.1 NonGMP-grade [⁶⁸Ga]Ga-DOTA-Siglec-9 using fractionated method (Subproject I)

Fractionated method was used for producing nonGMP-grade [⁶⁸Ga]Ga-DOTA-Siglec-9. QC was done using radio-HPLC. The reaction mixture was $\geq 95\%$ radiochemically pure. Molar activity was up to 70 MBq/nmol (63 ± 7 MBq/nmol, when the lowest amount of precursor (3 nmol) was used in the synthesis). In this context, molar activity is a theoretical value using all analogues of DOTA-Siglec-9 independent of binding or not and assuming that all of the peptide used will end up in the product. RCY of the radiosynthesis was $71 \pm 2\%$ (non decay-corrected). Overall yield (the yield of the radiosynthesis \times the radioactivity coming out of the ⁶⁸Ge/⁶⁸Ga generator) was $40 \pm 2\%$ ($n = 4$). Retention time of nonGMP-grade [⁶⁸Ga]Ga-DOTA-Siglec-9 was approximately 9.8 minutes.

5.1.2 GMP-grade [⁶⁸Ga]Ga-DOTA-Siglec-9 using acetone-based (Subproject II)

GMP-grade [⁶⁸Ga]Ga-DOTA-Siglec-9 was produced using acetone-based method. Radio-HPLC and radio-TLC were used for QC analyses (Figure 18.). Using radio-HPLC, RCP was $> 95\%$ ($n = 5$) and also chemical purity was $> 95\%$. RCP was also confirmed by iTLC. RCP was $> 95\%$ ($n = 3$). It was observed that [⁶⁸Ga]Ga-DOTA-Siglec-9 migrated clearly up from the baseline on iTLC plates. The decay-corrected RCY was $90 \pm 3\%$ ($n = 3$). As an example, in one of the produced batches, the radioactivity of the end product was 1106 MBq in 10 mL of physiological saline at EOS and molar activity was 67 GBq/ μ mol.

The amounts of radioactivity stuck on the reaction vial and tC18 cartridge were found to be insignificant ($< 2\%$). The automated process was programmed to wash the tC18 cartridge twice during the purification process in order to make sure that the acetone content in the end product would remain under the limit required for

human use (0.5%). In randomly selected batches ($n = 3$), GC using the standard protocols of the Turku PET Centre GMP production unit revealed no detectable amount of acetone (0.0%) in the final product. In addition, the EtOH content ($8.8 \pm 0.1\%$, $n = 3$) was observed to be under the limit (10%) as well. The product was stable at r.t. for 4 hours. Longer times were not tested.

The total content of DOTA-Siglec-9 peptide in each batch was below the limit of $4.1 \mu\text{g/mL}$. $[^{68}\text{Ga}]\text{Ga-DOTA-Siglec-9}$ is a new PET radiopharmaceutical. Because this tracer has not been studied in humans previously, it was critical to set a dose limit in terms of mass quantity (Koziorowski et al., 2016). In addition, single-dose acute toxicity studies in rats have been performed and no adverse effects have been observed (unpublished data). The concentration limit of the final product was set at $4.1 \mu\text{g/mL}$ in a total volume of 10 mL. This concentration limit was derived from the limit of ^{68}Ga -labeled bombesin antagonist $[^{68}\text{Ga}]\text{Ga-DOTA-4-amino-1-carboxymethylpiperidine-D-Phe-Gln-Trp-Ala-Val-Gly-His-Sta-Leu-NH}_2$. This tracer has been developed in Turku PET Centre earlier (Roivainen et al., 2013).

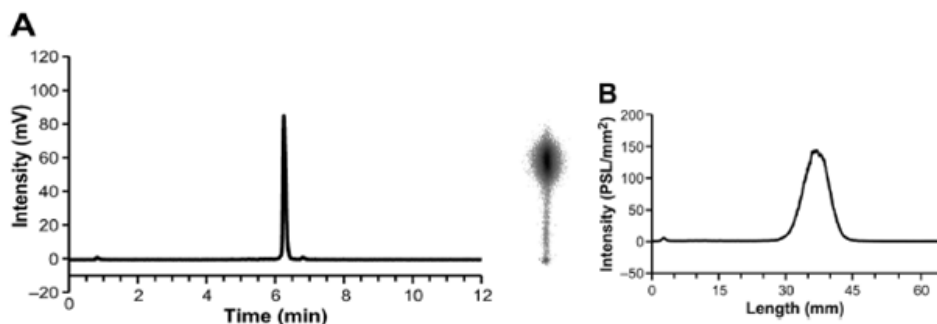


Figure 18. (A) Radiochromatogram of GMP-grade $[^{68}\text{Ga}]\text{Ga-DOTA-Siglec-9}$. (B) Photostimulated luminescence (PSL) imaging of the iTLC plate (the retention factor of $[^{68}\text{Ga}]\text{Ga-DOTA-Siglec-9}$ was 0.57 during 35 minutes of development) and iTLC profile of $[^{68}\text{Ga}]\text{Ga-DOTA-Siglec-9}$.

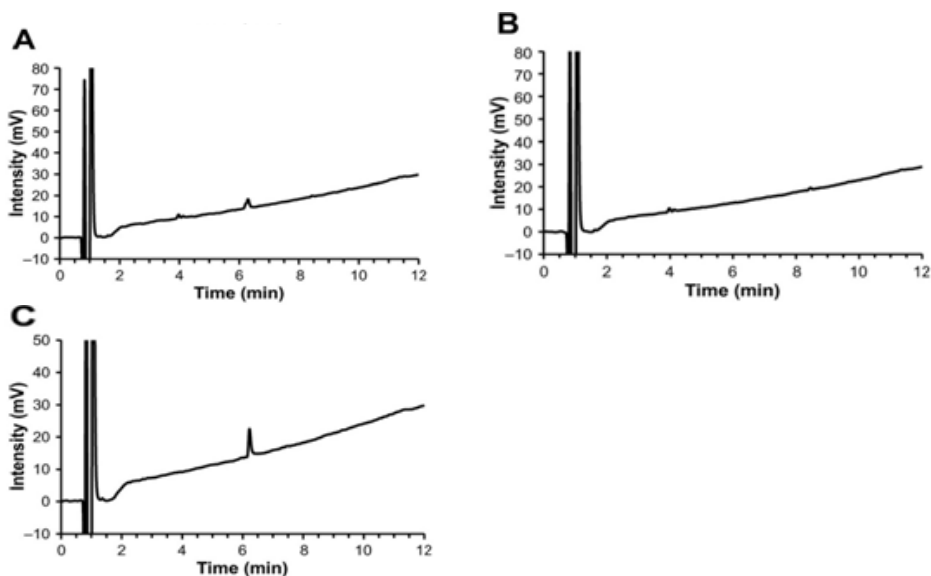


Figure 19. HPLC-chromatograms. (A) The UV peak of GMP-grade $[^{68}\text{Ga}]\text{Ga-DOTA-Siglec-9}$. The small size of the peak is due to the high molar activity at EOS. (B) UV detection of a control sample. The radiosynthesis is performed without addition of precursor DOTA-Siglec-9. (C) UV detection of DOTA-Siglec-9 (reference sample).

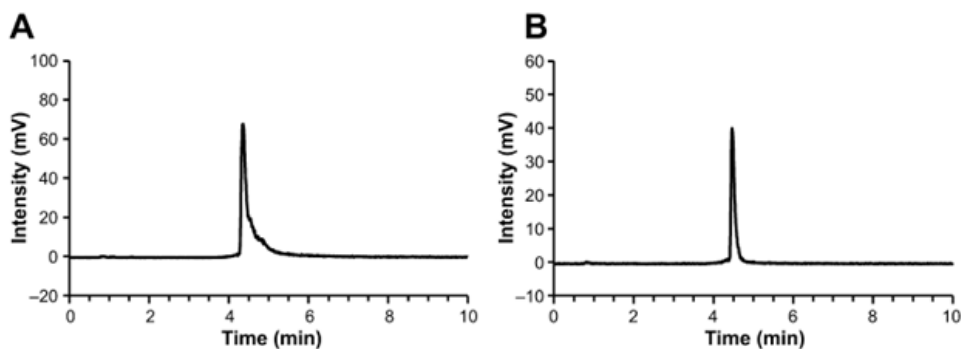
A couple of minor peaks at a retention time of approximately 4 minutes were observed in every produced batch in the UV trace of the HPLC chromatograms (Figure 19.). These minor peaks were not observed in the blank or reference samples. A control radiosynthesis was performed without the precursor compound DOTA-Siglec-9. Otherwise the exactly same protocol as for producing GMP-grade $[^{68}\text{Ga}]\text{Ga-DOTA-Siglec-9}$ was used. The “end product” solution was subjected to HPLC analysis and these minor peaks were observed to appear at the expected retention times. Thus, it was confirmed that these impurity peaks were derived from the radiosynthesis system rather than from the peptide itself.

Different concentrations of TFA in the HPLC solvents were tested before ending up using 0.16% TFA. 0.1% and 0.2% TFA in HPLC solvents were used to find the optimal concentration. C18 column (Phenomenex Kinetex, 4.6×75 mm, 100\AA , $2.6\ \mu\text{m}$) with the following HPLC conditions was used (Table 8.). Solvent A was water containing 0.1% or 0.2% TFA and solvent B was ACN containing 0.1% or 0.2% TFA. Flow rate was 1 mL/min. Retention time of GMP-grade $[^{68}\text{Ga}]\text{Ga-DOTA-Siglec-9}$ was 4.5 minutes when using the above mentioned concentrations of TFA. Using linear gradient and 0.16% TFA (cf. section 4.1.2.3), the retention time of GMP-grade $[^{68}\text{Ga}]\text{Ga-DOTA-Siglec-9}$ was approximately 6.3 minutes.

Table 8. Gradient used for analyzing GMP-grade [^{68}Ga]Ga-DOTA-Siglec-9 using 0.1% and 0.2% TFA.

t/min	TFA/H ₂ O (%)	TFA/ACN (%)
0.0	82	18
1.0	82	18
5.5	40	60
7.0	40	60
7.5	82	18
10.0	82	18

During the variation tests for the HPLC methods, it was observed that the concentration of TFA in the solvents plays an important role in the analysis. A typical TFA concentration for HPLC analysis of peptide-based PET radiopharmaceuticals is 0.1% by volume. However, this was not sufficient for the analysis of GMP-grade [^{68}Ga]Ga-DOTA-Siglec-9. When a higher TFA concentration (0.16% or 0.2%) was used, the peaks were sharp without tailing (Figure 20.).

**Figure 20.** HPLC analysis of GMP-grade [^{68}Ga]Ga-DOTA-Siglec-9 with different concentrations of TFA in the HPLC solvents. (A) [^{68}Ga]Ga-DOTA-Siglec-9 analysis, 0.1% TFA. (B) [^{68}Ga]Ga-DOTA-Siglec-9 analysis, 0.2% TFA.

5.1.2.1 Sticking problem and problem solving

Table 9. Troubleshooting table.

Place and initial loss of the radioactivity	Options	Solution
Waste vial: unreacted ^{68}Ga ~ 20 %	-	Acetone-based method (acidified acetone for elution of the cartridge)
Reaction vial: ~ 20 %	Lower temperature (50°C) Shorter reaction time (5 minutes) Decreased concentration of NaOAc buffer (0.08 M) Reduced concentration of NaCl for elution of SCX (from 5 M to 1.5 M)	Acetone-based method
tC18 cartridge: ~ 30 %	Increased concentration of EtOH Absolute EtOH Different cartridges (C18, C8, hydrophilic–lipophilic balance)	Acetone-based method
Injected radioactivity stuck at the head of the HPLC column	Modification of flow rate Properties of column (C4, C8, well-blocked silanols) Properties of solvent Addition of non-radiolabeled DOTA-Siglec-9	Acetone-based method

During the tests performed, it was observed that the decay-corrected RCY was approximately 30%. The unreacted ^{68}Ga was found in the waste vial and significant amount of radioactivity also remained in the reaction vial and on the tC18 cartridge (Table 9.). Several options to overcome the sticking problem were tried (Table 9.). 1.5 M NaCl was found to be the minimum applicable concentration for elution of an SCX cartridge in an experimental setting. After these modifications, it was observed that less radioactivity stuck to SPE cartridges and reaction vials. However, at reduced temperatures and with shortened reaction times the levels of free ^{68}Ga increased in the waste vial and the labeling efficiency weakened.

The injected radioactivity stuck at the head of the HPLC column. To solve this problem, the HPLC methods were modified in many different ways (Table 9). HPLC columns (e.g. XBridge Shield RP18) with well-blocked silanols were tested to exclude the possibility that sticking was caused by the net positive charge of the end product.

Also, varying amounts (60–120 $\mu\text{g}/\text{mL}$) of non-radiolabeled GMP-grade precursor compound DOTA-Siglec-9 were added to the HPLC samples of ^{68}Ga -labeled end product (Table 9.). By doing so, the radioactivity exited of the HPLC columns. The quantity of analyte is tiny in terms of mass or molarity, a known phenomenon for PET radiopharmaceuticals. This may partially explain why an addition of a “carrier” can help analytes travel through the materials packed into HPLC columns.

The sticking problem was caused by conformational changes in the peptide structure during radiosynthesis. The combination of high temperature, long reaction time and high salt content denatured the DOTA-Siglec-9 peptide. In brief, the acetone-based method (cf. section 4.1.2.1) means that acidified acetone was used to elute ^{68}Ga from the cation exchange cartridge, 0.2 M NaOAc buffer was used in the reaction vial and the reaction mixture was kept at 65°C for 6 minutes. Thus, lower temperature, shorter reaction time and decreased concentration of NaOAc buffer solved the above mentioned problems.

5.1.3 NonGMP-grade 3'-[^{68}Ga]Ga-NOTA-anti-microRNA-21 using fractionated method (Subproject III)

NonGMP-grade 3'-[^{68}Ga]Ga-NOTA-anti-microRNA-21 was produced successfully using fractionated method. QC was done using radio-HPLC. RCP of 3'-[^{68}Ga]Ga-NOTA-anti-microRNA-21 was determined to be $94 \pm 2\%$, molar activity was $6.3 \pm 0.6 \text{ GBq}/\mu\text{mol}$ at EOS. Retention time of nonGMP-grade 3'-[^{68}Ga]Ga-NOTA-anti-microRNA-21 was approximately 6.3 minutes (Figure 21., chromatogram A). Formation of the ^{68}Ga -labeled double helix was verified using radio-HPLC (Figure 21., chromatograms B and C).

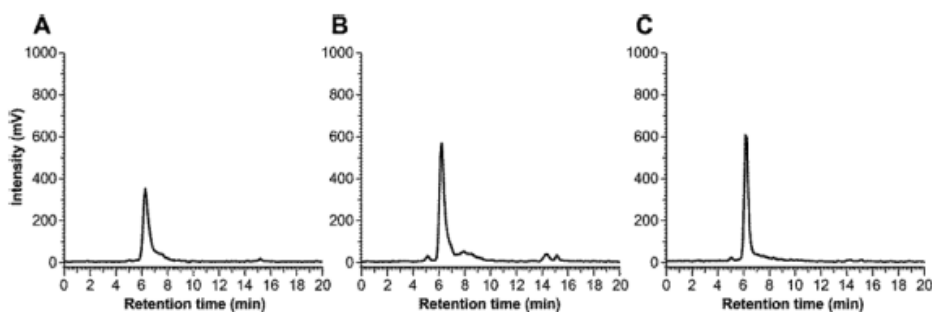


Figure 21. Radiochromatograms of (A) nonGMP-grade 3'-[^{68}Ga]Ga-NOTA-anti-microRNA-21 alone, (B) nonGMP-grade 3'-[^{68}Ga]Ga-NOTA-anti-microRNA-21 + 1 equivalent of 5'-alendronate-conjugated microRNA-21 and (C) a co injection of the mixed samples (A+B, 1:1).

5.2 *In vitro* experiments

5.2.1 Plasma protein binding of nonGMP-grade [^{68}Ga]Ga-DOTA-Siglec-9 (Subproject I)

In vitro experiments using blood from five different species were performed to determine how [^{68}Ga]Ga-DOTA-Siglec-9 translates between species. It was

observed that there are some species-specific differences (Figure 22.). At the first time point, 3 minutes, the highest *in vitro* plasma protein binding of [^{68}Ga]Ga-DOTA-Siglec-9 was seen in rats (34%) and mice (35%). The lowest was seen in pigs (22%). Fast initial binding was observed in all species and a very slow increase over time was seen for pigs (from 22% to 25%) and rats (from 34% to 41%) from 3 minutes to 250 minutes. Mice (from 35% to 55%) and humans (from 27% to 46%) had the highest relative increase in the plasma protein binding over time with an increase of approximately 60% from 3 minutes to 250 minutes. Rabbits (from 25% to 36%) had an increase of approximately 40% from 3 minutes to 250 minutes.

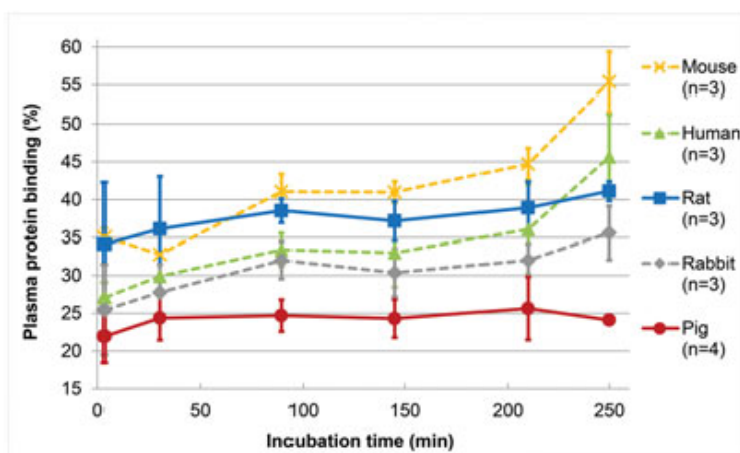


Figure 22. *In vitro* plasma protein binding of [^{68}Ga]Ga-DOTA-Siglec-9 as a function of time in five different species.

5.2.2 Stability of nonGMP-grade [^{68}Ga]Ga-DOTA-Siglec-9 (Subproject I)

The *in vitro* stability of [^{68}Ga]Ga-DOTA-Siglec-9 in human, mouse, pig, rabbit and rat plasma was examined at the same time points as the relative plasma protein binding (Table 10.). It was observed that, in plasma *in vitro*, the [^{68}Ga]Ga-DOTA-Siglec-9 stability depended heavily on which species the plasma came from (Figure 23.). For example, after 90 minutes of incubation, over 50% of the [^{68}Ga]Ga-DOTA-Siglec-9 had degraded in rabbit's plasma, whereas little degradation occurred in pig's plasma (only 5%). In rabbit's plasma, the fast degradation became even more pronounced at later time points and only approximately 30% of the radioactivity of [^{68}Ga]Ga-DOTA-Siglec-9 was intact after 250 minutes of *in vitro* incubation. According to the results, the *in vitro* plasma stabilities of [^{68}Ga]Ga-DOTA-Siglec-9 in the other three species (human, mouse and rat) were

in between those for pigs and rabbits. After 90 minutes of incubation, more than 80% of [^{68}Ga]Ga-DOTA-Siglec-9 was still intact in human's plasma.

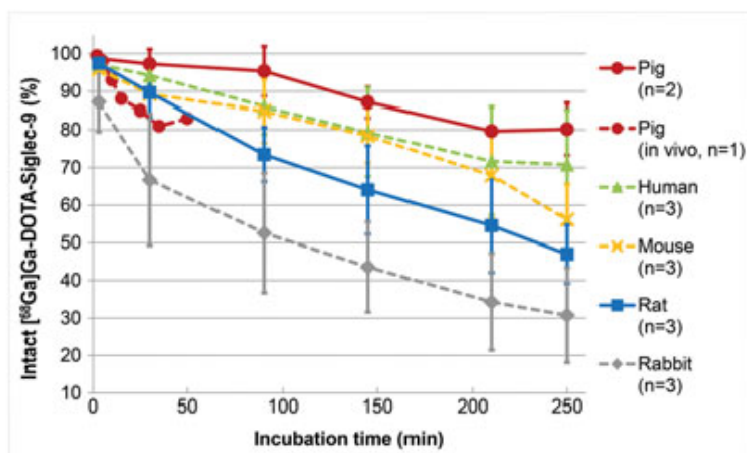


Figure 23. *In vitro* stability of [^{68}Ga]Ga-DOTA-Siglec-9 in animals and human plasma as a function of time.

Table 10. *In vitro* plasma protein binding (%) of [^{68}Ga]Ga-DOTA-Siglec-9 radioactivity.

t (min)	Male sprague-dawley rats (n=3)	Male C57B1N/6N mouse (n=3)	Male New Zealand White rabbit (n=3)	Female human (n=3)	Male Finnish landrace pig (n=1) Commercial porcine serum (n=3)
3	34.1 ± 8.2	35.1 ± 1.1	25.5 ± 6.0	27.1 ± 2.0	22.0 ± 3.5
30	36.1 ± 6.9	32.8 ± 3.5	27.8 ± 3.7	29.9 ± 0.2	24.4 ± 2.9
90	38.5 ± 1.6	41.0 ± 2.3	32.0 ± 2.5	33.4 ± 2.2	24.7 ± 2.1
145	37.2 ± 2.6	41.0 ± 1.4	30.4 ± 3.1	33.0 ± 4.5	24.3 ± 2.5
210	39.9 ± 3.5	44.7 ± 2.1	32.0 ± 2.1	36.1 ± 5.9	25.6 ± 4.2
250	41.1 ± 1.3	55.4 ± 4.0	35.6 ± 3.6	45.6 ± 5.5	24.1 ± 0.1*

Results are expressed as % (mean ± SD).

*Only two measurements were taken to determine the mean and SD at 250 minute time point.

5.2.3 Plasma protein binding of ^{68}Ga -labeled oligoribonucleotide (Subproject III)

According to the radio-HPLC analysis, the *in vitro* plasma protein binding of nonGMP-grade 3'-[^{68}Ga]Ga-NOTA-anti-microRNA-21 alone was observed to be clearly lower as compared with the ^{68}Ga -labeled double helix structure. Plasma protein binding measures at 10, 30 and 60 minutes time points are presented in Table 11.

Table 11. Plasma protein binding based on ⁶⁸Ga radioactivity measurements (mean ± SD, n = 3)

Oligoribonucleotide	Protein binding (%) <i>in vitro</i> , rat plasma +37°C / 10 min*	Protein binding (%) <i>in vitro</i> , rat plasma +37°C / 30 min*	Protein binding (%) <i>in vitro</i> , rat plasma +37°C / 60 min
1	40 ± 3.1	35 ± 5.4	31 ± 2.1
1 + 1 equivalent of 2	74 ± 0.8	74 ± 1.8	72 ± 2.3
1 + 2 equivalents of 2	77 ± 1.1	79 ± 4.4	80 ± 4.4
1 + 4 equivalents of 2	74 ± 0.1	77 ± 1.2	76 ± 0.5

1 is nonGMP-grade 3'-[⁶⁸Ga]Ga-NOTA-anti-microRNA-21

2 is 5'-alendronate-conjugated microRNA-21

* unpublished data

5.2.4 Stability of nonGMP-grade ⁶⁸Ga-labeled oligoribonucleotide (Subproject III)

According to the radio-HPLC analysis, the *in vitro* stability of nonGMP-grade 3'-[⁶⁸Ga]Ga-NOTA-anti-microRNA-21 alone at r.t. (Figure 25.) was observed to be weaker when compared with the ⁶⁸Ga-labeled double helix structure. Stability measures at 1, 2 and 3 hours time points are presented in Table 12.

Table 12. Stability based on ⁶⁸Ga radioactivity measurement (n = 1)

Oligoribonucleotide	Stability (%) <i>in vitro</i> r.t. / 1 h*	Stability (%) <i>in vitro</i> r.t. / 2 h*	Stability (%) <i>in vitro</i> r.t. / 3 h
1	76	79	77
1 + 1 equivalent of 2	92	93	91
1 + 2 equivalents of 2	92	93	93
1 + 4 equivalents of 2	90	91	90

1 is nonGMP-grade 3'-[⁶⁸Ga]Ga-NOTA-anti-microRNA-21

2 is 5'-alendronate-conjugated microRNA-21

* unpublished data

According to the radio-HPLC analysis, the *in vitro* stability of nonGMP-grade 3'-[⁶⁸Ga]Ga-NOTA-anti-microRNA-21 alone in rat's plasma (Figure 24.) was observed to be higher when compared with the ⁶⁸Ga-labeled double helix structure. Stability measures at 10, 30 and 60 minutes time points are presented in Table 13. Broadly speaking, the stability results in both conditions (in rat's plasma and at r.t.) were quite constant between different time points.

Table 13. Stability in rat's plasma based on ^{68}Ga radioactivity measurements (mean \pm SD, n = 3)

Oligoribonucleotide	Stability (%) <i>in vitro</i> , rat plasma +37°C / 10 min*	Stability (%) <i>in vitro</i> , rat plasma +37°C / 30 min*	Stability (%) <i>in vitro</i> , rat plasma +37°C / 60 min
1	98 \pm 0.2	98 \pm 0.4	98 \pm 0.4
1 + 1 equivalent of 2	84 \pm 7.5	87 \pm 2.3	89 \pm 3.2
1 + 2 equivalents of 2	83 \pm 10.5	89 \pm 2.9	87 \pm 3.4
1 + 4 equivalents of 2	91 \pm 2.6	92 \pm 0.2	90 \pm 0.8

1 is nonGMP-grade 3'- ^{68}Ga]Ga-NOTA-anti-microRNA-21

2 is 5'-alendronate-conjugated microRNA-21

* unpublished data

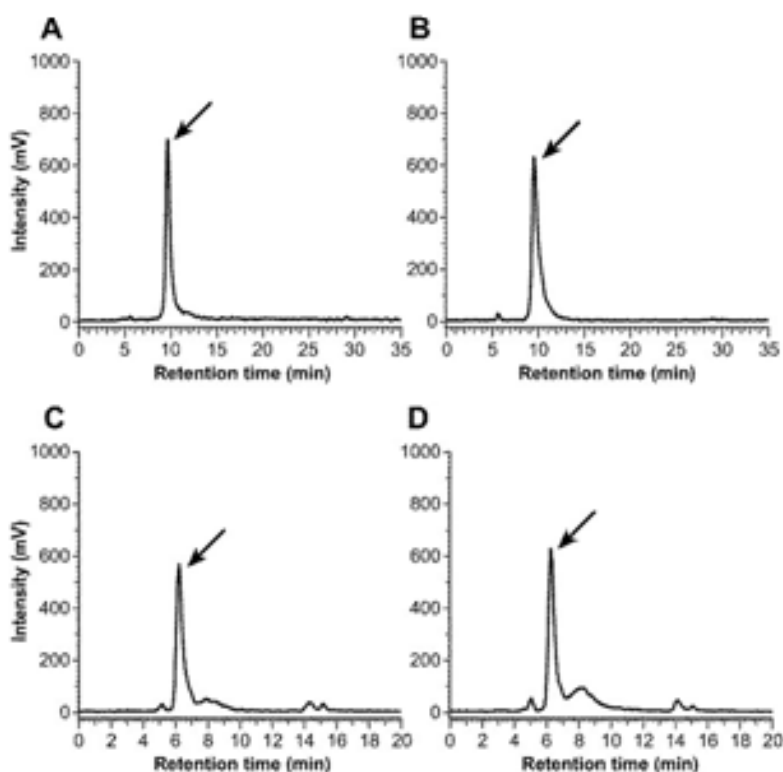


Figure 24. Radio-HPLC chromatograms of the *in vitro* stability experiments. (A) nonGMP-grade 3'- ^{68}Ga]Ga-NOTA-anti-microRNA-21 (retention time 9.65 min) incubated for 3 hours at r.t.; (B) nonGMP-grade 3'- ^{68}Ga]Ga-NOTA-anti-microRNA-21 (retention time 9.53 min) incubated for 1 hour, rat plasma *in vitro*, + 37°C; (C) nonGMP-grade 3'- ^{68}Ga]Ga-NOTA-anti-microRNA-21 + 1 equivalent of 5'-alendronate-conjugated microRNA-21 (retention time 6.22 min) incubated for 3 hours at r.t.; and (D) nonGMP-grade 3'- ^{68}Ga]Ga-NOTA-anti-microRNA-21 + 1 equivalent of 5'-alendronate-conjugated microRNA-21 (retention time 6.23 min) incubated for 1 hour, rat plasma *in vitro*, + 37°C. Gradient 1 (A–B) (Table 5.) and gradient 2 (C–D) (Table 6.) were used.

5.3 *In vivo* studies

5.3.1 *In vivo* imaging with ^{68}Ga -radiolabeled oligoribonucleotide (Subproject III)

The administration of nonGMP-grade 3'-[^{68}Ga]Ga-NOTA-anti-microRNA-21 with 5'-alendronate-conjugated microRNA-21 changed the bone uptake remarkably as compared with nonGMP-grade 3'-[^{68}Ga]Ga-NOTA-anti-microRNA-21 alone (Figures 25–27.). The increased radioactivity in knees is seen in whole-body coronal PET images (Figure 25.) and even more clearly in PET/CT images (Figure 26.). The prolonged radioactivity (nonGMP-grade 3'-[^{68}Ga]Ga-NOTA-anti-microRNA-21 alone versus 3'-[^{68}Ga]Ga-NOTA-anti-microRNA-21 + 1, 2 or 4 equivalents of 5'-alendronate-conjugated microRNA-21) in knees can be observed in the TACs across the distribution (0–60 min, Figure 27.).

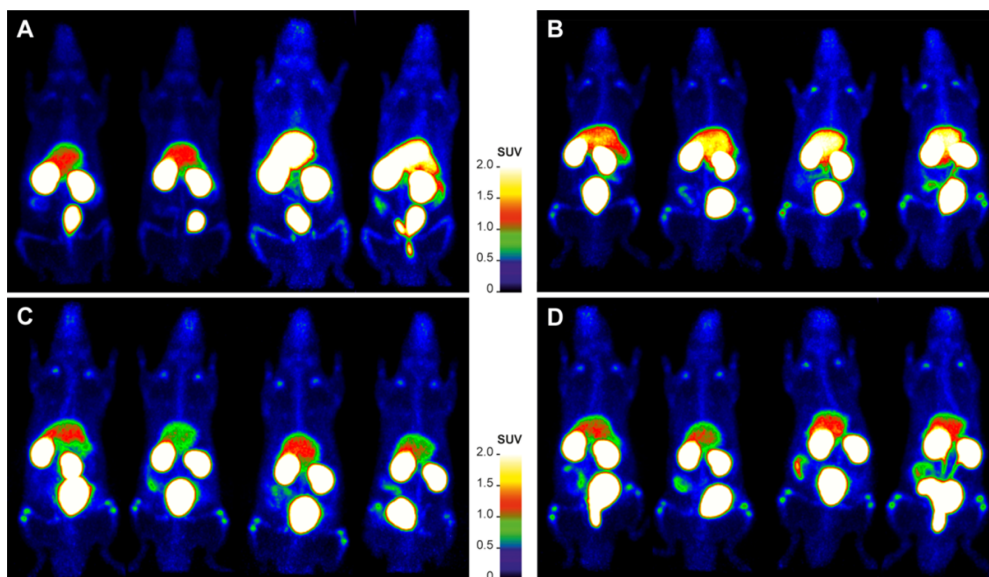


Figure 25. Whole-body coronal PET images of healthy rats i.v. injected with ^{68}Ga -labeled oligoribonucleotide. Images are summation from 50–60 minutes post injection and they are presented in the same colour scale. (A) nonGMP-grade 3'-[^{68}Ga]Ga-NOTA-anti-microRNA-21 alone; (B) nonGMP-grade 3'-[^{68}Ga]Ga-NOTA-anti-microRNA-21 + 1 equivalent of 5'-alendronate-conjugated microRNA-21; (C) nonGMP-grade 3'-[^{68}Ga]Ga-NOTA-anti-microRNA-21 + 2 equivalents of 5'-alendronate-conjugated microRNA-21; and (D) nonGMP-grade 3'-[^{68}Ga]Ga-NOTA-anti-microRNA-21 + 4 equivalents of 5'-alendronate-conjugated microRNA-21.

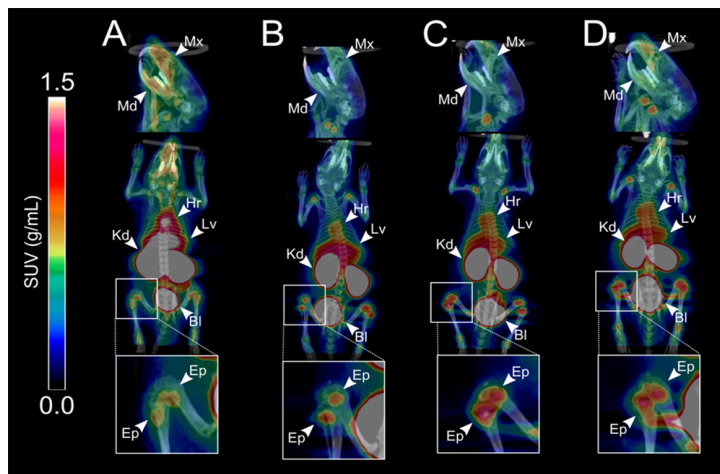


Figure 26. PET/CT images of healthy rats i.v. injected with ^{68}Ga -labeled oligoribonucleotide. Images are summation from 0–60 minutes post injection and they are presented in the same colour scale. (A) nonGMP-grade 3'- ^{68}Ga]Ga-NOTA-anti-microRNA-21 alone; (B) nonGMP-grade 3'- ^{68}Ga]Ga-NOTA-anti-microRNA-21 + 1 equivalent of 5'-alendronate-conjugated microRNA-21; (C) nonGMP-grade 3'- ^{68}Ga]Ga-NOTA-anti-microRNA-21 + 2 equivalents of 5'-alendronate-conjugated microRNA-21; and (D) nonGMP-grade 3'- ^{68}Ga]Ga-NOTA-anti-microRNA-21 + 4 equivalents of 5'-alendronate-conjugated microRNA-21 (BI = urinary bladder, Ep = epiphysis bone, Hr = heart, Kd = kidney, Lv = liver, Md = mandible bone, Mx = maxilla bone).

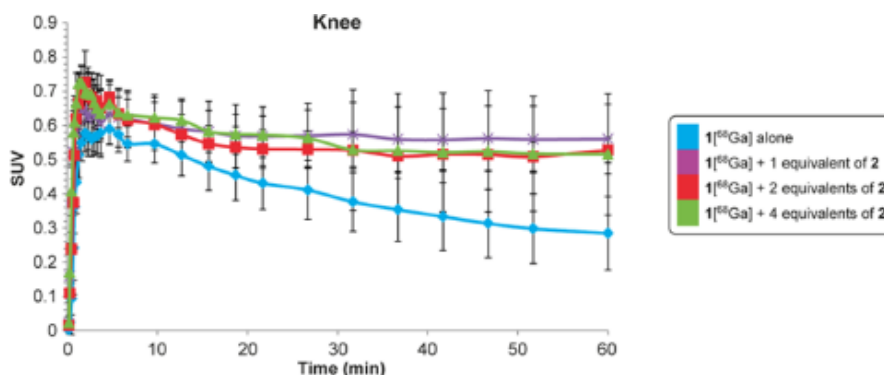


Figure 27. TACs (RAC as a function of time) of the distribution kinetics of nonGMP-grade ^{68}Ga -labeled oligoribonucleotide in rat's knee (1 ^{68}Ga] = nonGMP-grade 3'- ^{68}Ga]Ga-NOTA-anti-microRNA-21, 2 = 5'-alendronate-conjugated microRNA-21, error bars denote SD, n = 4).

5.3.2 Blood and urine samples (Subproject III)

According to the radio-HPLC analysis of an aliquot taken from plasma 60 minutes after the i.v. administration, 11% of nonGMP-grade 3'- ^{68}Ga]Ga-NOTA-anti-microRNA-21 and 28% of nonGMP-grade 3'- ^{68}Ga]Ga-NOTA-anti-microRNA-21/2-duplex (with 1 equivalent of 5'-alendronate-conjugated microRNA-21) were still intact (Figure 28.). The corresponding values of the samples taken from urine

were 81% for nonGMP-grade 3'-[⁶⁸Ga]Ga-NOTA-anti-microRNA-21 and 88% for nonGMP-grade 3'-[⁶⁸Ga]Ga-NOTA-anti-microRNA-21/2-duplex (Figure 30.). *In vivo* stability results at 1 hour time point are presented in Table 14.

Table 14. Stability (%) *in vivo* based on ⁶⁸Ga radioactivity measurement (n = 1).

Oligoribonucleotide	Stability (%) <i>in vivo</i> , rat plasma / 1 h	Stability (%) <i>in vivo</i> , rat urine / 1 h
1	11	81
1 + 1 equivalent of 2	28	88
1 + 2 equivalents of 2	18	84
1 + 4 equivalents of 2	38	91

1 is nonGMP-grade 3'-[⁶⁸Ga]Ga-NOTA-anti-microRNA-21

2 is 5'-alendronate-conjugated microRNA-21

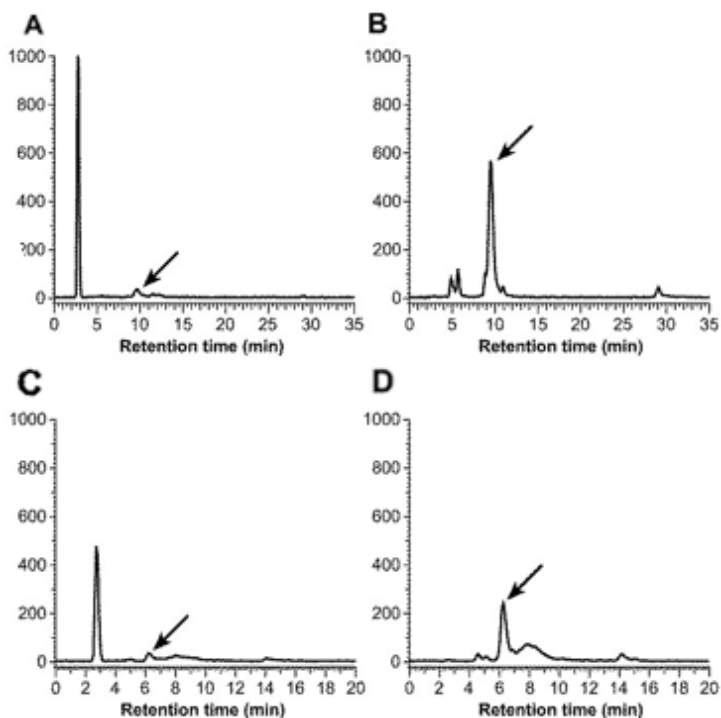


Figure 28. Radio-HPLC chromatograms of the *in vivo* stability experiments. (A) nonGMP-grade 3'-[⁶⁸Ga]Ga-NOTA-anti-microRNA-21 (retention time 9.64 min), 1 hour, rat's plasma; (B) nonGMP-grade 3'-[⁶⁸Ga]Ga-NOTA-anti-microRNA-21 (retention time 9.46 min), 1 hour, rat's urine; (C) nonGMP-grade 3'-[⁶⁸Ga]Ga-NOTA-anti-microRNA-21 + 1 equivalent of 5'-alendronate-conjugated microRNA-21 (retention time 6.21 min), 1 hour, rat's plasma; and (D) nonGMP-grade 3'-[⁶⁸Ga]Ga-NOTA-anti-microRNA-21 + 1 equivalent of 5'-alendronate-conjugated microRNA-21 (retention time 6.27 min), 1 hour, rat's urine. Gradient 1 (A–B) (Table 5.) and gradient 2 (C–D) (Table 6.) were used.

5.4 *Ex vivo* biodistribution experiments (Subproject III)

Observations obtained during PET studies were supported in a more detailed analysis of the *ex vivo* by gamma counting measurements of excised tissues (Figure 29.). The separate tibia and bone marrow uptakes verified the increased (ca. 40%) tibia accumulation of nonGMP-grade 3'-[⁶⁸Ga]Ga-NOTA-anti-microRNA-21/5'-alendronate-conjugated microRNA-21/2-duplex, whereas nonGMP-grade 3'-[⁶⁸Ga]Ga-NOTA-anti-microRNA-21 alone accumulated to larger extent to bone marrow. The administration of nonGMP-grade 3'-[⁶⁸Ga]Ga-NOTA-anti-microRNA-21 without 5'-alendronate-conjugated microRNA-21 showed higher uptake in all other tissues studied: kidneys, liver, spleen, salivary glands, pancreas, lungs, heart and skin, in comparison with uptakes of nonGMP-grade 3'-[⁶⁸Ga]Ga-NOTA-anti-microRNA-21 with 5'-alendronate-conjugated microRNA-21. Additionally, the double helical administration decreased the radioactivity in plasma but increased the radioactivity excreted to urine.

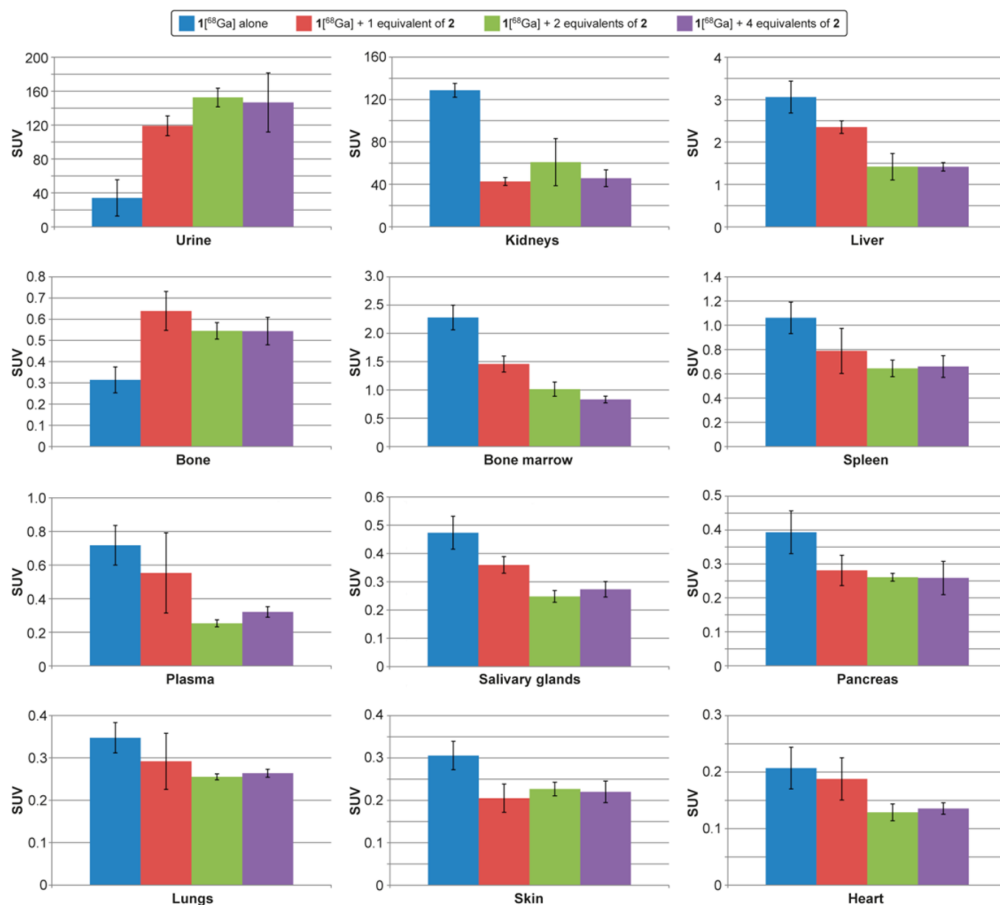


Figure 29. RAC at 60 minutes after i.v. injection of nonGMP-grade ⁶⁸Ga-oligoribonucleotide. Measured *ex vivo* by gamma counting of excised tissues of healthy rats (1[⁶⁸Ga] = nonGMP-grade 3'-[⁶⁸Ga]Ga-NOTA-anti-microRNA-21, 2 = 5'-alendronate-conjugated microRNA-21, error bars denote SD, n = 4). Bone = tibia.

5.5 UV melting profile analysis of ⁶⁸Ga-labeled double helix (Subproject III)

UV-melting profile analysis was used to evaluate the thermal stability of the double helix between 3'-NOTA-anti-microRNA-21 and 5'-alendronate-conjugated microRNA-21. The melting curves were presented as normalized absorbance versus temperature profiles (Figure 30.). A mixture ($T_m = 88^\circ\text{C}$, 3'-[^{69/71}Ga]Ga-NOTA-anti-micro-RNA-21 and 5'-alendronate-conjugated microRNA-21, 0.2 M NaOAc and 0.05 M NaCl) that mimics the ⁶⁸Ga-labeling conditions was used and a relatively stable double helix was observed in this mixture. However, the stability of the duplex *in vitro* is not comparable to that in the bloodstream.

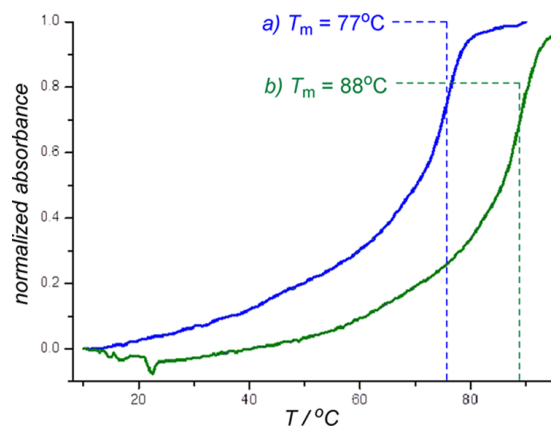


Figure 30. UV-melting profiles of the double helix. Conditions used: a) 2 μM of 3'-NOTA-anti-microRNA-21 in 10 mM sodium cacodylate and 0.1 M NaCl (pH 7.0); b) 2 μM 3'- $^{69/71}\text{Ga}$ -NOTA-anti-microRNA-21 and 5'-alendronate-conjugated microRNA-21, 0.2 M NaOAc and 0.05 M NaCl (pH 9.0).

6 Discussion

6.1 Radiolabeling

6.1.1 Fractionated method and ^{68}Ga -radiolabeling

In Subprojects I and III, fractionated method was used successfully for producing nonGMP-grade ^{68}Ga -labeled tracers. The advantage of the fractionated method is that no organic solvent is required. Previously, the fractionated method has been used successfully for radiolabeling DOTA-peptides (Breeman et al., 2005, Ujula et al., 2009, Ahtinen et al., 2014, Virtanen et al., 2015) and NOTA-oligonucleotides (Kiviniemi et al., 2012, Mäkilä et al., 2014).

The key point of this method is that the fraction with highest volume radioactivity is collected and buffered to an appropriate pH for radiolabeling (de Blois et al., 2011). Fractionated method is potentially effective but the drawback is that only a fraction of the eluted ^{68}Ga radioactivity is used. This reduces the achievable molar activity of the final product (Mueller et al., 2012). In Subproject I, when radiolabeling nonGMP-grade ^{68}Ga -DOTA-Siglec-9, the amount of peptide used was 3 nmol. Because of the small amount of peptide, the molar activity of the final nonGMP-grade ^{68}Ga -DOTA-Siglec-9 was high despite of the application of the fractionation method.

In Subproject III, 20 nmol of 3'-NOTA-chelated anti-microRNA-21 was used for ^{68}Ga -labeling. Thus, molar activity of nonGMP-grade 3'- ^{68}Ga -NOTA-anti-microRNA-21 was rather low. Conditions used for the ^{68}Ga -labeling of nonGMP-grade 3'-NOTA-chelated anti-microRNA-21 had previously been optimized for oligonucleotides (Roivainen et al., 2004) and were only slightly modified here. To improve the molar activity, the labeling procedure needs still further optimization.

Fractionated elution results in a ready-to-use eluate (de Blois et al., 2011). In Subprojects I and III, the eluate was used without any pre-purification. The major limitations for direct use of ^{68}Ga for radiolabeling are ^{68}Ge breakthrough, potential metal ion impurities, high proton concentration and large volume of generator eluate (Breeman et al., 2005, Zhernosekov et al., 2007, Asti et al., 2008, de Blois et al., 2011, Boschi et al., 2013). In our studies, a small volume of ^{68}Ga -eluate (0.5

mL) was used. Due to the low eluate volume used, the contents of ^{68}Ge and metallic impurities are reduced. (Zhernosekov et al., 2007)

In Subproject I, HEPES buffer was used in the reaction mixture for radiolabeling nonGMP-grade $[^{68}\text{Ga}]\text{Ga-DOTA-Siglec-9}$. HEPES has been reported, along with NaOAc and sodium succinate, to be the most favorable buffer for ^{68}Ga -labeling (Bauwens et al., 2010). Our results revealed that HEPES dissolved completely in the ^{68}Ga -eluate and the pH of the reaction mixture was optimal for radiolabeling DOTA-Siglec-9 peptide. Virtanen and co-workers have earlier used HEPES for radiolabeling $[^{68}\text{Ga}]\text{Ga-DOTA-Siglec-9}$. (Ahtinen et al., 2014, Virtanen et al., 2015)

One disadvantage of HEPES is that, at the moment, it is not allowed for human use. Ph. Eur. defines it as an impurity and sets a limit for HEPES in the final ^{68}Ga -labeled product (Ph. Eur., 2013, Pfaff et al., 2018). However, Theodore and co-workers have proved that HEPES has no deleterious effects even when administered daily in high doses to cancer patients over a period of 10 weeks (Theodore et al., 1997). As regards the automated synthesis protocol, SPE purification is considered to remove HEPES completely during the purification process (Pohle et al., 2012, Pfaff et al., 2018). In Subproject I, nonGMP-grade $[^{68}\text{Ga}]\text{Ga-DOTA-Siglec-9}$ was radiolabeled for preclinical experiments. Therefore, use of HEPES in the radiolabeling procedure was possible. The amount of HEPES in the final product was not determined.

In Subproject III, NaOAc buffer was used in the reaction mixture for radiolabeling nonGMP-grade $3'-[^{68}\text{Ga}]\text{Ga-NOTA-anti-microRNA-21}$. Unlike HEPES, NaOAc is allowed for human use. Previously, Mäkilä and co-workers have used NaOAc successfully for radiolabeling oligoribonucleotides (Mäkilä et al., 2014). In Subproject III, nonGMP-grade $3'-[^{68}\text{Ga}]\text{Ga-NOTA-anti-microRNA-21}$ was radiolabeled for preclinical studies, but it is assumed that these radiolabeling conditions can be used as such or slightly modified for human studies as well.

In Subproject III, reaction time for radiolabeling nonGMP-grade $3'-[^{68}\text{Ga}]\text{Ga-NOTA-anti-microRNA-21}$ was 10 minutes. Mäkilä and co-workers have previously used a similar reaction time (Mäkilä et al., 2014). In Subproject I, reaction time for radiolabeling nonGMP-grade $[^{68}\text{Ga}]\text{Ga-DOTA-Siglec-9}$ was 15 minutes. This kind of a reaction time has also been used earlier (Virtanen et al., 2015). We performed some tests with nonGMP-grade $[^{68}\text{Ga}]\text{Ga-DOTA-Siglec-9}$ using a decreased temperature (80°C or 90°C) and prolonged reaction time (approximately 17 minutes). However, we observed that non-chelated ^{68}Ga remained in the reaction mixture even after the extended reaction time. Minor modifications to the reaction time have no significant impact on the overall yield. The influence of the small changes to the temperature was also supposed to be

insignificant. Several reported ^{68}Ga -radiolabeling experiments have been conducted at a temperature exceeding 50°C . Tsionou and co-workers have concluded that, for the majority of the chelators, heating the reaction does not significantly increase RCY. They have also concluded that DOTA chelator is an exception, meaning that heating and low pH conditions are favourable in the case of DOTA. (Tsionou et al., 2017)

DOTA- and NOTA-chelators require a relatively long reaction time at a high temperature in order to provide a high RCY. This is because of the slow kinetics of these chelate reactions. Therefore, decreasing the temperature may result in a lower RCY. However, peptides can be sensitive to harsh conditions like high temperature. Thus, decrease of the temperature can be necessary to obtain desirable RCY.

In Subproject III, our conclusion was that hybridization of the alendronate moiety (5'-alendronate-conjugated microRNA-21, none, 1, 2 or 4 equivalents) has to be carried out after the ^{68}Ga -chelation of 3'-NOTA-anti-microRNA-21. We had problems in performing the tests for producing ^{68}Ga -labeled NOTA-chelated bis(phosphonate) conjugate of oligoribonucleotide. Several HPLC -analyses demonstrated that most of the radioactivity in the reaction mixture after the radiolabeling was free ^{68}Ga . After the tested and modified radiolabeling conditions including, for example, prolonged reaction time, it was established that successful ^{68}Ga -labeling only occurred in the absence of 5'-alendronate-conjugated microRNA-21. Most likely, this is because of a plausible interaction between the bis(phosphonate) and NOTA-chelate which is able to interfere with ^{68}Ga -chelation. Similar problems have been reported previously (Holub et al., 2015).

[^{68}Ga]Ga-DOTA-Siglec-9 peptide contains DOTA chelator. DOTA is a widely used chelator, mainly because of its exceptional *in vivo* stability, commercial availability and well studied coordination chemistry (Price and Orvig, 2014, Gijs et al., 2016). Previously, researchers in Turku PET Centre have studied Siglec-9 containing DOTA and its potential as a PET tracer has been proven (Aalto et al., 2011, Ahtinen et al., 2014, Virtanen et al., 2015, Silvola et al., 2016, Virtanen et al., 2017).

Researchers in Turku PET Centre have jointly with collaborative parties studied NOTA-chelated oligonucleotides previously (Kiviniemi et al., 2012, Mäkilä et al., 2014). Kiviniemi and co-workers have successfully labeled 3'-NOTA and 3'-DOTA conjugated oligonucleotides with ^{68}Ga (Kiviniemi et al., 2012). In Subproject III, ^{68}Ga -labeled oligoribonucleotide contains NOTA chelator. NOTA has ideal radiolabeling properties and stability with ^{68}Ga for diagnostic applications because its Ga(III) complex is thermodynamically more stable than that of DOTA (Price and Orvig, 2014, Gijs et al., 2016). However, thermodynamic stability is not critical here, meaning that DOTA chelator could also have been coupled to

oligoribonucleotide. When radiolabeling DOTA chelators, reaction solutions are heated since the purpose is to overcome substantial kinetic barriers. Radiolabeling of NOTA can be performed under mild conditions and at r.t. (Price and Orvig, 2014, Gijss et al., 2016). Thus, the kinetic barriers to Ga^{3+} complexation are likely to be lower for NOTA than DOTA. Peptides like Siglec-9 can be sensitive to harsh conditions. For example, disruption of bonds can be seen. Accordingly, NOTA chelator coupled to Siglec-9 peptide could be even favored when compared with DOTA. (Tsionou et al., 2017)

In Subproject III, three slightly different gradients were tested for the study of plasma protein binding and stability of ^{68}Ga -labeled oligoribonucleotide. During the project, the gradient of solvent A (50 mM NH_4OAc) was modified in order to obtain a sharper main peak. After the tested modifications, it was concluded that the original gradient (gradient 1) gave the sharpest main peak. Radioisotope ^{68}Ga is a short-lived isotope ($t_{1/2} = 68$ minutes). This means that all the steps during the radiolabeling process (starting from the elution of $^{68}\text{Ge}/^{68}\text{Ga}$ generator until the ^{68}Ga -labeled final product is ready for injection) have to be optimized. It is useful that the gradient used for QC analysis of the ^{68}Ga -labeled PET radiopharmaceuticals is optimized. In Subproject III, the duration of the gradient used for the QC analysis of nonGMP-grade 3'- ^{68}Ga]Ga-NOTA-anti-microRNA-21 was 17 minutes, in addition to washing with H_3PO_4 for 8 minutes. Optimizing the gradient duration by shortening it would be justified in the future.

6.1.2 Acetone-based method and ^{68}Ga -radiolabeling

The purpose of Subproject II was to develop a production method for radiopharmaceutical ^{68}Ga]Ga-DOTA-Siglec-9 in compliance with GMP. To our knowledge, Subproject II was the first study to represent a protocol for generating GMP-grade ^{68}Ga]Ga-DOTA-Siglec-9, the first radiopharmaceutical for PET imaging of VAP-1 protein.

A sticking problem was observed during the development work of GMP-grade ^{68}Ga]Ga-DOTA-Siglec-9. During the development process, we concluded that although it is not large, the DOTA-Siglec-9 peptide is sensitive to radiolabeling conditions, for example, the combination of relatively high reaction temperature and high salt content. In order to solve the problem, we applied an acetone-based method for producing GMP-grade ^{68}Ga]Ga-DOTA-Siglec-9 with a lower temperature, shorter reaction time, decreased concentration of NaOAc buffer and reduced concentration of NaCl . We concluded that introducing the acetone-based method solved the problems related to low RCY and sticking problem of the HPLC column.

One purpose of the development process was to establish milder reaction conditions. In order to reduce the salt content of the reaction mixture and the temperature of the radiolabeling reactions without compromising the potential RCY, we decided to test radiosynthesis with an acetone-based method. Acetone-based method has been proven to deliver ^{68}Ga -labeled compounds in high RCP and molar activity (Mueller et al., 2012). A cationic based post-processing method has been successfully applied to different types of radiolabeling precursors and it provides highly reproducible radiolabeling yields (Seemann et al., 2015). It has become more popular as opposed to the fractionated method (Prince et al., 2018). Purification of ^{68}Ga -eluate using an acetone-based method has been described previously (Zhernosekov et al., 2007) and the acetone-based method is widely used for radiolabeling DOTA-conjugated peptides. (Poepfel et al., 2011, Schultz et al., 2013, Wild et al., 2013, Ghai et al., 2018)

However, acetone has its limitations. The acetone-HCl-based solution may contain breakdown impurities like mesityloxide and 4-methyl-3-penten-2-on which can be detected in the final products. Acetone is classified as Class 3 solvent, in other words, a solvent with low toxic potential, and its amount in medicinal products has to be measured. Determination of residual acetone level requires extra steps in the QC process. It calls for intensified production efforts for technical staff (Mueller et al., 2012) as well as maintenance and purchase of GC equipment. Acetone has to be eliminated from the final formulation. The boiling point of acetone is low (56°C). Thus, it is possible to remove acetone by heating up the reaction vial. During the development process of GMP-grade [^{68}Ga]Ga-DOTA-Siglec-9, we observed that acetone evaporated gradually into the waste vial via vent tubing.

Development work of GMP-grade [^{68}Ga]Ga-DOTA-Siglec-9 was done taking into account the requirements set for GMP production. An automated synthesis device (initially Modular-Lab Standard, later on Modular-Lab PharmTracer) was used. Modular-Lab Standard is more like a manual system than Modular-Lab PharmTracer. It contains re-usable plastic tubes and vials made of glass. Modular-Lab PharmTracer is a cassette-based system using disposable cassettes. The trend towards using fully automated systems has been increasing in the recent years to overcome the intrinsic limitations of manual or semi-automated systems, and pre-loaded cassette-based modules have represented improvement in terms of compliance and safety. (Boschi et al., 2013)

6.2 *In vivo* imaging and *ex vivo* biodistribution experiments

The hypothesis that an appropriate conjugation with bis(phosphonate) would increase the bone accumulation of a potential oligoribonucleotide *in vivo* was proven in Subproject III. The excess (2 or 4 equivalents versus 1 equivalent) of 5'-alendronate-conjugated microRNA-21 used for the hybridization did not show marked variation in the accumulation or distribution kinetics. Accordingly, it was argued that an incomplete hybridization did not interfere with the desired systemic bone-targeted delivery and neither did the excess of 5'-alendronate-conjugated microRNA-21 do so. In previous studies, a high bone uptake potential, accumulation in bone and a high bone to blood ratio of $^{67/68}\text{Ga}$ -labeled DOTA- and NOTA-bis(phosphonates) using PET imaging have been proven (Ogawa et al., 2011, Suzuki et al., 2011, Meckel et al., 2013, Holub et al., 2015).

It is possible that this bone accumulation proof of concept will find further applications in targeting of double-helical RNAs to bone-forming surfaces. However, several important issues must be resolved prior to plausible therapeutic applicability. In the future, independent studies considering the bone cell internalization of the single strand RNA or the double helical RNA are required. Another important issue is the sequence complementarity. The stable double helix facilitates the systemic bone matrix-targeted delivery. The action of the potential therapeutically active single strand (anti-microRNA-21) could be hampered. In the future, the bone accumulation should be further enhanced. It can be assumed that multiple bis(phosphonate) units may provide the desired enhancement.

6.3 Plasma protein binding and stability *in vivo* and *in vitro* experiments

In Subproject I, the purpose was to set up an experiment to look at the species-specific variation of the ^{68}Ga]-Ga-DOTA-Siglec-9 *in vitro* behavior in plasma. It is highly important to understand the plasma protein binding of potential PET radiopharmaceuticals. This is because binding has great implications for the kinetics of PET radiopharmaceuticals. Plasma protein binding in human plasma was part of the experiment. It is useful to study how ^{68}Ga]-Ga-DOTA-Siglec-9 behaves in human plasma *in vitro*. In the future, these results can be compared with the *in vivo* results obtained. We concluded that the binding efficiency cannot be directly compared because the plasma concentrations of soluble VAP-1 and the sequence of VAP-1 vary greatly between different species. It is pointed out that any *in vitro* or animal data should be used with caution in assessing the properties of ^{68}Ga]-Ga-DOTA-Siglec-9 for human use. The plasma protein binding experiment was justified because it is known that ^{68}Ga]-Ga-DOTA-Siglec-9 binds

to plasma proteins when injected into the bloodstream (Retamal et al., 2016). High plasma protein binding reduces glomerular filtration and increases bloodstream half-life.

It is essential to understand the stability of potential PET radiopharmaceuticals. It is necessary to determine that PET radiopharmaceuticals will be stable enough in the organism so that they can be used for PET imaging. According to our results, the stability of [^{68}Ga]Ga-DOTA-Siglec-9 varied greatly between species. Differences in stability between species are possibly due to the differences in metabolism between species, for example how fast [^{68}Ga]Ga-DOTA-Siglec-9 is metabolized in blood. It is assumed that [^{68}Ga]Ga-DOTA-Siglec-9 may bind to different plasma proteins depending on species and this could explain the differences between species.

For example, there was a huge difference in stability between pig's plasma and rabbit's plasma. We observed that the decrease of the stability was moderate for human plasma. Virtanen and co-workers have reported previously that, after incubation at 37°C for 60 minutes in rabbit's plasma, the radioactivity associated with intact [^{68}Ga]Ga-DOTA-Siglec-9 was $94 \pm 1.0\%$ ($n = 2$) (Virtanen et al., 2015). In comparison, our results were different. We observed that, at the same time point, approximately 60% of [^{68}Ga]Ga-DOTA-Siglec-9 was intact ($n=3$). The experimental setup was quite similar in both studies. Differences between the results can be explained by, for example, differences between individual animals. Larger experimental materials would be justified in the future.

In Subproject III, one aim was to study plasma protein binding and stability of both nonGMP-grade 3'-[^{68}Ga]Ga-NOTA-anti-microRNA-21 and ^{68}Ga -labeled double helix structure. We concluded, that according to the radio-HPLC analysis, the *in vitro* plasma protein binding of nonGMP-grade 3'-[^{68}Ga]Ga-NOTA-anti-microRNA-21 alone was clearly lower as compared with the ^{68}Ga -labeled double helix structure. The reason for this difference of plasma protein bindings could be either that single-stranded oligonucleotide is bound to plasma protein more weakly in this context or that the bis(phosphonate) conjugated to double helix affects the plasma protein binding by increasing it.

We observed that the ^{68}Ga -labeled double helix structure was quite stable at r.t. ($\geq 90\%$) and more stable when compared with nonGMP-grade 3'-[^{68}Ga]Ga-NOTA-anti-microRNA-21 alone. The results obtained by Ogawa and co-workers and Suzuki and co-workers support our observation that ^{68}Ga -labeled bis(phosphonate) complexes are stable *in vitro* (Ogawa et al., 2011, Suzuki et al., 2011).

In Subproject III, we found that ^{68}Ga -labeled double helix was more stable in rat's plasma *in vivo* when compared with nonGMP-grade 3'-[^{68}Ga]Ga-NOTA-anti-microRNA-21 alone. Our results are in agreement with previous studies reporting that the rates of *in vivo* degradation of double helical

oligoribonucleotides are usually lower than those of the corresponding single strands (Braasch et al., 2004, Roivainen et al., 2004, Viel et al., 2008, Lendvai et al., 2009, Rettig and Behlke, 2012).

6.4 Future considerations

The increasing clinical demand of ^{68}Ga -labeled tracers has prompted the need for extensive automation of the production process for ^{68}Ga -radiopharmaceuticals. Nowadays, various automation strategies tailored to different needs are available and several commercial automatic devices have been developed. All of the automated systems approved for marketing provide a safe and effective synthesis of ^{68}Ga -radiolabeled tracers and ensure that the safety and quality of ^{68}Ga -radiopharmaceuticals is adequate for their intended use. These technologies have implemented different pre-purification approaches. They lead to an increased radionuclidic purity, RCP and high molar activity of the final preparation. High and reproducible throughput, robustness of the synthesis and radioprotection aspects have led to a great diffusion of automated technology in cGMP compliant environments. (Boschi et al., 2013)

$^{68}\text{Ge}/^{68}\text{Ga}$ generators and cyclotrons are used for the production of ^{68}Ga . Cyclotron-produced ^{68}Ga is proven to be, at least, as high-quality as generator-produced ^{68}Ga for the production of ^{68}Ga -labeled tracers. A cyclotron is an economical alternative to $^{68}\text{Ge}/^{68}\text{Ga}$ generators and it shows potential for large scale production of ^{68}Ga . (Pandey et al., 2014, Lin et al., 2018, Riga et al., 2018)

^{68}Ga has several benefits. The labeling synthesis is amenable to kit type preparation and automation. ^{68}Ga provides sufficient levels of radioactivity for high quality images and short scanning time, thus facilitating fast patient examination. However, it should be pointed out that this performance depends on the *in vivo* kinetics of the imaging probe. ^{68}Ga also makes possible to minimize the radiation dose to the patient and personnel and allows fast discharge of the patient. Moreover, repetitive examinations within the same day are possible. (Velikyan et al., 2010, Velikyan, 2014)

It has been proposed that the future development of ^{68}Ga -radiopharmaceuticals must be put in the context of several aspects, such as production and availability of ^{68}Ga , automation of the radiopharmaceutical production, PET radiopharmaceutical regulations as well as radiopharmaceutical chemistry advances, identification of new biomarkers, targets and corresponding ligands, role of PET in nuclear medicine, unmet medical needs and progress of PET technologies and image analysis methodologies for improved quantitation accuracy. (Velikyan, 2014)

In Subproject III, the bone accumulation of a potential small-interfering anti-microRNA-21/microRNA-21 double helix was shown to be increased by an

appropriate conjugation with bis(phosphonate). This was done using ^{68}Ga -labeled NOTA-chelated oligoribonucleotide and PET imaging. ^{68}Ga -labeling and QC of NOTA-chelated oligoribonucleotide were studied. In the future, it is recommended to optimize the radiolabeling protocol for oligoribonucleotide radiolabeling conditions and amount of precursor. Additional tests to collect more data and study the potential of this PET tracer in animal experiments are recommended. It is desirable that its potential as a PET tracer in human studies could be established in the future.

^{68}Ga]Ga-DOTA-Siglec-9 has been shown to be a promising PET tracer for imaging of inflammation in animal studies. The intention is to use this novel PET radiopharmaceutical in human studies and investigate its potential for clinical use in the future. The synthesis protocol for GMP-grade ^{68}Ga]Ga-DOTA-Siglec-9 developed here has made the first-in-human studies possible. In the future, it is possible that ^{68}Ga]Ga-DOTA-Siglec-9 can be utilized as a PET radiopharmaceutical for imaging of inflammation in routine clinical production.

7 Conclusions

Problems encountered in the PET radiopharmaceutical production of GMP-grade [^{68}Ga]Ga-DOTA-Siglec-9 were solved. *In vitro* experiments concerning the plasma protein binding and stability of nonGMP-grade [^{68}Ga]Ga-DOTA-Siglec-9 were performed and compared among different species. In addition, bis(phosphonate)-induced bone accumulation of nonGMP-grade ^{68}Ga -labeled NOTA-chelated bis(phosphonate)-conjugated oligoribonucleotide and its biodistribution were studied. The main conclusions were:

1. GMP-grade [^{68}Ga]Ga-DOTA-Siglec-9 is produced efficiently and rapidly using a fully automated acetone-based method. The GMP-grade tracer is suitable for human use.
2. The stability of nonGMP-grade [^{68}Ga]Ga-DOTA-Siglec-9 in plasma *in vitro* depends heavily on which species the plasma comes from. Plasma protein binding of nonGMP-grade [^{68}Ga]Ga-DOTA-Siglec-9 *in vitro* shows species-specific differences. Fast initial binding is observed in all examined species.
3. NonGMP-grade 3'-[^{68}Ga]Ga-NOTA-anti-microRNA-21 is produced successfully using the fractionated method. ^{68}Ga -radiolabeled NOTA-chelated bis(phosphonate)-conjugated anti-microRNA-21/microRNA-21 double helix forms successfully at r.t. within 10 minutes.
4. Bis(phosphonate)-induced bone accumulation of the double helical RNA in healthy rats is verified. ^{68}Ga -radiolabeled double helix structure is more stable at r.t. *in vitro* in comparison with nonGMP-grade 3'-[^{68}Ga]Ga-NOTA-anti-microRNA-21 alone. NonGMP-grade 3'-[^{68}Ga]Ga-NOTA-anti-microRNA-21 alone is more stable in rat's plasma *in vitro* as compared with ^{68}Ga -radiolabeled double helix structure.

Synthesis protocols for producing GMP-grade [^{68}Ga]Ga-DOTA-Siglec-9 and nonGMP-grade 3'-[^{68}Ga]Ga-NOTA-anti-microRNA-21 were developed and used successfully. The radiolabeling protocol for nonGMP-grade 3'-[^{68}Ga]Ga-NOTA-anti-microRNA-21 needs further optimization. *In vitro*, *in vivo* and *ex vivo* experiments as well as PET imaging were used for studying the stability, plasma protein binding and bone accumulation of the ^{68}Ga -radiolabeled tracers. However, a larger number of experimental animals should be used in the future. Bis(phosphonate)-induced bone accumulation can be utilized when developing medicinal treatments for diseases involved micro-RNA-21 like osteoporosis and osteosarcoma.

Acknowledgments

This study was conducted at the Turku PET Centre and the Department of Chemistry, University of Turku during the years 2014–2019. I would like to express my deepest gratitude to my supervisors, Professor Anne Roivainen and Adjunct Professor Xiang-Guo Li. It has been a great opportunity to conduct my research under your professional supervision. Both of you have provided me with cooperative and persistent guidance throughout this process. Anne, your extensive experience has steered and encouraged me during my work. Your sympathetic and supportive attitude has given me strength whenever I needed it. Xiang, you contacted me while I was working outside the University of Turku. I want to thank you for encouraging me to accept the challenge and write a thesis. Your positive attitude and great sense of humor have helped me so much during this process.

I wish to express my gratitude to Professor Vladimir Tolmachev and Adjunct Professor Kim Bergström for reviewing my thesis. Your critical comments and justified observations were necessary and valuable and helped me to improve and clarify this thesis. I am also grateful for your positive feedback. I wish to thank the members of the follow-up committee, Professor Pasi Virta and Head of Radiopharmaceutical Chemistry Laboratory Jörgen Bergman, for your guidance, feedback and professional attitude during this process.

I wish to thank Professor Juhani Knuuti for providing the facilities for my research. I wish to thank Associate Professor Erika Savontaus, Director of Drug Research Doctoral Programme, University of Turku for your expertise. I am grateful to Drug Research Doctoral Programme coordinator Eeva Valve for her assistance throughout my doctoral studies. I also want to acknowledge Chief Academic Officer Outi Irjala, who has kindly answered to my many questions. I am grateful to MA Lea Heinonen-Eerola for editing the language in my thesis.

I sincerely and equitably want to thank all my co-authors and collaborators involved in the research projects. I wish to express my gratitude to collaborators Svend B. Jensen, Lars Jødal and Aage K.O. Alstrup in Aalborg, Aarhus and Copenhagen, Denmark. I am grateful to Satish Jadhav, Kiira Rimpilä, Päivi Poijärvi-Virta and Harri Lönnberg for collaboration within the Department of Chemistry, University of Turku. I also want to thank Jussi Mäkilä, Matthieu

Bourgery and Tiina Laitala at the Department of Cell Biology and Anatomy, University of Turku. I am grateful to Professor Sirpa Jalkanen. I warmly thank Laboratory Technicians Erica Nyman and Marja-Riitta Kajaala for their assistance and flexibility.

I wish to express my gratitude to Radiochemist Pauliina Luoto. As an experienced radiochemist, she helped me in so many ways and supported me in solving the problems. She also encouraged me to step up to the challenge of acting as a substitute to her. I warmly thank Radiochemistry Manager Sarita Forsback and Radiochemist Olli Eskola for their support. Your professional experience was of great help to me while I was working as a researcher at the Turku PET Centre. I also want to thank Radiochemist Tapio Viljanen.

I wish to thank Hospital Physicist Tuula Tolvanen for guidance in radiation safety and PET technology. I also wish to thank Chief Physicist Mika Teräs for guidance in radiation safety. I wish to thank MSc Vesa Oikonen for his expertise and help with modeling and pharmacokinetics. Systems Analyst Rami Mikkola and IT-Manager Marko Tättäläinen are acknowledged for all their help and guidance with IT.

I want to thank the current and former members of the pre-clinical group at the Turku PET Centre, Helena Virtanen, Riikka Viitanen, Mia Ståhle, Jenni Virta, Sanna Hellberg, Olli Moisio, Petri Elo, Maria Grönman, Max Kiugel, Anu Autio, Johanna Silvola, Miikka Tarkia and Tiina Saanijoki. I especially thank Heidi Liljenbäck for your excellent expertise, organizing skills and flexibility. I am indebted to Olli Metsälä, you guided and helped me a lot.

I am grateful to the current and former members of the Turku PET Centre personnel, especially Eija Salo, Emilia Puhakka, Sanna Suominen, Heidi Partanen, Leena Tokoi-Eklund, Hanna Liukko-Sipi, Tiina Tuominen and Minna Tuominen, and all the radiographers. I also want to acknowledge Inkeri Laine for being a great colleague. I especially want to thank Eija Salo for your positive attitude, excellent expertise and help during the years at Turku PET Centre and later on. Thank you for all those difficult questions you asked just to make me think over various things. I wish to thank you for all the past discussions we have had as well as for those we are going to have in the future. I am grateful for your friendship.

I wish to express my gratitude to Senior Researcher Päivi Marjamäki. I want to thank you for all those discussions on science and life we had in the lab in the evenings. I highly appreciate your experience, wisdom and support. You gave me excellent advice and listened to me when I needed it most. I express my gratitude to Research Coordinator Aake Honkaniemi. Your performance in PET imaging has been essential for this study. I want to thank you for your flexibility and excellent organizing skills.

I sincerely want to thank all my dear friends in my life. Some of you have already defended your own doctoral theses and lent me your support during this process. Some of you are working outside of the academic world and have supported me in many different ways. You have given a great and highly important balance to this process. You have reminded me that there is life outside the research chamber.

I express my deepest gratitude to my parents, Pirkko and Markku Käkälä for all the support in life. I also wish to thank my brother, Jarno Käkälä, for your support. I wish to thank Pauliina Levy, it has been a great pleasure to get to know you.

I want to thank my uncle and godfather Pauli Natunen and his wife, Pastor Seija Jokilehto. You have been part of my life for so many years now. I highly appreciate your support and interest in my thesis. I also want to thank my godparents Aino and Otto Korhonen. You are wonderful persons.

Most of all, I want to thank my common-law husband Ville Vartiainen. You have given me strength, space and time when I have needed them most. You made it possible for me to accomplish this process. Together we make a good team.

The study was conducted within the Finnish Centre of Excellence in Cardiovascular and Metabolic Diseases supported by the Academy of Finland, University of Turku, Turku University Hospital and Åbo Akademi University. The Drug Research Doctoral Programme, University of Turku Graduate School, Academy of Finland, Business Finland, Jane and Aatos Erkkö Foundation and Sigrid Jusélius Foundation are acknowledged.

January 2020
Meeri Käkälä

References

- Aalto, K., Autio, A. & Kiss, EA., 2011. Siglec-9 is a novel leukocyte ligand for vascular adhesion protein-1 and can be used in PET imaging of inflammation and cancer. *Blood* 118(13), p. 3725–33.
- Afshar-Oromieh, A., Hetzheim, H., Kratochwil, C., et al. 2015. The Theranostic PSMA Ligand PSMA-617 in the Diagnosis of Prostate Cancer by PET/CT: Biodistribution in Humans, Radiation Dosimetry, and First Evaluation of Tumor Lesions. *J Nucl Med* 56(11), p. 1697–705.
- Ahtinen, H., Kulkova, J., Lindholm, L., et al. 2014. ⁶⁸Ga-DOTA-Siglec-9 PET/CT imaging of periimplant tissue responses and staphylococcal infections. *EJNMMI Res* 4(45), p. 1–11.
- Alves, F., Alves, VHP., Do Cormo, SJC., et al. 2017. Production of copper-64 and gallium-68 with a medical cyclotron using liquid targets. *Mod Phys Lett A* 32(17), p. 1–21.
- Ambrosini, V., Castellucci, P., Rubello, D., et al. 2009. ⁶⁸Ga-DOTA-NOC: a new PET tracer for evaluating patients with bronchial carcinoid. *Nuclear Medicine Communications* 30(4), p. 281–6.
- André, JP., Maecke, HR., Zehnder, M. et al. 1998. 1,4,7-Triazacyclononane-1-succinic acid-4,7-diacetic acid (NODASA): a new bifunctional chelator for radio gallium-labelling of biomolecules. *Chem Commun* p. 1301–2.
- Antunes, P., Ginj, M., Zhang, H., et al. 2007. Are radiogallium-labelled DOTA-conjugated somatostatin analogues superior to those labelled with other radiometals? *Eur J Nucl Med Mol Imaging* 34(7), p. 982–93.
- Arino, H., Skraba, WJ., Kramer, HH., 1978. A new ⁶⁸Ge/⁶⁸Ga radioisotope generator system. *Int J Appl Radiat Isot* 29(2), p. 117–20.
- Asti, M., De Pietri, G., Fraternali, A., et al. 2008. Validation of ⁶⁸Ge/⁶⁸Ga generator processing by chemical purification for routine clinical application of ⁶⁸Ga-DOTATOC. *Nucl Med Biol* 35(6), p. 721–4.
- Autio, A., Henttinen, T., Sipilä, HJ., et al. 2011. Mini-PEG spacing of VAP-1-targeting ⁶⁸Ga-DOTAVAP-P1 peptide improves PET imaging of inflammation. *EJNMMI Res* 1(10), p. 1–7.
- Ballinger, JR & Koziorowski, J., 2017. Regulation of PET Radiopharmaceuticals Production in Europe. In: Khalil, MM., (ed.) *Basic Science of PET Imaging*. Springer International Publishing AG, Switzerland.
- Banerjee, SR. & Pomper, MG., 2013. Clinical Applications of Gallium-68. *Appl Radiat Isot* 76(0), p. 2–13.
- Baranski, A-C., Schäfer, M., Bauder-Wüst, U., et al. 2018. PSMA-11-Derived Dual-Labeled PSMA Inhibitors for Preoperative PET Imaging and Precise Fluorescence-Guided Surgery of Prostate Cancer. *J Nucl Med* 59(4), p. 639–45.
- Barrio, M., Czernin, J., Fanti, S., et al. 2017. The Impact of Somatostatin Receptor-Directed PET/CT on the Management of Patients with Neuroendocrine Tumor: A Systematic Review and Meta-Analysis. *J Nucl Med* 58(5), p. 756–61.
- Bartholomä, MD., 2012. Recent developments in the design of bifunctional chelators for metal-based radiopharmaceuticals used in Positron Emission Tomography. *Inorg Chim Acta* 389, p. 36–51.
- Bauwens, M., Chekol, R., Vanbilloen, H., et al. 2010. Optimal buffer choice of the radiosynthesis of ⁶⁸Ga-Dotatoc for clinical application. *Nucl Med Commun* 31(8), p. 753–8.

- Benešová, M., Schäfer, M., Bauder-Wüst, U., et al. 2015. Preclinical Evaluation of a Tailor-Made DOTA-Conjugated PSMA Inhibitor with Optimized Linker Moiety for Imaging and Endoradiotherapy of Prostate Cancer. *J Nucl Med* 56(6), p. 914–20.
- Berry, DJ., Ma, Y., Ballinger, JR., et al. 2011. Efficient bifunctional gallium-68 chelators for positron emission tomography: tris(hydroxypyridinone) ligands. *Chem Commun (Camb)* 47(25), p. 7068–70.
- bin Othman, MF., Mitry, NR., Lewington, VJ., et al. 2017. Re-assessing gallium-67 as a therapeutic radionuclide. *Nucl Med Biol* 46, p. 12–8.
- Blower, PJ., 2016. The Future Direction of Radiopharmaceutical Development. In: McCready R, Gnanasegaran G, Bomanji JB (eds.) A history of radionuclide studies in UK. *Springer International Publishing AG*, Switzerland.
- Blumberg, LM., 2012. Theory of Gas Chromatography. In: Poole CF (ed.) Gas Chromatography. *Elsevier*, Unites States.
- Bornhöfft, KF., Goldammer, T., Rebl, A., et al. 2018. Siglecs: A journey through the evolution of sialic acid-binding immunoglobulin-type lectins. *Dev Comp Immunol* 86, p. 219–31.
- Boros, E., Ferreira, CL., Cawthray, JF., et al. 2010. Acyclic Chelate with Ideal Properties for ^{68}Ga PET Imaging Agent Elaboration. *J Am Chem Soc* 132(44), p. 15726–33.
- Boschi, S. and Lodi, F., 2017. Chemistry of PET Radiopharmaceuticals: Labelling Strategies. In: Khalil, MM., (ed.) Basic Science of PET Imaging. *Springer International Publishing AG*, Switzerland.
- Boschi, S., Lodi, F., Malizia, C., et al. 2013. Automation synthesis modules review. *Appl Radiat Isot* 76, p. 38–45.
- Boschi, S., Malizia, C., Lodi, F., et al. 2013. Overview and Perspectives on Automation Strategies in ^{68}Ga Radiopharmaceutical Preparations. In: Baum, R., and Rösch, F., (eds.) Theranostics, Gallium-68, and Other Radionuclides. Recent Results in Cancer Research, vol 194. *Springer International Publishing AG*, Germany.
- Braasch, DA., Paroo, Z., Constantinescu, A., et al. 2004. Biodistribution of phosphodiester and phosphorothioate siRNA. *Bioorg Med Chem Lett* 14(5), p. 1139–43.
- Breeman, WAP., de Jong, M., de Blois, E., et al. 2005. Radiolabelling DOTA-peptides with ^{68}Ga . *Eur J Nucl Med Mol Imaging* 32(4), p. 478–85.
- Burke, BP., Clemente, GS., Archibald, SJ., et al. 2014. Recent advances in chelator design and labelling methodology for ^{68}Ga radiopharmaceuticals. *J Label Comp. Radiopharm* 57, p. 239–43.
- Calin, GA. & Croce, CM., 2006. MicroRNA signatures in human cancers. *Nat Rev Cancer* 6(11), p. 857–66.
- Cardinale, J., Schäfer, M., Benešová, M., et al. 2017. Preclinical Evaluation of ^{18}F -PSMA-1007, a New Prostate-Specific Membrane Antigen Ligand for Prostate Cancer Imaging. *J Nucl Med* 58(3), p. 425–31.
- Carroll, DJ., O'Sullivan, JA., Nix, DB., et al. 2018. Sialic acid-binding immunoglobulin-like lectin 8 (Siglec-8) is an activating receptor mediating β_2 -integrin-dependent function in human eosinophils. *J Allergy Clin Immunol* 141(6), p. 2196–207.
- Chakravarty, R., Chakraborty, S., Dash, A., et al. 2013. Detailed evaluation on the effect of metal ion impurities on complexation of generator eluted ^{68}Ga with different bifunctional chelators. *Nucl Med Biol* 40, p. 197–205.
- Chakravarty, R., Shukla, R., Ram, R., et al. 2011. Development of a nano-zirconia based $^{68}\text{Ge}/^{68}\text{Ga}$ generator for biomedical application. *Nucl Med Biol* 38(4), p. 575–83.
- Charron, CL., Farnsworth, AL., Roselt, PD., et al. 2016. Recent developments in radiolabelled peptides for PET imaging of cancer. *Tetrahedron Lett* 57, p. 4119–27.
- Chen, H., Niu, G., Wu, H., et al. 2016. Clinical Application of Radiolabeled RGD Peptides for PET Imaging of Integrin $\alpha_v\beta_3$. *Theranostics* 6(1), p. 78–92.
- Chen, X., 2011. Integrin Targeted Imaging and Therapy. *Theranostics* 1, p. 28–9.

- Chi, Y-T., Chu, P-C., Chao, H-Y., et al. 2014. Design of CGMP Production of ^{18}F - and ^{68}Ga -Radiopharmaceuticals. *Biomed Res Int* Article ID 680195, p. 1–8.
- Clarke, ET. & Martell, AE., 1991. Stabilities of the Fe(III), Ga(III) and In(III) chelates of N,N',N''-triazacyclononanetriacetic acid. *Inorg Chim Acta* 181, p. 273–80.
- Cole, LE., Vargo-Gogola, T., Roeder, RK., et al. 2016. Targeted delivery to bone and mineral deposits using bisphosphonate ligands. *Ad Drug Delivery Rev* 99(Part A), p.12–27.
- Costello, F., Langhorst, S., Mattmuller, S., et al. 2015. Germanium-68 (^{68}Ge) Decommissioning Funding Plan (DFP) Final Report. *Advisory Committee on the Medical Use of Isotopes (ACMUI)*, p. 1–26.
- Cusnir, R., Imberti, C., Hider, RC., et al. 2017. Hydroxypyridinone Chelators: From Iron Scavenging to Radiopharmaceuticals for PET Imaging with Gallium-68. *Int J Mol Sci* 18(116), p. 1–23.
- Decristoforo, C., Knopp, R., von Guggenberg, E., et al. 2007. A fully automated synthesis for the preparation of ^{68}Ga -labelled peptides. *Nucl Med Commun* 28(11), p. 870–5.
- Decristoforo, C., Pickett, RD., Verbruggen, A. et al. 2012. Feasibility and availability of ^{68}Ga -labelled peptides. *Eur J Nucl Med Mol Imaging* 39:(Suppl 1), p. S31–S40.
- de Blois, E., Chan, HS., Naidoo, C., et al. 2011. Characteristics of SnO_2 -based $^{68}\text{Ge}/^{68}\text{Ga}$ generator and aspects of radiolabelling DOTA-peptides. *Appl Radiat Isot* 69:308–15.
- de Carvalho, LL., Elovaara, H., de Ruyck, J., et al. 2018. Mapping the interaction site and effect of the Siglec-9 inflammatory biomarker on human primary amine oxidase. *Sci Rep* 8, p. 1–12.
- Deppen, SA., Liu, E., Blume, JD., et al. 2016. Safety and Efficacy of ^{68}Ga -DOTATATE PET/CT for Diagnosis, Staging, and Treatment Management of Neuroendocrine Tumors. *J Nucl Med* 57(5), p. 708–14.
- Dijkgraaf, I., Yim, C-B., Franssen, GM., et al. 2011. PET imaging of $\alpha_v\beta_3$ integrin expression in tumours with ^{68}Ga -labelled mono-, di- and tetrameric RGD peptides. *Eur J Nucl Med Mol Imaging* 38, p. 128–37.
- Ebenhan, T., Wagener, C., Bambarger, LE., et al. 2017. Radiochemistry. In: Jain, SK. (ed.) *Imaging Infections – From Bench to Bedside*. Springer International Publishing AG, Switzerland.
- Eckert & Ziegler Eurotope 2019. Modular-Lab PharmTracer® schematic.
- Eder, M., Neels, O., Müller, M., et al. 2014. Novel Preclinical and Radiopharmaceutical Aspects of [^{68}Ga]Ga-PSMA-HBED-CC: A New PET Tracer for Imaging of Prostate Cancer. *Pharmaceuticals* 7, p. 779–96.
- Eder, M., Wängler, B., Knackmuss, S., et al. 2008. Tetrafluorophenolate of HBED-CC: a versatile conjugation agent for ^{68}Ga -labeled small recombinant antibodies. *Eur J Nucl Med Mol Imaging* 35, p. 1878–86.
- Elsinga, P., Todde, S., Penuelas, I., et al. 2010. Guidance on current good radiopharmacy practice (cGRPP) for the small-scale preparation of radiopharmaceuticals. *Eur J Nucl Med Mol Imaging* 37, p. 1049–62.
- Fani, M., André, JP., Maecke, HR., 2008. ^{68}Ga -PET: a powerful generator-based alternative to cyclotron-based PET radiopharmaceuticals. *Contrast Media Mol Imaging* 3, p. 53–63.
- Farkas, E., Nagel, J., Waldron, BP., et al. 2017. Equilibrium, Kinetic and Structural Properties of Gallium(III) and Some Divalent Metal Complexes Formed with the New DATA^m and DATA^{5m} Ligands. *Chemistry* 23(43), p. 10358–71.
- Fellner, M., Biesalski, B., Bausbacher, N., et al. 2012. ^{68}Ga -BPAMD: PET-imaging of bone metastases with a generator based positron emitter. *Nucl Med Biol* 39:993–9.
- Fellner, M., Riss, P., Loktionova, NS., et al. 2011. Comparison of different phosphorus-containing ligands complexing ^{68}Ga for PET-imaging of bone metabolism. *Radiochim Acta* 99(1), p. 43–51.
- Fermi, E., 2009. Quality Control of PET Radiopharmaceuticals. In: Vallabhajosula, S., (ed.) *Molecular Imaging – Radiopharmaceuticals for PET and SPECT*. Springer, Germany.
- Francis, MD., Russell, RGG., Fleisch, H., 1969. Diphosphonates Inhibit Formation of Calcium Phosphate Crystals *in vitro* and Pathological Calcification *in vivo*. *Science* 165, p. 1264–6.

- Franck, D., Nann, H., Davi, P., et al. 2009. Faster analysis of radiopharmaceuticals using ultra performance liquid chromatography (UPLC®) in combination with low volume radio flow cell. *App Radiat Isot* 67, p. 1068–70.
- Gabriel, M., Decristoforo, C., Kendler, D., et al. 2007. ⁶⁸Ga-DOTA-Tyr³-Octreotide PET in Neuroendocrine Tumors: Comparison with Somatostatin Receptor Scintigraphy and CT. *J Nucl Med* 48(4), p. 508–18.
- Ghai, A., Singh, B., Li, M., et al. 2018. Optimizing the radiosynthesis of [⁶⁸Ga]DOTA-MLN6907 peptide containing three disulfide cyclization bonds – a GCC specific chelate for clinical radiopharmaceuticals. *Appl Radiat Isot* 140, p. 333–41.
- Giesel, FL., Cardinale, J., Schäfer, M. et al. 2016. ¹⁸F-Labelled PSMA-1007 shows similarity in structure, biodistribution and tumour uptake to the theragnostic compound PSMA-617. *Eur J Nucl Med Mol Imaging* 43, p. 1929–30.
- Giesel, FL., Hadaschik, B., Cardinale, J. et al. 2017. F-18 labelled PSMA-1007: biodistribution, radiation dosimetry and histopathological validation of tumor lesions in prostate cancer patients. *Eur J Nucl Med Mol Imaging* 44, p. 678–88.
- Gijs, M., Dammico, S., Warnier, C., et al. 2016. Gallium-68-labelled NOTA-oligonucleotides: an optimized method for their preparation. *J Labelled Compd Radiopharm* 59, p. 63–71.
- Gilad, Y., Firer, M., Gellerman, G, et al. 2016. Recent Innovations in Peptide Based Targeted Drug Delivery to Cancer Cells. *Biomedicines* 4(11), p. 1–24.
- Gleason, GI., 1960. A positron cow. *Int J Appl Radiat Isot* 8, p. 90–4.
- Gnesin, S., Mitsakis, P., Cicone, F., et al. 2017. First in-human radiation dosimetry of ⁶⁸Ga-NODAGA-RGDyK. *EJNMMI Res* 7(43), p. 1–10.
- Greene, MW. & Tucker, WD., 1961. An Improved Gallium-68 Cow. *Int J Appl Radiat Isot* 12, p. 62–3.
- Ha, NS., Sadeghi, S., van Dam, RM., 2017. Recent Progress toward Microfluidic Quality Control Testing of Radiopharmaceuticals. *Micromachines* 8(337), p. 1–28.
- Haubner, R., Finkenstedt, A., Stegmayr, A., et al. 2016. [⁶⁸Ga]NODAGA-RGD – Metabolic stability, biodistribution, and dosimetry data from patients with hepatocellular carcinoma and liver cirrhosis. *Eur J Nucl Med Mol Imaging* 43, p. 2005–13.
- Haukkala, J., Laitinen, I., Luoto, P., et al. 2009. ⁶⁸Ga-DOTA-RGD peptide: biodistribution and binding into atherosclerotic plaques in mice. *Eur J Nucl Med Mol Imaging* 36, p. 2058–67.
- Heppeler, A., Froidevaux, S., Mäcke, HR., et al. 1999. Radiometal-Labelled Macrocyclic Chelator-Derivatised Somatostatin Analogue with Superb Tumour-Targeting Properties and Potential for Receptor-Mediated Internal Radiotherapy. *Chem Eur J* 5(7), p. 1974–81.
- Hofman, MS., Kong, G., Neels, OC., et al. 2012. High management impact of Ga-68 DOTATATE (GaTate) PET/CT for imaging neuroendocrine and other somatostatin expressing tumours. *J Med Imaging Radiat Oncol* 56, p. 40–7.
- Hofmann, M., Maecke, H., Börner, AR., et al. 2001. Biokinetics and imaging with the somatostatin receptor PET radioligand ⁶⁸Ga-DOTATOC: preliminary data. *Eur J Nucl Med* 28(12), p. 1751–7.
- Holub, J., Meckel, M., Kubiček, V., et al. 2015. Gallium(III) complexes of NOTA-bis(phosphonate) conjugates as PET radiotracers for bone imaging. *Contrast Media Mol Imaging* 10, p. 122–34.
- Huang, Y-Y., 2018. An Overview of PET Radiopharmaceuticals in Clinical Use: Regulatory, Quality and Pharmacopeia Monographs of the United States and Europe. In: Nuclear Medicine Physics, *IntechOpen*.
- Jalilian, AR., 2016. An overview on Ga-68 radiopharmaceuticals for positron emission tomography applications. *Iran J Nucl Med* 24(1), p. 1-10.
- Jeong, JM., Hong, MK., Chang, YS., et al. 2008. Preparation of a Promising Angiogenesis PET Imaging Agent: ⁶⁸Ga-Labeled c(RGDyK)-Isothiocyanatobenzyl-1,4,7-Triazacyclononane-1,4,7-Triacetic Acid and Feasibility Studies in Mice. *J Nucl Med* 49(5), p. 830–6.
- Jindal, T., Kumar, A., Venkitaraman, B., et al. 2010. Role of ⁶⁸Ga-DOTATOC PET/CT in the Evaluation of Primary Pulmonary Carcinoids. *Korean J Intern Med* 25(4), p. 386–91.

- Kerlin, R.L. & Li, X., 2013. Pathology in Non-Clinical Drug Safety Assessment. In: Haschek, W., Rousseaux, C., Wallig, M., (eds.) Haschek and Rousseaux's Handbook of Toxicologic Pathology (3rd ed.), *Academic Press*, United States.
- Kiugel, M., Dijkgraaf, I., Kytö, V., et al. 2014. Dimeric [⁶⁸Ga]DOTA-RGD Peptide Targeting $\alpha_v\beta_3$ Integrin Reveals Extracellular Matrix Alterations after Myocardial Infarction. *Mol Imaging Biol* 16, p. 793–801.
- Kiviniemi, A., Mäkelä, J., Mäkilä, J., et al. 2012. Solid-Supported NOTA and DOTA Chelators Useful for the Synthesis of 3'-Radiometalated Oligonucleotides. *Bioconjugate Chem* 23, p. 1981–8.
- Kopecký, P. & Mudrová, B., 1974. ⁶⁸Ge - ⁶⁸Ga Generator for the Production of ⁶⁸Ga in an Ionic Form. *Int J Appl Radiat Isot* 25(6), p. 263–8.
- Koziorowski, J., Behe, M., Decristoforo, C., et al. 2016. Position paper on requirements for toxicological studies in the specific case of radiopharmaceuticals. *EJNMMI Radiopharm Chem* 1, p. 1–6.
- Kryza, D. & Janier, M., 2013. Radio-UHPLC: A tool for rapidly determining the radiochemical purity of technetium-99m radiopharmaceuticals? *Appl Radiat Isot* 78, p. 72–6.
- Kubíček, V., Havlíčková, J., Kotek, J., et al. 2010. Gallium(III) Complexes of DOTA and DOTA-Monoamide: Kinetic and Thermodynamic Studies. *Inorg Chem* 49(23), p. 10960–9.
- Lamesa, C., Rauscher, A., Lacoueille, F., et al. 2015. ⁶⁸Ga somatostatin analog radiolabelling: The radiopharmacist's point of view. *Méd Nucl* 39, p. 3–10.
- Lankinen, P., Mäkinen, T.J., Pöyhönen, T.A., et al. 2008. Ga-68-DOTAVAP-P1 PET imaging capable of demonstrating the phase of inflammation in healing bones and the progress of infection in osteomyelitic bones. *Eur J Nucl Med Mol Imaging* 35(2), p. 352–64.
- Lendvai, G., Estrada, S., Bergstrom, M., 2009. Radiolabelled Oligonucleotides for Imaging of Gene Expression with PET. *Curr Med Chem* 16(33), p. 4445–61.
- Li, X-G., Autio, A., Ahtinen, H., et al. 2013. Translating the concept of peptide labeling with 5-deoxy-5-[¹⁸F]fluororibose into preclinical practice: ¹⁸F-labeling of Siglec-9 peptide for PET imaging of inflammation. *Chem Commun* 49, p. 3682–4.
- Lin, M., Waligorsky, G.J. & Leper, C.G., 2018. Production of curie quantities of ⁶⁸Ga with a medical cyclotron via the ⁶⁸Zn (p,n)⁶⁸Ga reaction. *Appl Radiat Isot* 133:1–3.
- Lobeck, D., Franssen, G.M., Ma, M.T., et al. 2018. *In Vivo* Characterization of 4 ⁶⁸Ga-Labeled Multimeric RGD Peptides to Image $\alpha_v\beta_3$ Integrin Expression in 2 Human Tumor Xenograft Mouse Models. *J Nucl Med* 59(8), p. 1296–301.
- Lodi, F. & Boschi, S., 2017. Quality Control of PET Radiopharmaceuticals. In: Khalil, M.M., (ed.) Basic Science of PET Imaging. *Springer International Publishing AG*, Switzerland.
- Ma, M.T., Cullinane, C., Imberti, C., et al. 2016. New Tris(hydroxypyridinone) Bifunctional Chelators Containing Isothiocyanate Groups Provide a Versatile Platform for Rapid One-Step Labeling and PET Imaging with ⁶⁸Ga³⁺. *Bioconjugate Chem* 27, p. 309–18.
- Ma, R., Welch, M.J., Reibenspies, J., et al. 1995. Stability of metal ion complexes of 1,4,7-tris(2-mercaptoethyl)-1,4,7-triazacyclononane (TACN-TM) and molecular structure of In (C₁₂H₂₄N₃S₃). *Inorg Chim Acta* 236, p. 75–82.
- Maecke, H.R. & André, J.P., 2007. ⁶⁸Ga-PET Radiopharmacy: A Generator-Based Alternative to ¹⁸F-Radiopharmacy. *Ernst Schering Res Found Workshop* 62, p. 215–42.
- Mahajan, A. & Cook, G., 2017. Physiologic and Molecular Basis of PET in Cancer Imaging. In: Khalil, M.M., (ed.) Basic Science of PET Imaging. *Springer International Publishing AG*, Switzerland.
- Maisey, M.N., 2005. Positron emission tomography in clinical medicine. In: Bailey DL, Townsend DW, Valk, P.E., et al. (ed.) Positron emission tomography – Basic sciences. *Springer-Verlag*, Singapore.

- Mathias, C.J., Lewis, M.R., Reichert, D.E., et al. 2003. Preparation of ^{66}Ga - and ^{68}Ga -labeled Ga(III)-deferoxamine-folate as potential folate-receptor-targeted PET radiopharmaceuticals. *Nucl Med Biol* 30, p. 725–31.
- Meckel, M., Fellner, M., Thieme, N., et al. 2013. *In vivo* comparison of DOTA based ^{68}Ga -labelled bisphosphonates for bone imaging in non-tumour models. *Nucl Med Biol* 40, p. 823–30.
- Meyer, G.-J., Mäcke, H., Schuhmacher, J., et al. 2004. ^{68}Ga labelled DOTA-derivatised peptide ligands. *Eur J Nucl Med Mol Imaging* 31(8), p. 1097–1104.
- Mueller, D., Klette, I., Baum, R.P., et al. 2012. Simplified NaCl Based ^{68}Ga Concentration and Labeling Procedure for Rapid Synthesis of ^{68}Ga Radiopharmaceuticals in High Radiochemical Purity. *Bioconjugate Chem* 23, p. 1712–7.
- Myasoedov, B.F., 2000. Century of Radiochemistry: History and Future. *J Nucl Radiochem Sci* 1(1), p. 23–6.
- Mäkilä, J., Jadhav, S., Kiviniemi, A., et al. 2014. Synthesis of multi-galactose-conjugated 2'-O-methyl oligoribonucleotides and their *in vivo* imaging with positron emission tomography. *Bioorg Med Chem* 22, p. 6806–13.
- Nakayama, M., Haratake, M., Koiso, T., et al. 2002. Separation of ^{68}Ga from ^{68}Ge using a macroporous organic polymer containing *N*-methylglucamine groups. *Anal Chim Acta* 453(1), p. 135–41.
- Neirinckx, R.D. & Davis, M.A., 1979. Potential Column Chromatography Generators for Ionic Ga-68. *J Nucl Med* 20(10), p. 1075–9.
- Nock, B.A., Kaloudi, A., Nagel, J., et al. 2017. Novel bifunctional DOTA chelator for quick access to site-directed PET ^{68}Ga -radiotracers: preclinical proof-of-principle with [Tyr^3]octreotide. *Dalton Trans* 46, p. 14584–90.
- Notni, J., Šimeček, J., Wester, H.J., et al. 2014. Phosphinic Acid Functionalized Polyazacycloalkane Chelators for Radiodiagnostics and Radiotherapeutics: Unique Characteristics and Applications. *Chem Med Chem* 9(6), p. 1107–15.
- Nunn, A.D. & Fritzberg, A.R., 1986. Components for the Design of a Radio-HPLC System. In: Wieland, D.M., Tobes, M.C. & Mangner, T.J., (eds.) Analytical and Chromatographic Techniques in Radiopharmaceutical Chemistry. *Springer-Verlag*, United States.
- Ocak, M., Antretter, M., Knopp, R., et al. 2010. Full automation of ^{68}Ga labelling of DOTA-peptides including cation exchange prepurification. *Appl Radiat Isot* 68, p. 297–302.
- Ocak, M., Demirci, E., Kabasakal, L., et al. 2013. Evaluation and comparison of Ga-68 DOTA-TATE and Ga-68 DOTA-NOC PET/CT imaging in well-differentiated thyroid cancer. *Nucl Med Commun* 34(11), p. 1084–9.
- Ogawa, K., Takai, K., Kanbara, H., et al. 2011. Preparation and evaluation of a radiogallium complex-conjugated bisphosphonate as a bone scintigraphy agent. *Nucl Med Biol* 38(5), p. 631–6.
- Pandey, M.K., Byrne, J.F., Jiang, H., et al. 2014. Cyclotron production of ^{68}Ga via the $^{68}\text{Zn}(p,n)^{68}\text{Ga}$ reaction in aqueous solution. *Am J Nucl Med Mol Imaging* 4(4), p. 303–10.
- Petrik, M., Knetsch, P.A., Knopp, R., et al. 2011. Radiolabelling of peptides for PET, SPECT and therapeutic applications using a fully automated disposable cassette system. *Nucl Med Commun* 32(10), p. 887–95.
- Pfaff, S., Nehring, T., Pichler, V., et al. 2018. Development and evaluation of a rapid analysis for HEPES determination in ^{68}Ga -radiotracers. *EJNMI Research* 8, p. 1–10.
- Pfob, C.H., Ziegler, S., Graner, F.P., et al. 2016. Biodistribution and radiation dosimetry of ^{68}Ga -PSMA HBED CC – a PSMA specific probe for PET imaging of prostate cancer. *Eur J Nucl Med Mol Imaging* 43, p. 1962–70.
- Ph. Eur., 2013. Gallium (^{68}Ga) edotreotide injection. *01/2013:2482, corrected 9.6*: 5979–81.
- Pillay, K.K.S., 1986. A review of the radiation stability of ion exchange materials. *Akadémiai Kiadó* 102(1), p. 247–68.
- Poeppl, T.D., Binse, I., Petersenn, S., et al. 2011. ^{68}Ga -DOTATOC Versus ^{68}Ga -DOTATATE PET/CT in Functional Imaging of Neuroendocrine Tumors. *J Nucl Med* 52(12), p. 1864–70.

- Pohle, K., Notni, J., Bussemer, J., et al. 2012. ^{68}Ga -NODAGA-RGD is a suitable substitute for ^{18}F -Galacto-RGD and can be produced with high specific activity in a cGMP/GRP compliant automated process. *Nucl Med Biol* 39:777–84.
- Poli, M., Petroni, D., Berton, A., et al. 2014. The role of quality management system in the monitoring and continuous improvement of GMP-regulated short-lived radiopharmaceutical manufacture. *Accred Qual Assur* 19(5), p. 343–54.
- Prata, M., Santos, AC., Geraldes, CFGC., et al. 1999. Characterisation of $^{67}\text{Ga}^{3+}$ Complexes of Triaza Macrocyclic Ligands: Biodistribution and Clearance Studies. *Nucl Med Biol* 26, p. 707–10.
- Prata, MIM., Santos, AC., Geraldes, CFGC., et al. 2000. Structural and *in vivo* studies of metal chelates of Ga (III) relevant to biomedical imaging. *J Inorg Biochem* 79, p. 359–63.
- Price, EW. & Orvig, C., 2014. Matching chelators to radiometals for radiopharmaceuticals. *Chem Soc Rev* 43(1), p. 260–90.
- Prince, D., Rossouw, D. & Rubow, S., 2018. Optimization of a Labeling and Kit Preparation Method for Ga-68 Labeled DOTATATE, Using Cation Exchange Resin Purified Ga-68 Eluates Obtained from a Tin Dioxide $^{68}\text{Ge}/^{68}\text{Ga}$ Generator. *Mol Imaging Biol* 20(6), p. 1008–41.
- Ramogida, CF., Murphy, L., Cawthray, JF., et al. 2016. Novel “bi-modal” H₂dedpa derivatives for radio- and fluorescence imaging. *J Inorg Biochem* 162, p. 253–62.
- Razbash, AA., Sevastianov, YuG., Krasnov, NN., et al. 2005. Germanium-68 row of products. In: Proceedings of the 5th International Conference on Isotopes 5ICI, p. 147–51.
- Retamal, J., Sorensen, J., Lubberink, M., et al. 2016. Feasibility of (^{68}Ga) -labeled Siglec-9 peptide for the imaging of acute lung inflammation: a pilot study in a porcine model of acute respiratory distress syndrome. *Am J Nucl Med Mol Imaging* 6(1), p. 18–31.
- Rettig, GR. & Behlke, MA., 2012. Progress Toward *In Vivo* Use of siRNAs-II. *Mol Ther* 20(3), p. 483–512.
- Riga, S., Cicoria, G., Pancaldi, D., et al. 2018. Production of Ga-68 with a General Electric PETtrace cyclotron by liquid target. *Phys Med* 55, p. 116–26.
- Riss, PJ., Kroll, C., Nagel, V., et al. 2008. NODAPA-OH and NODAPA-(NCS)_n: Synthesis, ^{68}Ga -radiolabelling and *in vitro* characterisation of novel versatile bifunctional chelators for molecular imaging. *Bioorg Med Chem Lett* 18, p. 5364–7.
- Roivainen, A., Kähkönen, E., Luoto, P., et al. 2013. Plasma Pharmacokinetics, Whole-Body Distribution, Metabolism, and Radiation Dosimetry of ^{68}Ga Bombesin Antagonist BAY 86-7548 in Healthy Men. *J Nucl Med* 54(6), p. 867–72.
- Roivainen, A., Tolvanen, T., Salomäki, S., et al. 2004. ^{68}Ga -Labeled Oligonucleotides for *In Vivo* Imaging with PET. *J Nucl Med* 45(2), p. 347–55.
- Ruoslahti, E., 2016. RGD and Other Recognition Sequences for Integrins. *Annu Rev Cell Dev Biol* 12, p. 697–715.
- Rösch, F., 2013. Past, present and future of $^{68}\text{Ge}/^{68}\text{Ga}$ generators. *Appl Radiat Isot* 76, p. 24–30.
- Salmi, M. & Jalkanen, S., 2014. Ectoenzymes in leukocyte migration and their therapeutic potential. *Semin Immunopathol* 36, p. 163–76.
- Satpati, D., Sharma, R., Sarma, HD., et al. 2018. Comparative evaluation of ^{68}Ga -labeled NODAGA, DOTAGA, and HBED-CC-conjugated cNGR peptide chelates as tumor-targeted molecular imaging probes. *Chem Biol Drug Des* 91, p. 781–8.
- Schmidt, A., Schottelius, M., Herz, M., et al. 2017. Production of clinical radiopharmaceuticals: general pharmaceutical and radioanalytical aspects. *J Radioanal Nucl Chem* 311:1551–7.
- Schuhmacher, J., Klivényi, G., Hull, WE., et al. 1992. A Bifunctional HBED-derivative for Labeling of Antibodies with ^{67}Ga , ^{111}In and ^{59}Fe . Comparative Biodistribution with ^{111}In -DPTA and ^{131}I -labeled Antibodies in Mice Bearing Antibody Internalizing and Non-internalizing Tumors. *Nucl Med Biol* 19(8), p. 809–24.
- Schuhmacher, J. & Maier-Borst, W., 1981. A New $^{68}\text{Ge}/^{68}\text{Ga}$ Radioisotope Generator System for Production of ^{68}Ga in Dilute HCl. In *J Appl Radiat Isot* 12, p. 31–6.

- Schultz, MK., Mueller, D., Baum, RP., et al. 2013. A new automated NaCl based robust method for routine production of gallium-68 labeled peptides. *Appl Radiat Isot* 76, p. 46–54.
- Seemann J, Waldron BP, Roesch F et al. (2015) Approaching 'Kit-Type' Labelling with ⁶⁸Ga: The DATA Chelators. *ChemMedChem*. 10:1019–26.
- Silver DA, Pellicer I, Fair WR et al. (1997) Prostate-specific Membrane Antigen Expression in Normal and Malignant Human Tissues. *Clin. Cancer Res*. 3:81–5.
- Silvola, J., Autio, A., Luoto, P., et al. 2010. Preliminary evaluation of novel 68Ga-DOTAVAP-PEG-P2 peptide targeting vascular adhesion protein-1. *Clin Physiol Funct Imaging* 30(1), p. 75–8.
- Silvola, JMU., Virtanen, H., Siitonen, R., et al. 2016. Leukocyte trafficking-associated vascular adhesion protein 1 is expressed and functionally active in atherosclerotic plaques. *Sci Rep* 6, p. 1–10.
- Šimeček, J., Schulz, M., Notni, J., et al. 2012. Complexation of Metal Ions with TRAP (1,4,7-Triazacyclononane Phosphinic Acid) Ligands and 1,4,7-Triazacyclononane-1,4,7-triacetic Acid: Phosphinate-Containing Ligands as Unique Chelators for Trivalent Gallium. *Inorg Chem* 51, p. 577–90.
- Smith-Jones, PM., Stolz, B., Bruns, C., et al. 1994. Gallium-67/Gallium-68-[DFO]-Octreotide – A Potential Radiopharmaceutical for PET Imaging of Somatostatin Receptor-Positive Tumors: Synthesis and Radiolabeling *In Vitro* and Preliminary *In Vivo* Studies. *J Nucl Med* 35(2), p. 317–25.
- Suzuki, K., Satake, M., Suwada, J., et al. 2011. Synthesis and evaluation of a novel 68Ga-chelate-conjugated bisphosphonate as a bone-seeking agent for PET imaging. *Nucl Med Biol* 38(7), p. 1011–18.
- Syed, MA. &Pervaiz, S., 2010. Advances in aptamers. *Oligonucleotides* 20(5), p. 215–24.
- Theodore, TR., Van Zandt, RL. & Carpenter, RH., 1997. Preliminary evaluation of a fixed dose of zwitterionic piperazine (TVZ-7) in clinical cancer. *Cancer Biother Radiopharm* 12(5), p. 351–3.
- Theodore, TR., Van Zandt, RL. & Carpenter, RH., 1997. Preliminary evaluation of a fixed dose of zwitterionic piperazine (TVZ-7) in clinical cancer. *Cancer Biother Radiopharm* 12(5), p. 351–3.
- Tsang, BW., Mathias, CJ. & Green, MA., 1993. A Gallium-68 Radiopharmaceutical That is Retained in Myocardium: ⁶⁸Ga[(4,6-MeO₂sal)₂BAPEN]⁺. *J Nucl Med* 34(7), p. 1127–31.
- Tsionou, MI., Knapp, CE., Foley, CA., et al. 2017. Comparison of macrocyclic and acyclic chelators for gallium-68 radiolabelling. *RSC Adv* 7, p. 49586–99.
- Ujula, T., Salomäki, S., Virsu, P., et al. 2009. Synthesis, ⁶⁸Ga labeling and preliminary evaluation of DOTA peptide binding vascular adhesion protein-1: a potential PET imaging agent for diagnosing osteomyelitis. *Nucl Med Biol* 36, p. 631–41.
- Uludag, H., Kousiniaris, N., Gao, T., et al. 2000. Bisphosphonate conjugation to proteins as a means to impart bone affinity. *Biotechnol Progr* 16(2), p. 258–67.
- Varga, J., 2012. An Introduction to Nuclear Medicine. In: Kónya, J. & Nagy, N., (eds.) Nuclear and Radiochemistry. *Elsevier Inc.*, Great Britain.
- Varki, A. & Angata, T., 2006. Siglecs – the major subfamily of I-type lectins. *Glycobiology* 16:1R–27R.
- Velikyan, I., 2011. Positron emitting [⁶⁸Ga]Ga-based imaging agents: chemistry and diversity. *Med Chem* 7(5), p. 338–72.
- Velikyan, I., 2013. The Diversity of ⁶⁸Ga-Based Imaging Agents. In: Baum, RP.& Rösch, F., (eds.) Theranostics, Gallium-68, and Other Radionuclides - A Pathway to Personalized Diagnosis and Treatment. *Springer-Verlag*, Germany.
- Velikyan, I., 2014. Prospective of ⁶⁸Ga-Radiopharmaceutical Development. *Theranostics* 4(1), p. 47–80.
- Velikyan, I., Beyer, GJ., Bergström-Pettermann, E., et al. 2008. The importance of high specific radioactivity in the performance of ⁶⁸Ga-labeled peptide. *Nucl Med Biol* 35(5), p. 529–36.
- Velikyan, I., Lendvai, G., Váčilá, M., et al. 2004. Microwave accelerated ⁶⁸Ga-labelling of oligonucleotides. *J Labelled Compd Radiopharm* 47(1), p. 79–89.

- Velikyán, I., Maecke, H. & Langstrom, B., 2008. Convenient Preparation of ^{68}Ga -Based PET-Radiopharmaceuticals at Room Temperature. *Bioconjugate Chem* 19(2), p. 569–73.
- Velikyán, I., Sundin, A., Eriksson, B., et al. 2010. *In vivo* binding of [^{68}Ga]-DOTATOC to somatostatin receptors in neuroendocrine tumours – impact of peptide mass. *Nucl Med Biol* 37(3), p. 265–75.
- Viel, T., Boisgard, R., Kuhnast, B., et al. 2008. Molecular Imaging Study on *In Vivo* Distribution and Pharmacokinetics of Modified Small Interfering RNAs (siRNAs). *Oligonucleotides* 18(3), p. 201–12.
- Viola, N.A., Rarig, Jr. R.S., Ouellette, W., et al. 2006. Synthesis, structure and thermal analysis of the gallium complex of 1,4,7,10-tetraazacyclo-dodecane-N,N',N'',N'''-tetraacetic acid (DOTA). *Polyhedron* 25(18), p. 3457–62.
- Virtanen, H., Autio, A., Siitonen, S., et al. 2015. ^{68}Ga -DOTA-Siglec-9 – a new imaging tool to detect synovitis. *Arthritis Res Ther* 17(308), p. 1–11.
- Virtanen, H., Silvola, J.M.U., Autio, A., et al. 2017. Comparison of ^{68}Ga -DOTA-Siglec-9 and ^{18}F -Fluorodeoxyribose-Siglec-9. *Contrast Media & Molecular Imaging* 31, p. 1–10.
- Wadsak, W. & Mitterhauser, M., 2010. Basics and principles of radiopharmaceuticals for PET/CT. *Eur J Radiol* 73(3), p. 461–9.
- Waters Corporation, 2014. *Beginners Guide to Liquid Chromatography*. Wiley, United States.
- Wild, D., Bomanji, J.B., Benkert, P., et al. 2013. Comparison of ^{68}Ga -DOTANOC and ^{68}Ga -DOTATATE PET/CT Within Patients with Gastroenteropancreatic Neuroendocrine Tumors. *J Nucl Med* 54(3), p. 364–72.
- Wild, D., Schmitt, J.S., Ginj, M., et al. 2003. DOTA-NOC, a high-affinity ligand of somatostatin receptor subtypes 2, 3 and 5 for labelling with various radiometals. *Eur J Nucl Med Mol Imaging* 30(10), p. 1338–47.
- Winkler, J., 2013. Oligonucleotide conjugates for therapeutic applications. *Ther Deliv* 4(7), p. 791–809.
- World Health Organization, 2003. Annex 3 - Guidelines on Good Manufacturing Practices for radiopharmaceutical products. © World Health Organization. *Technical Report Series* No. 908, p. 26–35.
- Xia, H., Zhang, W., Zhang, B., et al. 2017. miR-21 modulates the effect of EZH2 on the biological behavior of human lung cancer stem cells *in vitro*. *Oncotarget* 8(49), p. 85442–51.
- Yamamoto, T., Nakatani, M., Narukawa, K., et al. 2011. Antisense drug discovery and development. *Future Med Chem* 3(3), p. 339–65.
- Yang, C.-T., Sreerama, S.G., Hsieh, W.-Y., et al. 2008. Synthesis and Characterization of a Novel Macrocyclic Chelator with 3-Hydroxy-4-Pyrone Chelating Arms and Its Complexes with Medically Important Metals. *Inorg Chem* 47(7), p. 2719–27.
- Yang, J., Kan, Y., Ge, B.H., et al. 2014. Diagnostic role of Gallium-68 DOTATOC and Gallium-68 DOTATATE PET in patients with neuroendocrine tumors: a meta-analysis. *Acta Radiol* 55(4), p. 389–98.
- Zhernosekov, K.P., Filosofov, D.V., Baum, R.P., et al. 2007. Processing of Generator-Produced ^{68}Ga for Medical Application. *J Nucl Med* 48(10), p. 1741–8.
- Zhuang, H. & Alavi, A., 2002. ^{18}F -Fluorodeoxyglucose positron emission tomographic imaging in the detection and monitoring of infection and inflammation. *Semin Nucl Med* 32(1), p. 47–59.
- Ziyan, W., Shuhua, Y., Xiufang, W., et al. 2011. MicroRNA-21 Is Involved in Osteosarcoma Cell Invasion and Migration. *Med Oncol* 28(4), p. 1469–74.



**UNIVERSITY
OF TURKU**

ISBN 978-951-29-7975-2 (PRINT)
ISBN 978-951-29-7976-9 (PDF)
ISSN 0355-9483 (Print)
ISSN 2343-3213 (Online)